# Lawrence Berkeley National Laboratory
## Recent Work

**Title**

CHEMICAL MODIFICATION AND SPIN-LABEL STUDIES OF CARBOXYL RESIDUES IN BACTERIORHODOPSIN

**Permalink**

https://escholarship.org/uc/item/3wq5v9q9

**Author**

Herz, J.M.

**Publication Date**

1983-06-01

# Lawrence Berkeley Laboratory
## UNIVERSITY OF CALIFORNIA

# ENERGY & ENVIRONMENT DIVISION
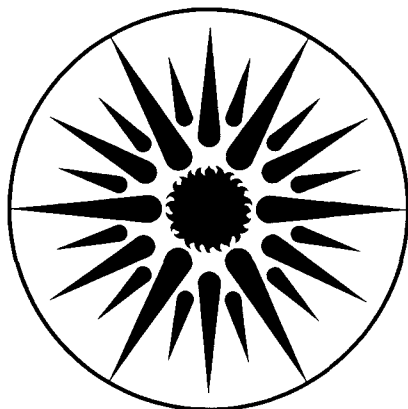
CHEMICAL MODIFICATION AND SPIN-LABEL STUDIES OF
CARBOXYL RESIDUES IN BACTERIORHODOPSIN

J.M. Herz
(Ph.D. Thesis)

June 1983

**ENERGY
AND ENVIRONMENT
DIVISION**

## DISCLAIMER

CHEMICAL MODIFICATION AND SPIN-LABEL STUDIES
OF CARBOXYL RESIDUES IN BACTERIORHODOPSIN

by

Jeffrey Mark Herz

(Ph.D. Thesis)

June, 1983

Lawrence Berkeley Laboratory
University of California
Berkeley, California 94720

# CHEMICAL MODIFICATION AND SPIN-LABEL STUDIES OF

# CARBOXYL RESIDUES IN BACTERIORHODOPSIN

Jeffrey Mark Herz

Membrane Bioenergetics Group
Lawrence Berkeley Laboratory
and
Department of Physiology-Anatomy
University of California
Berkeley, California

## ABSTRACT

The structural and functional roles of carboxyl residues in bacteriorhodopsin have been investigated by amino acid chemical modification and electron paramagnetic resonance studies of spin-labeled bacteriorhodopsin. Carboxyl modification of bacteriorhodopsin using either the water-soluble reagent, 1-ethyl-3-(3-dimethylaminopropyl) carbodiimide, or a hydrophobic reagent, N-(ethoxycarbonyl)-2-ethoxy-1,2-dihydroquinoline, resulted in no changes in the absorption spectra or visible circular dichroism spectra, and the modified protein retained proton pumping activity.

A structural role for a carboxyl residue in the bacteriorhodopsin photocycle was found by analyzing the kinetics for the decay of the $M_{412}$ intermediate. It was found that both carboxyl activating reagents strongly inhibited $M_{412}$ decay kinetics. The inhibition was prevented if modification occurred in the presence of a nucleophile, glycine methyl ester, or if lysine residues were first blocked by reaction with a monofunctional imidoester. It was found that one carboxyl-lysine

cross-link that was a result of carboxyl modification was prevented if lysines were first modified. These results showed that the formation of zero-length intramolecular cross-link strongly inhibited the reprotonation phase of the photocycle.

Evidence for interactions between a carboxyl group and the retinal-protein chromophore was obtained by labeling a carboxyl residue with a pH-sensitive chromophoric reporter group, nitrotyrosine methyl ester. The spectral and ionization properties of the reporter group were substantially different than the model compound in solution. Similar studies of the reporter group-labeled bacterioopsin in white membranes demonstrated that the immediate protein microenvironment and not retinal interactions "per se" were responsible for the elevated pK value of 10-11 and unusual spectral properties. Alkaline titration resulted in a protein configurational change that transferred the reporter group from a hydrophobic environment to the aqueous membrane surface, and eliminated interactions with the retinal chromophore. The ionization state of the reporter group also influenced photocycling activity by inhibiting $M_{412}$ decay kinetics.

The topography and mobility of carboxyl residues in different membrane protein domains was studied by chemical modification with spin-label reporter groups. Carboxyl groups were covalently spin-labeled with 4-amino,2,2,6,6-tetramethylpiperidine-N-oxyl (Tempamine) using the hydrophobic activating reagent. Spin-labeled bacteriorhodopsin (2 spins/mole) retained photocycling and proton pumping functions. Accessibility to the paramagnetic broadening agents, $Fe(CN)_6^{-3}$ and $Ni^{+2}$, demonstrated the existence of two distinct spin populations: a highly mobile surface group and a buried immobilized group. A series

of stearic acid spin labels bound to purple membranes showed that paramagnetic interactions of $Fe(CN)_6^{-3}$ were limited to surfaces whereas $Ni^{+2}$ and $Cu^{+2}$ effects extended into hydrophobic domains. A double modification procedure, which first blocked surface groups, selectively spin-labeled only a buried carboxyl group having a strongly immobilized signal. Comparison of the quenching behavior of stearic acid spin labels with this double modified sample indicated that one carboxyl residue is buried about 20 Å from the membrane surface.

In summary, chemical modification and spin-label studies have identified several distinct functional roles for the buried carboxyl residues of BR in the mechanism of the light-driven proton pump. In addition, these studies obtained structural information which supports current models of BR protein structure in the purple membrane.

## DEDICATION

This dissertation is dedicated to Mona and my parents, for all their love and encouragement.

## ACKNOWLEDGEMENTS

TABLE OF CONTENTS

ABBREVIATIONS

AES, 2-aminoethanesulfonic acid

BO, bacterioopsin

BR, bacteriorhodopsin

CD, circular dichroism

CMC, 1-cyclohexyl-3-(2-morpholino-4-ethyl)carbodiimide

EA, ethyl acetimidate

EDC, 1-ethyl-3-(3-dimethylaminopropyl)carbodiimide

EEDQ, N-(ethoxycarbonyl)-2-ethoxy-1,2-dihydroquinoline

EPR, electron paramagnetic resonance

ESR, electron spin resonance

ETC, 1-ethyl-3-(3-trimethylpropylammonium)carbodiimide iodide

GME, glycine methyl ester

HEPES, N-2-hydroxyethylpiperazine-N'-2-ethanesulfonic acid

MES, 2-(N-morpholino)ethanesulfonic acid

NTME, nitrotyrosine methyl ester

PM, purple membrane

SDS, sodium dodecyl sulfate

TA-BR, tempamine-spin labeled bacteriorhodopsin

Tempamine, 4-amino-2,2,6,6-tetramethyl-piperindine-N-oxyl

TRIS, tris(hydroxymethyl)aminomethane

WM, white membrane

5NS, 2-(3-carboxypropyl)-4,4-dimethyl-2-tridecyl-3-oxazolidinyloxyl

10NS, 2-(8-carboxyoctyl)-2-octyl-4,4-dimethyl-3-oxazolidinyloxyl

16NS, 2-(14-carboxytetradecyl)-2-ethyl-4,4-dimethyl-3-oxazolidinyloxyl

## IV. INTRODUCTION

Biological membranes provide barriers that regulate the exchange of materials and information between a cell's internal compartments and the external environment. These membranes are permeable to nonpolar molecules and water, less permeable to polar molecules, and virtually impermeable to charged molecules and ions. However, most membranes include specific proteins that selectively mediate the transport of certain polar solutes and ions. Ion translocation by integral membrane proteins serves several important physiological processes: 1) energy production by the electron transport system of mitochondria, chloroplasts, and bacteria; 2) the maintenance of intracellular pH and ionic composition within a narrow range; and 3) the generation of ionic gradients and ion fluxes essential for nerve and muscle excitability. Of the numerous examples of ion transport proteins, many are large macromolecular complexes composed of multiple subunits, such as the acetylcholine-receptor sodium channel, cytochrome oxidase, and the proton-ATPase/synthase of the electron transport system. Other ion translocators such as the red blood cell Band 3 and $H^+$-ATPase of yeast plasma membrane are single, large polypeptides with molecular weights near 100,000. Only recently, knowledge of the primary sequence of a few of these integral membrane proteins has become available, but the secondary and tertiary structures remain almost completely unknown. At a molecular level, the mechanism by which membrane proteins translocate ions across the membrane remains an unanswered question. In order to gain insight into translocation mechanisms, a simple system where membrane protein structure can be related to function is desirable for study.

The purple membrane of <u>Halobacterium</u> <u>halobium</u> is uniquely suited

as a model system to study ion translocation. It contains only a single protein, bacteriorhodopsin, which utilizes light energy to translocate protons across the membrane. The light-driven proton pump creates an electrochemical gradient across the membrane that can be used by the cells to drive ATP synthesis, as described by Mitchell's chemiosmotic hypothesis. Purified purple membranes can be readily obtained in large quantities from Halobacteria. The protein is a small, single polypeptide of 26,000 molecular weight. Furthermore, its complete primary sequence (Khorana et al., 1979) and three-dimensional structure to 3.7 Å resolution has been determined (Hayward and Stroud, 1981). Thus, bacteriorhodopsin represents the simplest and structurally best defined ion-translocating membrane protein known to date.

This dissertation is a study of the structure-functional relationships of bacteriorhodopsin. Most studies of bacteriorhodopsin have focused mainly on the role of the Schiff-base linked retinal chromophore in the overall mechanism. Much less is known about the involvement of the protein moiety in the photochemical reaction cycle and proton translocation process. Since the complete primary sequence of bacteriorhodopsin is now known, it should be possible to use chemical modification techniques to gain information on the role of specific amino acid residues involved in bacteriorhodopsin function. Chemical modification techniques and spin-labeling have been used in this study to identify the role of the negatively charged amino acid residues of aspartate and glutamate in the structure and function of bacteriorhodopsin.

## V.  BACKGROUND

### A.  Halobacterial Physiology

The Halobacteria occupy a unique ecological niche that is characterized by a highly concentrated or saturated saline condition found in locations such as the Dead Sea, the Great Salt Lake in Utah, and solar evaporative ponds (Lanyi, 1978). They are classified as extreme halophiles since high concentrations of NaCl (3.5-5 M) are required for growth and maintenance of structure. The critical nature of their salt dependence becomes evident when the NaCl concentration is lowered below approximately 2 M: the cells lyse and the cellular components dissociate (Kushner, 1964).

The purple membrane was discovered in 1967 as part of careful investigation of the fragmentation products of H. halobium (Stoeckenius and Rowen, 1967; Stoeckenius and Kunau, 1968). The isolation of purple membranes is based on their stability in the absence of salt, a condition which results in fragmentation of the Halobacterium membranes. Differential centrifugation of the cell lysate yields a fraction containing the red membrane and purple membrane components. The red membrane functions as a typical bacterial cell plasma membrane containing the respiratory chain with b- and c-type cytochromes, and a cytochrome oxidase (White and Sinclair, 1971). The red color is due to an abundant $C_{50}$ carotenoid pigment, bacterioruberin (Kushwaha et al., 1975). The purple membranes can be purified by sucrose-density gradient centrifugation.

The purple membrane forms a discrete, differentiated functional site in the plasma membrane of Halobacteria. Freeze-fracture electron microscopy of whole cells shows oval areas with distinctly smooth and

regular structure that differ from the surrounding red membrane (Blaurock and Stoeckenius, 1971). The isolated purple membrane has the same morphological features as seen in intact cells. It appears in the form of planar sheets with a size corresponding to that of the original patches on the cell surface. There is no evidence for alteration of purple membrane structure as a result of the isolation procedure.

The biosynthesis of the purple membrane was found to be regulated by the $O_2$ concentration in the culture (Oesterhelt and Stoeckenius, 1973). Shifting a culture from growth at high $O_2$ in the dark to low $O_2$ in the light results in a large increase of purple membrane concentration in these cells, while cell number and protein concentration in the culture remain essentially constant (Stoeckenius et al., 1979). Low $O_2$ concentrations were found to not only trigger synthesis, but were necessary for continued formation of purple membrane. The yield of purple membrane from cultures grown in the light was about 6 to 7 times higher than in the dark.

The significance of the $O_2$ regulation is evident from bioenergetic considerations of Halobacteria energy production in its ecological environment. When the $O_2$ concentration in the environment is not limiting, Halobacteria cells use the respiratory chain present in the plasma membrane to generate an electrochemical gradient of protons across the membrane to drive ATP synthesis. However, when $O_2$ levels drop to very low levels, the lack of the terminal electron acceptor shuts down electron transport activity. These conditions induce synthesis of purple membrane, which acts as an alternate system to the respiratory chain to generate a proton gradient across the cell membrane. Fermentation pathways have not been found in Halobacteria containing

purple membranes. Thus, under low oxygen conditions, cells are forced to convert from oxidative phosphorylation to light-energy conversion by the synthesis of a single protein and incorporation of it into the plasma membrane. The simplicity and elegance of this system has played a large role in demonstrating the validity of the chemiosmotic theory of energy coupling advanced by Mitchell (1972).

The $\underline{H.}$ $\underline{halobium}$ strains frequently used for study are derived from a spontaneous mutant isolated by R. Rowen, designated $R_1$ (Stoeckenius $\underline{et}$ $\underline{al.}$, 1979). The $R_1$ strain does not produce gas vacuoles, which makes isolation of the purple membrane easier. A relatively stable mutant strain $R_1S_9$, prepared by nitrosoguanidine mutagenesis from $R_1$ (Stoeckenius $\underline{et}$ $\underline{al.}$, 1979), yields large amounts of purple membranes. A spontaneous mutant, $R_1mW$, isolated from its parent strain $R_1M_1$, lacks pathways for caretenoid synthesis (Matsuno-Yagi and Mukohata, 1980). These cells appear brownish-white since they also lack bacterioruberins and retinal, but contain respiratory enzymes. Addition of all-$\underline{trans}$ retinal converts $R_1mW$ into purple cells. White membrane patches were isolated from these cells by procedures similar to those used for purple membrane. A careful ultrastructural and spectroscopic study by Mukohata $\underline{et}$ $\underline{al.}$ (1981) demonstrated that white membranes are composed of bacterioopsin crystallized in hexagonal arrays. Addition of retinal leads to stoichiometric reconstitution of bacteriorhodopsin and formation of a functional purple membrane. The $R_1mW$ white membranes have advantages as material for use in spectroscopic studies of BR.

B. Purple Membrane Structure

1. Protein and lipid composition

Early experiments establishing the nature of the purple membrane by Oesterhelt and Stoeckenius (1971) showed that purple membranes contained only a single polypeptide. The molecular weight of bacteriorhodopsin is now firmly established to be 26,000 by amino acid analysis and from knowledge of the complete primary sequence. The amino acid compositions determined by several laboratories at an earlier date were found to be in general agreement (Keefer and Bradshaw, 1977). Among the interesting features of these compositions are the absence of cysteine and histidine. The number of negatively charged residues of aspartic and glutamic acid were found to compose approximately 10% (18/248) of the total. These negatively charged residues exceed the 14 positively charged residues of arginine and lysine.

The complete amino acid sequence of bacteriorhodopsin (Fig. 1), which contains 248 amino acids, has been determined independently by Khorana et al. (1979) and Ovchinnikov et al. (1979). The extreme hydrophobicity of the protein required the development of novel techniques for fragmentation and separation of peptides. A combination of reverse-phase HPLC and gel permeation in formic acid/ethanol mixtures was employed to separate cyanogen-bromide generated peptides (Khorana, 1979). Sequence analysis was carried out with the combined use of automated Edman degradation and gas chromatographic mass spectrometry.

The extreme hydrophobicity of bacteriorhodopsin is evident from its amino acid composition. Over 70% of the residues are hydrophobic amino acids, as might be expected for an integral membrane protein. There is significant clustering of both hydrophobic and hydrophilic

Figure 1. Complete amino acid sequence of bacteriorhodopsin according to Khorana et al. (1979).

```
          5                    10                   15                   20 ·                  25
< GLU ALA GLN ILE THR GLY ARG PRO GLU TRP ILE TRP LEU ALA LEU GLY THR ALA LEU MET GLY LEU GLY THR LEU

          30                   35                   40                   45                   50
  TYR PHE LEU VAL LYS GLY MET GLY VAL SER ASP PRO ASP ALA LYS LYS PHE TYR ALA ILE THR THR LEU VAL PRO

          55                   60                   65                   70                   75
  ALA ILE ALA PHE THR MET TYR LEU SER MET LEU LEU GLY TYR GLY LEU THR MET VAL PRO PHE GLY GLY GLU GLN

          80                   85                   90                   95                   100
  ASN PRO ILE TYR TRP ALA ARG TYR ALA ASP TRP LEU PHE THR THR PRO LEU LEU LEU LEU ASP LEU ALA LEU LEU

          105                  110                  115                  120                  125
  VAL ASP ALA ASP GLU GLY THR ILE LEU ALA ILE VAL GLY ALA ASP GLY LEU MET ILE GLY THR GLY LEU VAL GLY

          130                  135                  140                  145                  150
  ALA LEU THR LYS VAL TYR SER TYR ARG PHE VAL TRP TRP ALA ILE SER THR ALA ALA MET LEU TYR ILE LEU TYR

          155                  160                  165                  170                  175
  VAL LEU PHE PHE GLY PHE THR SER LYS ALA GLU SER MET ARG PRO GLU VAL ALA SER THR PHE LYS VAL LEU ARG

          180                  185                  190                  195                  200
  ASN VAL THR VAL VAL LEU TRP SER ALA TYR PRO VAL VAL TRP LEU ILE GLY SER GLU GLY ALA GLY ILE VAL PRO

          205                  210                  215                  220                  225
  LEU ASN ILE GLU THR LEU LEU PHE MET VAL LEU ASP VAL SER ALA LYS VAL GLY PHE GLY LEU ILE LEU LEU ARG

          230                  235                  240                  245
  SER ARG ALA ILE PHE GLY GLU ALA GLU ALA PRO GLU PRO SER ALA GLY ASP GLY ALA ALA ALA THR SER
```

∞

residues. The presence of long sequences (20 amino acids) of hydrophobic residues may create membrane-inserted segments through favorable thermodynamic considerations (Engelman, 1982). This may be a general property integral membrane proteins utilize to incorporate and stabilize buried membrane sequences.

Studies of the lipid composition of purple membranes from H. halobium have identified an unusual polar lipid content. Kushwaha et al. (1975) found that polar lipids constitute 90% of the total lipids, and has shown them to be derivatives of a glycerol diether, 2,3-di-0-phytanyl-sn-glycerol. The lipid content expressed as the respective contribution to the total lpid is as follows: phosphatidyl-glycerophosphate (49%), phosphatidylglycerol (5%), triglycosyl diether (15%), and several neutral lipids, largely squalenes (22%). In addition, two sulfolipid components, phosphatidylglycerosulfate (4%) and glycolipid sulfate (10%), are found exclusively in the purple membrane. Examples of structures of the major lipid components are shown in figure 2. The unusual dihydrophytol chains are saturated branched chain hydrocarbons. It has been suggested that the additional methyl groups on the straight chain may prevent undesirable close packing of the lipids in the membrane.

Chemical analyses of the purple membrane shows that it contains 75% protein and 25% lipid on a weight basis - a very high ratio of protein to lipid (exclusive of retinal). It has been calculated that there are 7 lipids per molecule of bacteriorhodopsin, of which 6 are polar lipids (Kates et al., 1982). One consequence of the highly polar lipid composition and its close association with the protein is the resultant high density of negative charge at the membrane surface.

Figure 2.  Major lipid components of H. halobium purple membrane.

    a)  Phosphatidylglycerophosphate composes 49% of the total lipids.

    b)  Glycolipid sulfate composes 10% of the total lipids; Glc =

glucose, Man = mannose, Gal = galactose.

A.

B.
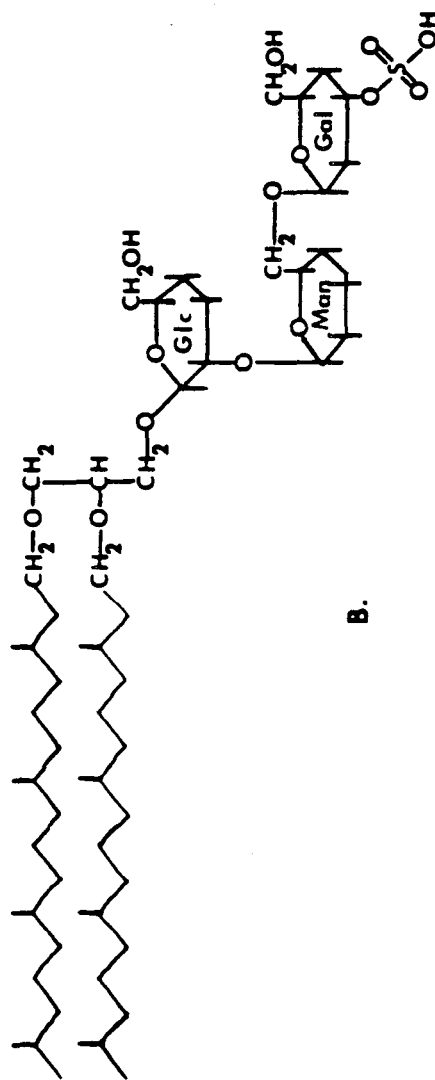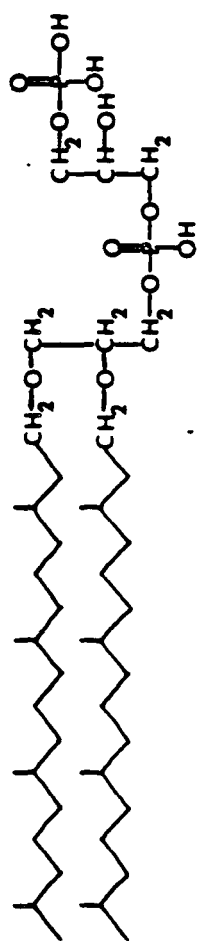
XBL 832-8069

## 2. Arrangement of protein in a hexagonal crystal lattice

X-ray diffraction patterns obtained by Blaurock and Stoekenius (1971) first demonstrated the unusual regular arrangement of the protein and lipid components in a well-ordered hexagonal crystal lattice. Additional x-ray observations from oriented multilayers showed that the hexagonal lattice existed in a plane parallel to the membrane, and that the thickness of the membrane was 49 Å. From the lattice parameters, the membrane density, the ratio of lipid to protein, and molecular weight of BR, it was calculated that each unit cell of 63 Å contained 3 protein molecules. The packing arrangement of 3 molecules per unit cell is described by the crystallographic space group P3 (Blaurock, 1975, Henderson, 1975). This means that BR is in clusters of three, oriented about a three-fold axis at the center of each of the clusters, with the symmetry axis perpendicular to the plane of the membrane. As seen in figure 3, this has been termed a BR trimer.

The main feature of the diffraction pattern suggested a structure for BR that is composed largely of $\alpha$-helices arranged perpendicularly to the plane of the membrane and extending across its width. Ultra-violet circular dichroism measurements give a 73% $\alpha$-helix content when corrected for light-scattering distortions (Long et al., 1977).

## 3. Three-dimensional $\alpha$-helical model

Henderson and Unwin (1975) directly determined the three-dimensional structure of the BR polypeptide by novel electron diffraction techniques. They obtained a 7 Å resolution map and proposed that BR contains seven, closely packed $\alpha$-helical rods about 40 Å long, and with a center-to-center distance of 10 Å that extended across the membrane (Fig. 3). The three helices (on the interior side of the

Figure 3.   Projected structure of purple membrane at 7.1 Å resolution

obtained from an electron diffraction image.   Center-to-center

spacing is ˜ 62 Å.   Three BR monomers are delineated.

Figure from Hayward et al. (1978).
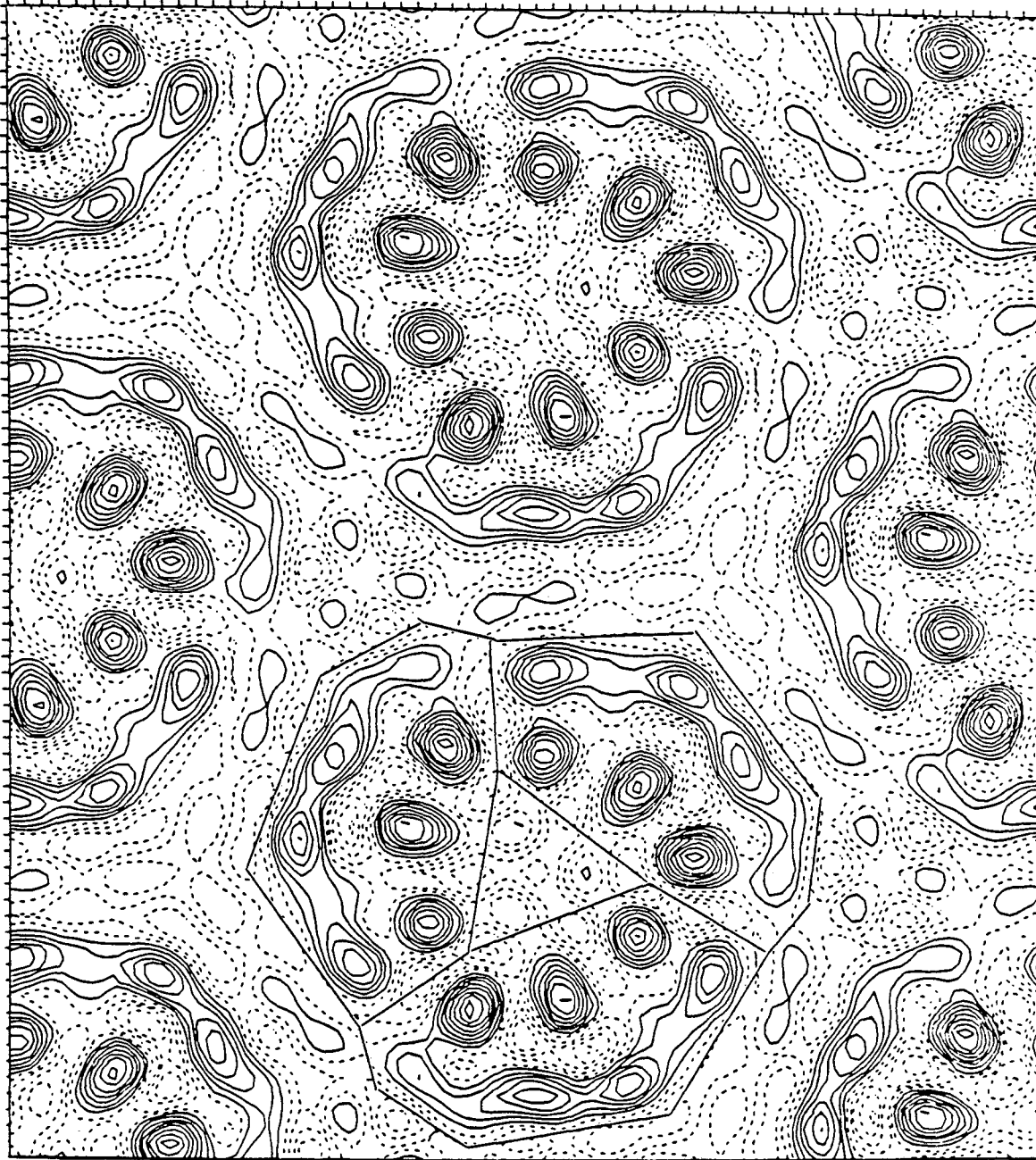
trimer) were almost exactly perpendicular while the outer four were tilted at angles from 10° to 20° from the perpendicular plane. A subsequent study (Agard and Stroud, 1982) applied an iterative Fourier refinement procedure to the data of Henderson and Unwin (1975). The refined model showed helices 45 Å thick that extended to both membrane surfaces. In addition, linking regions between helices were revealed: three on the extracellular surface and one on the cytoplasmic surface. The projected structure of BR determined to 3.7 Å resolution has been obtained by low temperature electron microscopy (Hayward and Stroud, 1981). At this resolution, which approaches the resolution limit of the electron microscope, the amino acid side chains of the protein are not resolved. However, new features resolved in the 3.7 Å map are the possible identification of the retinal chromophore between helices 4 and 6 and the location of the lipids on one side of the bilayer; three at the trimer center and four per monomer in the interstitial region.

Although 70-80% of the polypeptide is embedded in the membrane, specific sites of cleavage by proteolytic enzymes have identified helix linking segments and other surface structures. A small region at the carboxyl terminus of 1500 molecular weight is cleaved by trypsin and pronase (Gerber et al., 1977; Huang et al., 1980). The released water-soluble 15 amino acid peptide has been termed the "C-terminal tail." An additional site becomes available for cleavage by trypsin in the apoprotein, which creates two fragments of 19,700 and 6,300 molecular weight. The orientation of BR in the purple membrane was determined by comparison of proteolysis patterns of purple membrane sheets, reconstituted vesicles, and whole cells. It was found that

the carboxyl terminus faces the cytoplasmic side, and the blocked amino terminus faces the extracellular surface (Gerber et al., 1977).

### 4. Identification and position of the retinal chromophore

One molecule of retinal bound to an ε-amino group of a lysine residue by a Schiff base linkage is the BR chromophore (Oesterhelt and Stoeckenius, 1971). The structure of the retinyl-lysine chromophore is shown in figure 4. Bridgen and Walker (1976) determined that Lys-41 was the attachment site of retinal. However, this result now conflicts with the assignment from later investigations. Recent re-examination of the retinal attachment site by several groups (Bayley et al., 1981; Lemke and Oesterhelt, 1981; Katre et al., 1981) found that retinal is primarily linked to Lys-216 on helix G. Absorbance and circular dichroism spectra indicate that the retinyl residue is in its original binding site after reduction in the light. These findings place the Schiff base linkage in the seventh α-helical trans-membrane rod that directly connects the carboxyl terminal tail.

The protein bound retinal is responsible for the deep purple color of the membrane. The absorption spectra of BR shows a large peak at 570 nm ($\varepsilon_{570} = 63,000$ $M^{-1}cm^{-1}$), a broad band in the 300-500 nm range, and a sharp peak at 280 nm ($\varepsilon = 75,000$ $M^{-1}cm^{-1}$). The 280 nm peak, typical of most proteins, is primarily due to the 11 tyrosine and 8 tryptophan residues of BR. The bands in the visible spectra disappear when retinal-protein interactions are destroyed. Denaturation of the protein with charged detergents, SDS and CTAB, shifts the 570 nm absorption band to 370 nm. Chemical bleaching of BR by reaction with hydroxyl-amine under strong illumination forms retinaloxime ($\lambda_{max} = 360$ nm) and an apomembrane lacking a visible absorption band. Addition of

Figure 4.   Structure of the Bacteriorhodopsin Chromophore.

Retinal forms a Schiff base linkage with the $\varepsilon$-amino group of
the Lys-216 residue in BR.   The retinal configuration and protonation
state of the Schiff base are shown for $BR_{570}$ and the $M_{412}$ intermediate.

# BR~570~

all-trans retinyl-lysine
protonated Schiff base
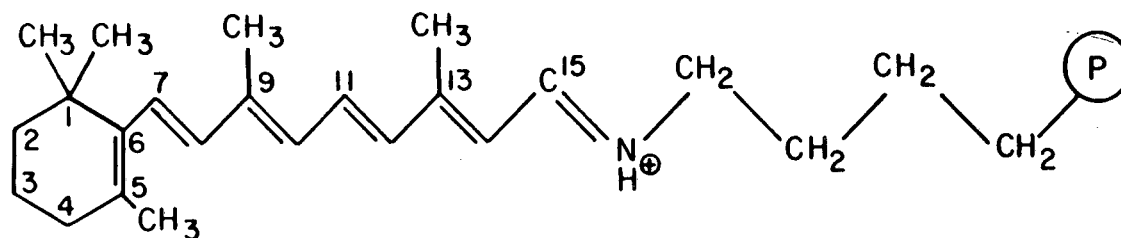


# M~412~

13-cis retinyl-lysine
unprotonated Schiff base



XBL 833-76

18
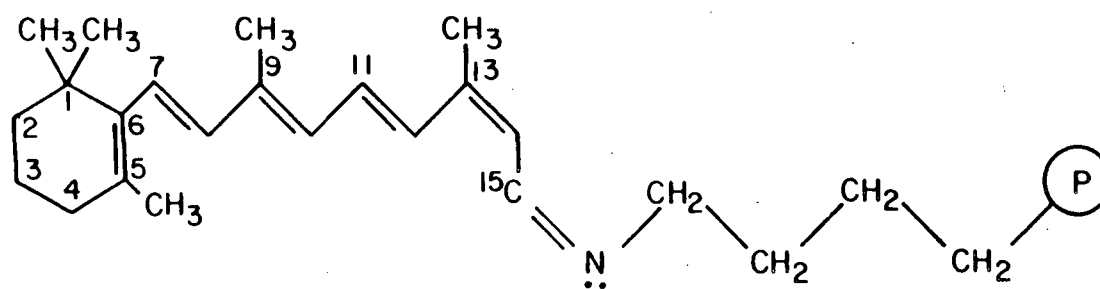
stoichiometric amounts of all-trans retinal to the apomembrane regenerates the characteristic purple complex.

The position of retinal polyene chain in BR has been investigated by several approaches. Linear dichroism at 570 nm of oriented purple membrane multilayers yielded an angle of 23.5 ± 2°, inclined from the plane of the membrane (Bogolmoni et al., 1977). The transmembrane location of retinal in purple membranes was determined by low-angle neutron diffraction studies (King et al., 1979). Membranes were bleached and regenerated with deuterated and with hydrogen containing retinal. The determination of position is based on the large differential neutron scattering power of protonated and deuterated retinal The difference map indicated the β -ionone ring was located approximately 17 Å from the membrane surface.

### C. Function of the Purple Membrane

#### 1. A light-driven proton pump

The purple membrane functions as a unique light-energy converter by pumping protons across the membrane. The electrochemical gradient of protons is then used by the cell to drive ATP synthesis, as postulated by Mitchell's chemiosmotic hypothesis (Mitchell, 1972). Experimental support of this idea came from experiments that showed a correlation between light-driven ATP synthesis and increases in the pH gradient and membrane potential of cells (Michel and Oesterhelt, 1976,1980). It was found that light induced a large increase in the total proton motive force of the cells. Photophosphorylation exhibited an action spectrum that exactly overlapped the absorption spectrum of BR (Hartmann and Oesterhelt, 1977). They also found a direct, linear correlation between the rate of photophosphorylation and BR content of the cells.

The major component of proton motive force was partitioned between the membrane potential or the pH gradient, depending on the initial external pH value.

The functional role of purified BR in establishing a proton motive force was elegantly demonstrated by Racker and Stoeckenius (1974). They showed uncoupler sensitive, light-dependent ATP synthesis in lipid vesicles reconstituted with mitochondrial ATPase and purple membranes. An number of elaborate studies have since shown that purple membrane sheets incorporated into liposomes establish a pH gradient and membrane potential by pumping protons to the vesicle interior. Proteolytic experiments show almost all BR (95%) is oriented with the cytoplasmic surface facing the liposome exterior (Gerber et al., 1977; Huang et al., 1981). The functional significance of the two-dimensional hexagonal lattice of structure of PM has been explored by performing proton pumping measurements in a lipid vesicle system. By changing the temperature from below the lipid phase transition to above, the state of BR aggregation can be altered in a reversible manner from aggregated to monomeric (Cherry et al., 1978). The results obtained by Dencher and Heyn (1979) show that monomeric BR itself is able to pump protons, most probably with an efficiency not significantly different from that of BR in the hexagonal array.

The role of the unusual purple membrane lipids in BR function has been examined. A detergent solubilization procedure was developed by Huang et al. (1980) that resulted in a BR preparation 99% free from endogenous lipid. The delipidated BR was then reconstituted with different phospholipids by the cholate dialysis method. The reconstituted vesicles all showed light-dependent proton translocation. The direction

of proton translocation in these vesicles was from outside to inside, as previously found for vesicles prepared directly from PM sheets. It is clear that the native PM lipids are not essential for proton pumping activity of the BR protein.

## 2. Photochemical reaction cycle of BR

Light initiates a photochemical reaction cycle in BR that involves configurational changes in retinal, as well as protein conformational changes. The photochemistry of BR has been extensively studied using laser flash photolysis at both low (-80 to -170°C) and room temperatures. It was first proposed that the results fit a linear, unidirectional reaction sequence composed of six intermediates: $BR_{570}$ (ground state), $K_{590}$, $L_{550}$, $M_{412}$, $N_{520}$, and $O_{640}$; denoted by their absorption maxima as shown in figure 5 (Lozier et al., 1976). Only the first reaction, $BR_{570} \rightarrow K_{590}$ (half-life < 10 ps), requires absorption of a photon, while the formation and decay of the other thermal intermediates proceeds in the dark. At room temperature, after absorption of a photon, BR passes through all reaction cycle intermediates to reform the $BR_{570}$ species within 10 msec. Branched pathways have also been suggested, one of which proposes that M converts both directly and via the $O_{640}$ intermediate to $BR_{570}$ (Sherman et al., 1976). These alternative photoreaction cycle proposals must be regarded critically since the resolution of the kinetic data for the reaction pathway requires extensive data collection and mathematical analysis.

The proton pumping function of the purple membrane is linked to the photochemical reaction cycle. The kinetics of the release and uptake of protons from purple membrane sheets, purple membrane reconstituted vesicles, and whole bacterial cells has been measured

Figure 5.  Photochemical Reaction Cycle of BR.  The light-adapted
photochemical cycle of $BRL_{570}$ is shown illustrating lifetimes
for the intermediates, the protonation state of the Schiff
base, the retinal configuration and proton release and uptake
from the purple membrane.

# Photoreaction cycle of bacteriorhodopsin



(X) $\longrightarrow$ 610

h$\nu$

37 msec

BRD$_{560}$

(13 – cis – all – trans = 1:1)

in the light    in the dark

Dark cycle

Light cycle

< 10 ~ 12 psec

BRL$_{570}$

$\oplus$

$-C=N-$
    |
   H

(all trans)

h$\nu$

~ 5 msec

O$_{660}$
(640)

K$_{590}$
(610)

2 ~ 5 $\mu$sec

~ 3 msec

N$_{520}$

L$_{550}$
(540)

~ 1 msec

M$_{412}$

50 ~ 300 $\mu$sec

$-C=\ddot{N}-$
(13 cis ?)

H$^+$

H$^+$
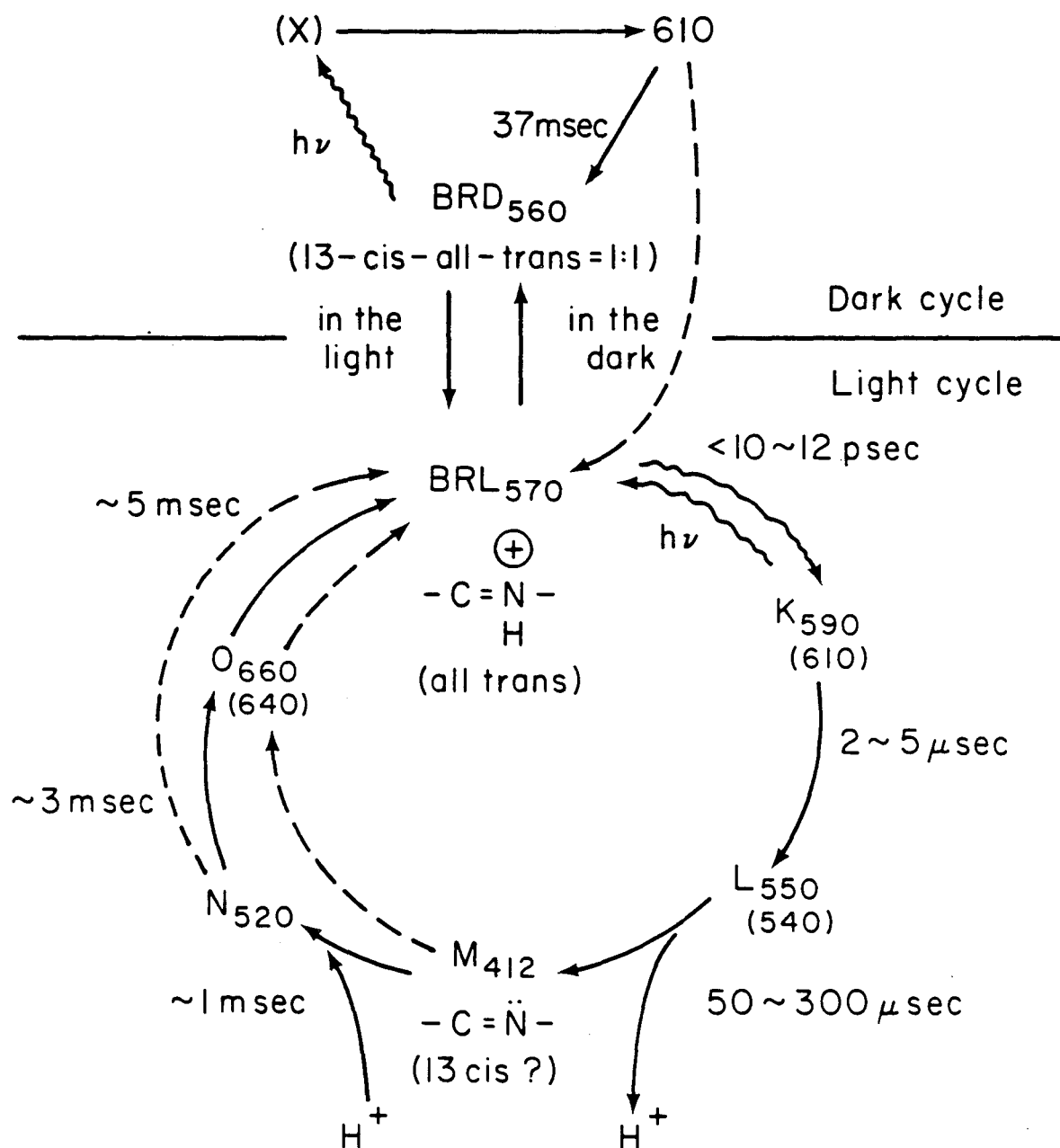
XBL 7811-12582

using a pH-sensitive dye and single turnover light flashes (Lozier et al., 1976; Govindjee et al., 1980). The release of a proton(s) from the membrane occurs subsequent to $M_{412}$ formation ($t_{1/2}$ = 0.8 - 1.5 msec), and rebinding occurs with kinetics almost identical to the decay of $M_{412}$. It was found that at low ionic strength the strength of the $H^+/M_{412}$ ratio is about 1, while at high salt concentrations the ratio is almost 2. However, the variable stoichiometry of protons released by light may be merely a reflection of the methodology employed, since the sensitivity of indicator dyes or buffer can be influenced by surface charge. Regardless of the proton pumping stoichiometry, it is clear that proton release occurs from the extracellular PM surface and uptake from the cytoplasmic surface. The parallel kinetics between the $M_{412}$ photocycle intermedate and observed pH changes strongly link the two processes in the mechanism of the proton pump.

The effect of ionic strength on the steady-state light-induced release of protons from purple membrane sheets has been investigated by Renthal (1981). He found that the steady state value of proton release increased by a factor of four between 0.015 and 0.5 M NaCl. Divalent cations ($Ca^{+2}$, $Mg^{+2}$) had a similar effect at much lower concentrations. Both the charge and concentration effects of salt can be explained by considering the presence of surface charge on the purple membrane. A negative surface charge will result in a surface potential, $\psi$, that attracts cations to the membrane surface in the diffuse double layer.

The cation concentration near the membrane surface, $C_m$, is greater than the bulk solution concentration, $C_b$, by an exponential factor (McLaughlin, 1977):

$$C_m = C_b \exp (- \psi F/RT)$$

where F = Faraday's constant, R = the gas constant, and T = absolute temperature. At low ionic strength, the effect will be to diminish the concentration of protons released in bulk solution ($C_b$), since some ions will remain in the diffuse double layer at the membrane surface. The results obtained by Renthal (1981) show that the Gouy-Chapman Theory quantitatively accounts for the effect of salt on light-induced changes in $H^+$ binding.

### 3. Retinal configuration during the photocycle

It has been suggested that a trans/cis isomerization of retinal is a key event in proton pumping. Extraction experiments has shown that the light-adapted form of $BR_{570}$ contains an all-trans isomer of retinal (Oesterhelt, 1973; Pettei et al., 1977). Similar extraction experiments of a stabilized $M_{412}$-intermediate showed almost complete conversion to 13-cis-retinal (Pettei et al., 1977). The configuration of retinal has also been determined by resonance Raman spectroscopy of the purple membrane and its photochemical intermediates. The advantage of Raman spectroscopy is that is provides an in situ probe of retinal configuration, whereas isomerization may occur during chemical extraction. Resonance Raman spectroscopy produces a frequency spectrum of the vibrational modes of the absorbing chromophore, with only minor contributions from the protein to which it is linked. Spectra of samples with specific isotopic substitutions have confirmed that light-adapted $BR_{570}$ contains the all-trans isomer and that the $M_{412}$ intermediate is 13-cis (Braiman and Mathies, 1980).

Resonance Raman has also been utilized to determine the protonation

state of the retinal-lysine Schiff base linkage. Lewis et al. (1974)
analyzed the stretching frequencies of the purple membrane Schiff base
in $H_2O$ and $D_2O$, and concluded that the $BR_{570}$ retinylidine-lysine linkage
is protonated, but unprotonated in the $M_{412}$ intermediate. Subsequently,
time-resolved resonance Raman spectroscopy (Terner et al., 1979) of
purple membranes determined that deprotonation of the Schiff base
occurs between $L_{550}$ and $M_{412}$, and that reprotonation occurs during
the $M_{412}$ to $O_{640}$ transition.

### 4. Protein conformational changes associated with photocycling activity

It is likely that conformational changes in the BR protein that are
intimately linked to intermediates of the photocycle are directly
involved in the proton pumping mechanism. However, the magnitude and
localization of these postulated structural changes is subject to
debate. Recently, x-ray diffraction studies of photocycle interme-
diates have been initiated. Although these studies are preliminary,
they indicate that major changes are not associated with the M inter-
mediate (Stamatoff et al., 1982; Frankel and Forsyth, 1982). These
observations are not surprising since: (1) spectral changes in the
retinal-protein chromophore may reflect very small structural changes
in the immediate chromophore environment, and (2) the purple membrane
is a rigid crystalline lattice in which BR possesses no protein rota-
tional mobility (Cherry et al., 1978) and the lipids are strongly
immobilized (Chignell and Chignell, 1975).

Low temperature spectroscopy has been used to trap photocycle
intermediates and to examine their ultraviolet absorption spectra.
The most striking changes were observed in the $BR_{570}$ - $M_{412}$ difference

spectra (Becher and Ebrey, 1977) which showed a decreased absorbance
at 280 nm. This can be explained by transient transfer of 50% of the
aromatic residues from a non-polar protein interior to a polar media
or by changes in orientation of originally interacting amino acids.

Time-resolved changes in protein fluorescence correlated with
photocycle intermediates have also been made by several groups
(Bogomolni et al., 1978; Fukumoto et al., 1981). Since the fluorescence
of proteins is generally thought to be dependent on the immediate
environment of the aromatic residues, the changes in fluorescence were
interpreted as evidence for light-dependent conformational changes.
Significant decreases in fluorescence intensity were observed that
correlated strongly to the $L_{550}$ and $M_{412}$ intermediates of the photocycle.
The remaining intermediates ($K_{610}$, $N_{520}$, and $O_{640}$) did not significantly
alter the protein fluorescence intensity from that of the initial $BR_{570}$
level. Bogomolni et al. (1978) also observed that CsCl specifically
quenched fluorescence at 350 nm and eliminated a large part of the
light-induced fluorescence change. Significant decreases in bacterio-
rhodopsin fluorescence occur exclusively in the $L_{550}$ and $M_{412}$ inter-
mediates, and closely follow the kinetics of $M_{412}$ intermediate.
The results may imply that intimate tryptophan and/or tyrosine charge
interactions with retinal change during the formation and decay of the
$M_{412}$ intermediate. Alternatively, deprotonation of 1-2 tyrosines
or charge perturbation of 1-2 tryptophans could account for the fluor-
escence changes. Evidence from chemical modification studies demon-
strates that tryptophan is necessary component of the BR chromophore
structure and required for photocycling activity (Konishi and Packer,
1977).

Chemical cross-linking of BR lysine residues by bifunctional imidoesters was carried out to determine the importance of protein movement during photocycling. Konishi et al. (1979) found that mono-functional agents, methyl acetimidate (3.0 Å) and methyl butyrimidate (6.8 Å) which reacted with 80% of the ε-amino groups had no effect on $M_{412}$ decay kinetics. However, the reaction of the bifunctional reagents, dimethyl adipimidate (8.3 Å in length) and dimethyl suberi-midate (11.2 Å), resulted in extensive dimer and trimer formation; as well as higher molecular weight oligomers due to cross-linking. The bifunctional treated purple membranes had slower $M_{412}$ decay kinetics, but still photocycled. The results indicate that protein conformational changes are small since intermolecular cross-linking had little effect on activity and that cooperative interactions between individual molecules are not significant for photocycling or proton pumping activity.

### 5. Changes in the protonation state of the BR protein

Spectroscopic methods for the determination of the protonation state of BR during the photocycle have been described for steady-state and transient-state conditions. The method relies on the intrinsic absorption changes of tyrosyl and tryptophanyl residues that reflect the protonation state and environment of these residues. Steady-state light-dark difference spectra show an absorption increase with a maxi-mum centered at 296 nm and a decrease centered at 275 nm (Hess and Kuschmitz, 1979). The kinetic measurements show that formation of the 275 nm and 295 nm specie(s) slightly precedes $M_{412}$ formation and almost coincide with $M_{412}$ decay. Linear dichroism values are high at 275 nm and 412 nm, but low at 295 nm. These results have been

interpreted as indicating either the deprotonation of 2-tyrosines or the deprotonation of one tyrosine and the charge displacement of 2 tryptophans.

The role of the tyrosyl residues in the photocycle of BR was also investigated by chemical modification of these residues by iodination (Scherrer et al., 1981). It was found that modification of a tyrosyl residue accelerated $M_{412}$ formation, whereas modification of another type of tyrosine residue(s) inhibited $M_{412}$ decay. The pH-rate profile for $M_{412}$ decay was shifted to a lower pK characteristic of the lower pK's of mono- and diiodotyrosine. The effect of iodination on $M_{412}$ kinetics strongly supports the hypothesis that reversible deprotonation of tyrosine residues prior to, and after $M_{412}$ formation in the photocycle, are steps in the proton translocation pathway of BR.

Proton transfer steps in the photoreaction cycle have also been identified by analyzing deuterium isotope effects on BR photocycle kinetics. It was found that rates of formation ($k^H/k^D = 5$) and decay ($k^H/k^D = 2$) of $M_{412}$ were strongly affected. The $O_{640}$ intermediate was also found to exhibit a small isotope effect -- $k^H/k^D = 2$ for rise and decay (Sherman et al., 1976; Lozier and Niederberger, 1977). Sullivan et al. (1980) found that group-specific chemical modification of either lysines, carboxyls, tyrosines, or arginines did not substantially alter the value of the isotope effects, even though the decay kinetics of $M_{412}$ had changed by two orders of magnitude in some cases. This indicates that the basic mechanism for the formation and decay of $M_{412}$ is unaltered by these chemical modifications.

D. Chemical Modification

1. Application to the study of structure-function
   relationships

Proteins are complex organic molecules to which an unique linear

amino acid sequence imparts a unique folding pattern for the polypeptide

in three dimensions. The function of a protein is in turn intimately

related to its precise three-dimensional structure. A large portion

of existing information concerning the chemical basis of enzyme function

has been obtained through chemical modification techniques. Identifi-

cation of groups essential for activity by chemical modification can

lead to a picture of the protein's catalytic mechanism. However,

there are several problems which must be overcome for unambiguous

interpretation of protein inactivation data. To directly correlate

the modification of a group with an effect on enzyme function, it is

essential to exclude the possibility that the modification has caused

a structural change in the protein. Harsh or extensive reaction

conditions are particulary likely to bring about undesired changes.

When a change in activity accompanies a modification of a single residue,

conformational changes are less likely to be responsible. On the

other hand, if chemical modification has no effect on the properties of

interest, it is reasonable to assume the modified residues are not

essential for activity.

In chemical modification studies, it is essential to determine

which amino acids have been modified, and the extent of modification.

This can be a formidable task for a large protein containing multiple

residues of the same type. Amino acid analysis may be used to determine

the stoichiometry of the reaction for some modifications. Alternatively,

if the modified residues are labeled (radioactive, fluorescent, etc.),

the physical properties may be directly monitored to obtain accurate quantitation. Another problem encountered with group-specific modification is "random" modification of sites with fractional occupancy. This may occur when several groups have similar reactivity. For example, the average degree of modification may be one per molecule; while the distribution of modification may be: 30% unmodified, 40% one group modified, 20% two groups modified, and 10% three or more groups modified. The problem of modification heterogeneity can only be resolved by amino acid sequencing procedures recently developed by Khorana et al. (1979) or Lemke and Oesterhelt (1981), although these are not routinely employed procedures at the present time. The particular problems described above are difficult to resolve, and this first chemical modification study of carboxyl residues has not defined all of these issues. However, these problems may be resolved by further work.

## 2. Site-specific modification

The general objectives for using site-specific modification to study native bacteriorhodopsin include: (1) the identification of amino acid residues at the active site involved in the catalytic mechanism and, (2) the introduction of physico-chemical reporter groups such as chromophoric, fluorescent, or spin-labeled probes to study protein topography. The site-specific modification of a native protein is not a routine procedure and its results cannot be guaranteed, even if the three-dimensional structure of the protein is already known. There are two approaches to achieve site-specific modification of a protein: modification with group-specific reagents and affinity labeling.

Affinity labels are designed to be structurally similar to known substrates, inhibitors, or ligands. This structural similarity directs

the label to a specific site and imparts a high probability of a tight-
interaction prior to covalent attachment. The use of affinity labels
as opposed to functional group modification may sometimes be advantageous.
However, several drawbacks to this route are: (1) the time-consuming
synthesis of the label, (2) an amino acid labeled by affinity reagent
must be in the vicinity of the active site, but it may not necessarily
be involved in catalysis, (3) the reactive group used for covalent
attachment usually does not exhibit protein side-chain specificity.

In the case of bacteriorhodopsin, the use of the affinity label
approach is limited to analogs of retinal. The "substrates" of BR,
light and protons, are not amenable to the synthesis of photoaffinity
derivatives. The photoaffinity label, 3-diazoacetoxyl derivative of
retinal was synthesized and was found to reconstitute a 525 nm absorbing
species when combined with bacteriorhodopsin (Balogh-Nair et al., 1981).
The properties of the 525 nm chromophore and the site of the photolabel
group interaction with the protein are currently unknown. In a recent
study, Huang et al. (1983) used a photosensitive m-diazirinophenyl analog
of retinal that bound to Lys-216 and regenerated a chromophore with a
$\lambda_{max}$ = 470 nm. Photolysis generated a cross-link between the retinal
analog and residues Ser-193 and Glu-194. Photoaffinity labeling with
modified retinals might lead to identification of amino acids involved
in the binding between the chromophore and apoprotein.

Group-specific reagents may also achieve site-specific modification
due to different relative reactive properties of a given side-chain.
The specificity is a consequence of the native protein's ability to
impose a unique chemical environment on a given amino acid. Differen-
tial reactivity of amino acid-side chains of a particular kind can be

due to some of the side-chains being "buried" and shielded from the
aqueous phase. However, it also depends on the size and polarity of
the reagent; small hydrophobic reagents are much more likely to
penetrate into membrane-inserted protein domains and react with groups
distant from the surface. Buried residues often have reduced reactivity
and only become accessible to modification when the protein is completely
denaturated (Means and Feeney, 1971). This factor emerges as a major
problem in chemical modification of completely integral membrane proteins
such as bacteriorhodopsin.

It is important to emphasize that site-specific modification of a
protein is a kinetic phenomenon that results from the protein's ability
to alter the reaction under one clearly defined condition of pH, ionic
strength, and temperature. Many of the reactive side chains can exist
in both a protonated or unprotonated form having vastly different
chemical properties. Of specific consideration to membrane protein
modification is the effect of the electrostatic surface potential on
the surface concentration of protons. Variation in pH often can be
used to control the course of modification reactions.

### 3. Reporter groups

Information about the local environment of particular groups in
proteins may be obtained by attaching to the protein small molecules
with characteristic spectra which are sensitive to changes in environment.
The reporter groups may be chromophores, fluorophores, or spin labels.
Ideally, only one reporter group should be introduced into each protein
molecule for easily interpretable results and the group should not change
the structure of the protein. With all probe techniques that involve
the use of an extrinsic reporter group, it is essential to anticipate

and evaluate the effect of that group on the structure and function of the protein under study.

Chromophoric groups whose spectral properties are sensitive to the environment were first termed reporter groups by Burr and Koshland (1964). The spectra of a reporter group covalently linked to protein will respond to changes in the pH or the polarity of their environment, and in this way act as internal monitors of protein structure. Reporter groups are well-suited to monitor protein conformational changes that result from denaturation, or ligand binding, as well as providing dynamic information on changes occurring during protein activity.

Nitroxyl radicals (spin labels) exhibit a number of chemical and physical properties that make them extremely useful molecules for studying biophysical properties of biological systems. Chemical modification techniques have been developed to attach spin labels to proteins. This allows one to employ electron paramagnetic resonance (EPR) spectroscopy to study the environmental properties of proteins in the vicinity of the covalently bound spin label. A spin label in free aqueous solution shows a characteristic sharp three-line spectrum (arising from interaction of the unpaired electron with the nitrogen nucleus), which primarily reflects the relative rotational freedom of the nitroxide group. When the motion of the group becomes anisotropic due to restricted rotation, the spectrum is broadened and asymmetric (Fig. 6). This restricted motion may occur in solutions of high viscosity, or when the spin-label is bound to a protein. Properties other than motional constraints, such as orientation of the spin label and polarity of the environment may also contribute to the EPR spectrum. In addition, spin label interactions with reducing agents or paramagnetic

Figure 6. Simulated Electron Spin Resonance Spectra of a Nitroxide Radical Illustrating Spectral Changes Associated with the Different Rotational Correlation Times ($\tau_c$).

The spectra correspond to a range of motion from rapid ($\tau_c = 1 \times 10^{-11}$ s) to slow ($\tau_c = 10^{-7}$ s) in which conventional EPR is capable of detecting motion. Figure from Mehlhorn and Keith (1972).
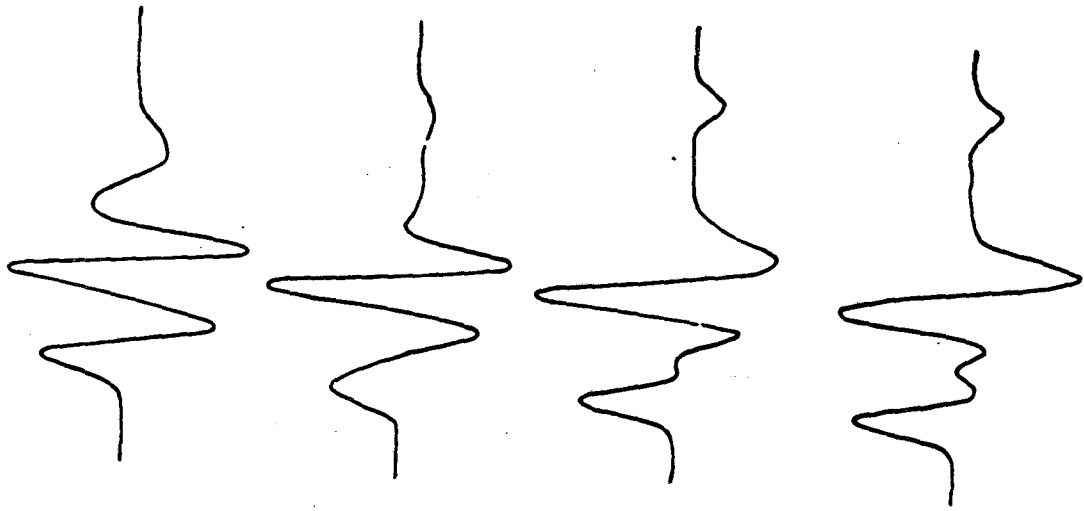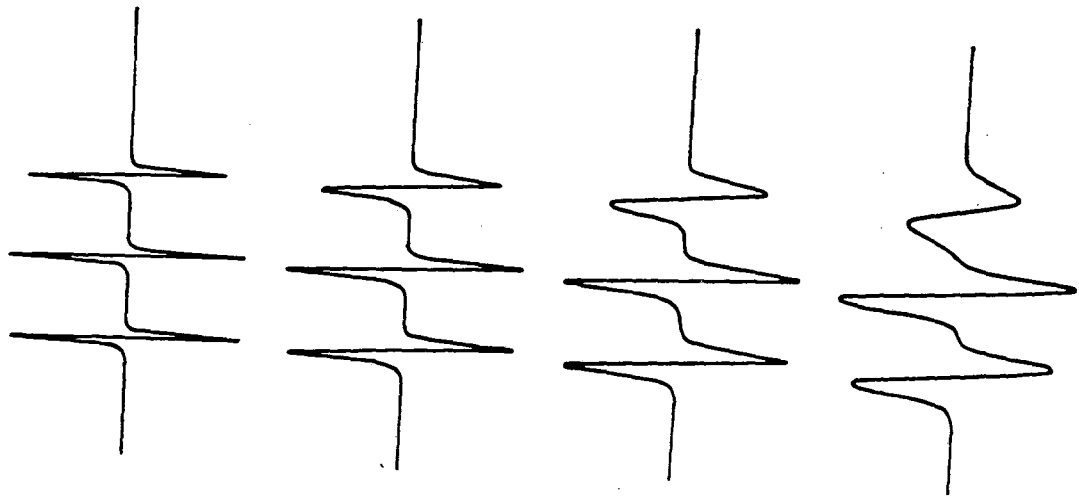
ions can be used to probe protein microenvironments. The information obtainable from spin-labeled proteins is extremely vast and Morrisett (1976) and Likhtenshtein (1976) have provided expert summaries.

### E. Postulated Roles of Carboxyl Residues in Bacteriorhodopsin

#### 1. Structural: Ion-pair formation

One consideration that must be addressed in the arrangement of the BR polypeptide in the purple membrane is the distribution of charged amino acid residues between the hydrophobic membrane environment and the polar surfaces. The folding pattern was largely determined by structural constraints given by the length of the seven $\alpha$-helices, proteolytic cleavage points, chemical modification data and energy calculations. Given these constraints, all models to date (Engelman et al., 1982; Agard and Stroud, 1982; Huang et al., 1983) place several aspartic and glutamic amino acid residues within the hydrophobic membrane phase, although the majority of such residues have been placed at the cytoplasmic and extracellular membrane surfaces. This distribution is also based on the generalization that it is energetically not favorable to bury single charged residues in the low dielectric environment of the membrane. An earlier model of Engelman et al. (1980) placed nine charged residues sufficiently far from the membrane surface to be considered buried. Engelman attempted to remedy the energetic problem this posed by burying all charges as "self-neutralizing" ion-pairs. The requirement that buried charges form ion-pairs was subsequently employed as an important criterion in selecting among models meeting other criteria.

The insertion of a charged ion from the aqueous medium ( $\epsilon_{water}$ = 80) into the membrane phase ( $\epsilon_{hydrocarbon}$ = 2) is extremely unfavorable due to a large change in electrostatic energy. The free energy

difference is described by the Born charging energy and has been calcu-
lated by Parsegian (1969) for several models including the case of
charge-pairing. Calculations showed that the energy cost for burying
an ion-pair is equal to the transfer energy of a single charge, about
40 kcal/mole. This value may be less if the dielectric constant of
the polypeptide is higher, as has been measured for $\beta$-sheet structure
( $\varepsilon = 20$). Thus, although the energy cost is indeed minimized by
ion-pairing of buried charges, the number of such groups is expected
to be small due to large energy changes involved.

Clearly, an ion-pair buried in the membrane could be an important
force in stabilization of the BR structure. Consequently, the separation
of charges due to conformational changes in BR during the photocycle
may represent a method to store the energy of photon in the protein.
The transient separation of a carboxyl-lysine or carboxyl-arginine ion
pair could play a role in the photocycle mechanism.

### 2. Chromophoric: Interactions with retinal and the Schiff base

Protein-chromophore interactions are thought to account for the
red-shift in the absorption maximum of the BR chromophore. Retinal
itself absorbs light maximally at about 380 nm, and thus interactions
with the bacteriorhodopsin protein must shift the absorption to 570 nm.
The factors that determine the spectroscopic properties of polyenes
such as retinal are well understood in model systems. It appears to be
a general principle that long-wavelength absorption is correlated with
increased electron delocalization and decreased single-bond alteration
(Callender and Honig, 1977). Protonation of the Schiff base of retinal
in solution results in a red-shift to 450 nm. This is due to the

positive charge being delocalized throughout the π system and increasing π electron delocalization. However, theoretical as well as experimental observations predict that an isolated protonated Schiff base should absorb near 600 nm. The 450 nm species obtained in solution is due primarily to the association with a counterion. Thus, the above findings, coupled with the energetic problem posed by burying a net charge in a low dielectric medium, suggests that the Schiff base in the protein is ion paired to a negatively charged amino acid.

### 3. Catalytic: Proton translocating groups

In order to elucidate the mechanism of proton transport in BR, it is necessary to obtain information about molecular changes occurring during the photocycle. Resonance Raman spectroscopy has been used to provide information on the retinylidene chromophore. Recently, infrared spectroscopy has been utilized to study specific groups of proteins. Fourier transform infrared difference spectroscopy of $BR_{570}-M_{412}$ transition was used by Rothschild et al. (1981) to identify a peak at 1762 $cm^{-1}$, characteristic of carboxyl groups in aspartic and glutamic acid. The vibration was shifted by 10 $cm^{-1}$ in deuterated samples, also a characteristic of a carboxyl group containing an exchangeable hydrogen. The vibration frequency of 1760 $cm^{-1}$ is 10-15 $cm^{-1}$ higher than in model compounds which suggests that the carboxyl group is perturbed by a nearby ionic charge.

Subsequently, kinetic infrared spectroscopy was used to obtain additional evidence for two carboxyl residues undergoing protonation and deprotonation during the photocycle (Siebert et al., 1982). The protonation of one group (1765 $cm^{-1}$) occurs simultaneously with formation of the $M_{412}$ intermediate, while the second group is slower and does

not reflect kinetics observed for chromophoric changes. The time constant for reprotonation of both groups is similar and coincides with the kinetics for the reformation of $BR_{570}$ from $M_{412}$. The absorbance changes at 1755 $cm^{-1}$ and 1765 $cm^{-1}$ were both shifted 10 $cm^{-1}$ by deuteration and exhibited kinetic isotope effects for the rise and decay. These studies provide strong experimental evidence for the role of carboxyl residues as proton exchangeable groups in BR.

## VI. OBJECTIVES OF THIS STUDY

Despite the fact that the structure of BR has been well characterized, the overall molecular mechanism of proton translocation remains essentially unknown. The role of the Schiff base in the mechanism is well established, but the involvement of the protein moiety in chromophore structure, the photochemical cycle, and proton translocation process is still largely open to speculation. Several models have been proposed for the above mechanisms. In particular, the carboxyl residues of aspartic and glutamic acid have been suggested for the following roles: (i) interacting directly with the Schiff base nitrogen to form an ion-pair (Fischer and Oesterhelt, 1979; Honig et al., 1979), (ii) interacting with the -ionone ring or polyene chain of retinal (Warshel, 1978), (iii) forming ion-pairs within the membrane with the positively charged groups of arginine and/or lysine and (Lewis et al., 1978; Packer et al., 1979), and (iv) participating in a sequence of proton translocating groups (Packer et al., 1979; Engelman et al., 1980).

Since the complete primary sequence of BR has been reported and the retinal binding site identified, chemical modification techniques can be used to gain information on the role of specific amino acid residues. This project seeks to identify both the structural and functional roles of carboxyl residues in BR.

Specific objectives are:

(1) to determine if carboxyl residues are essential for photocycling activity of BR (see Chapter VIIIA),

(2) to determine if carboxyl residues form ion-pairs with the positively charged residues of lysine or arginine in

BR structure (see Chapter VIIIB),

(3) to determine whether carboxyl residues are involved in protein-chromophore interactions (see Chapter VIIIC),

(4) to study the topography, mobility, and local environment of carboxyl residues in BR by the introduction of physico-chemical reporter groups, such as chromophores and spin-labels (see Chapter VIIID), and

(5) to identify carboxyl residues that may directly be involved in proton translocation activity by the protein (see General Discussion).

The detailed findings relating to each of the above objectives will be discussed separately in the following chapters while the overall findings will be related to a model of BR structure in the General Discussion.

VII. MATERIALS AND METHODS

1. Growth of H. halobium, strain S9

H. halobium strain S9 was grown according to Lanyi and MacDonald (1979) in 10-liter batches in a sterilized LF-14 Chemapec Fermenter. The growth media contained the following per liter: 250 gms NaCl, 20 mgs $MgSO_4 \cdot 7H_2O$, 2 gms KCl, 200 mgs $CaCl_2 \cdot H_2O$, 1 ml of 3.58 gms/liter $FeCl_2 \cdot 4H_4O$, 1 ml of 190 mg/liter $MnSO_4 \cdot H_2O$, 10 gms Inolex peptone, and 10 mg NaOH was added to adjust the final pH to 7.0. A small amount of AF-72 Antifoam Emulsion was added to prevent foaming during mixing. The solution was mixed with a magnetic stirrer until it was clear. The media was then autoclaved 20 minutes at 121°C.

The cooled media was inoculated either with a small amount of media containing colonies from either agar slants, or with a test tube or 250 ml starter culture. Agar slants were prepared by adding 1.5% agar to the culture media in sealed test tubes, autoclaving 20 minutes at 121°C and positioning the test tubes at a slant to gel at room temperature. Petri plates were filled with 1.5% agar in media, auto- claved and left to gel covered at room temperature. 1 ml of late log phase liquid cell culture was spread on agar plates or slants. Agar slants were maintained in tightly sealed test tubes and agar plates were sealed in plastic bags. Slants and plates were grown at room temperature in a tightly sealed box illuminated by GE "Cool-white" fluorescent lights. Established slants could be stored at 4°C for one year.

Starter test tube cultures were prepared by picking desired cul- tures from plates or slants and placing 5-7 ml of liquid culture medium in a loosely capped test tube. The test tube culture was either grown

on a shaker in a stationary test tube rack under illumination. 250 ml
starter cultures were prepared from a test tube starter culture or
from colonies picked from plates or slants in culture media. This
starter culture was grown on a shaker platform (180 rpm) at 25-35°C.
The cultures were illuminated by a band of 6 GE "Cool-White" fluorescent
lights. The 250 ml culture used to inoculate 10-15 liter batches of
media when the cell growth had produced a light scattering intensity
of $A_{660}$ = 0.4-0.5.

It was also possible to serial culture the S9 colonies, provided
that not more than five serial transfers were made without starting
with fresh colonies. To serial transfer a culture, 250 ml of a culture
that had reached the stationary growth phase was diluted into 10 liters
of new media.

Aeration in the Chemapec Fermenter was achieved by flowing com-
pressed air into the fermenter at a flow rate of 2 liters/minute and
monitoring oxygen concentration in the media polarographically with
the Il 530 Industrial Dissolved Oxygen Monitoring System. The oxygen
electrode was initially calibrated in distilled water that had been
bubbled with compressed air for 10 minutes and set at 160 mm $O_2$, or
21.1% atmospheric pressure. The oxygen was gradually depleted by the
growing cells. Just before S9 cultures reached the stationary growth
phase ($A_{660}$ = 0.8-1.0 at about 4 days of growth), the air was turned
off and the anaerobic culture stirred about 2 more days. The fermenter
was maintained at 37°C, stirred at 460 rpm, and surrounded by seven
18" GE "Cool-White" fluorescent lights mounted on a circular wooden
stand 2 cm from the fermenter.

After the cells had remained at the stationary phase of growth for

two days, they were harvested by centrifugation at 7,000 x g for 15 minutes. The cell pellet was either used immediately or frozen at −40°C and stored for up to 3-4 months.

## 2. Isolation of purple membrane

The cell pellet was resuspended in 400 ml of cold distilled water and 5 mg Deoxyribonuclease I was added. This suspension was blended in a Waring Blender 5 x 5 seconds, and 600 ml of cold distilled water was added. This cell lysate was stirred for not more than one night in an 8°C room.

A preliminary low speed centrifugation at 7,000 x g for 10 minutes pelleted cell debris. The supernatant was then centrifuged at 100,000 x g for 30 minutes. After this spin, the pellet was resuspended with a Pasteur pipette into a minimal volume of distilled water and the above centrifugations of the cell lysate supernatant were repeated until the entire cell lysate was pelleted together. After each spin the reddish supernatant was discarded. The combined pellet was resuspended in 30-40 ml of distilled water and centrifuged at 100,000 x g for 30 minutes. This pellet was resuspended to a concentration of 5 mg/ml of bacteriorhodopsin (BR) protein, based on the molar extinction coefficient of 63,000 $M^{-1}cm^{-1}$ at 570 nm and approximate molecular weight of BR of 26,000 (Khorana et al., 1979).

The following discontinuous sucrose density gradient was carried out to remove any remaining red membrane (175,000 x g for 16-20 hours) from the purple membrane (PM) lysate:

> 0.5 ml 60% sucrose (w/v)
>
> 2.0 ml 52% sucrose (w/v)
>
> 2.0 ml 45% sucrose (w/v)

         2.0 ml 40% sucrose (w/v)

         2.0 ml 38% sucrose (w/v)

         2.0 ml 36% sucrose (w/v)

1.5 ml of the cell lysate combined pellet was loaded onto this gradient in six separate centrifuge tubes. The PM fraction sedimented primarily at 45% sucrose. The sucrose was removed from the collected PM fraction by diluting PM into a large volume of distilled water and centrifuging at 100,000 x g for 30 minutes. The combined pellet was washed by centrifuging at 180,000 x g for 20 minutes and resuspending in 25 ml distilled water, three times. The final pellet was resuspended in distilled water to a BR concentration of 10 mg/ml.

The resulting PM was examined for microheterogeneity by gel electrophoresis in slabs using a 5% polyacrylamide stacking gel and 12.5% polyacrylamide separation gel according to the method of Laemmli (1970) and found to be free of contaminating proteins. The overall yield was determined by comparing the final BR weight to the initial weight of the total protein in the cell lysate analyzed by a modified Lowry method. The usual overall yield of PM per 10 liter culture batch was 250 mg of BR protein, representing a 60% yield. This preparation was stable for more than 4 months if stored in 4 M NaCl at 5°C.

3.  Isolation of white membranes from H. halobium, strain $R_1mW$

H. halobium, strain $R_1mW$ was obtained from Dr. Yasuo Mukohata, Osaka University, Japan. $R_1mW$ cells were cultured in 4 M NaCl medium as described previously for strain $S_9$, with the following differences in media composition:

         $MgSO_4 \cdot 7H_2O$          10 g

>Inolex peptone     3.3 g
>
>No trace metals and
>
>pH adjusted to 7.4.

The culture conditions and isolation procedures have been described by Mukohata and Sugiyama (1982).

Cells were harvested by centrifugation at 5000 x g for 30 min and suspended in basal salt solution (100 ml) and 2 mg of deoxyribonuclease I (Sigma Chemical Co.) added. The lysate was dialyzed overnight against 0.1 M NaCl, 0.01 M Tris-HCl, pH 7.6. A low speed spin (7000 rpm, 10 min) in the Sorvall GSA rotor was used to pellet cell debris from the lysate. The clear, brown supernatant was then centrifuged at high speed (100,000 x g, 30 min) to pellet the white membranes (WM). The pellets were resuspended in 0.1 M NaCl and washed two additional times. Pellets from the wash were collected and resuspended in a small volume of water. The white membrane was purified by ultracentrifugation on a discontinuous sucrose density gradient composed as follows: 26%, 30%, 38%, 45%, and 52%. The sucrose gradient was run at 37,000 rpm for 16 hr in a Beckman SW40 TI rotor. The white membrane was collected at a buoyant density of 1.18 g/ml and subsequently washed free of sucrose by resuspension in a large volume of 0.10 M NaCl (100,000 x g, 30 min).

4. Formation of purple membrane from white membrane

The white membrane containing bacterioopsin can be converted to bacteriorhodopsin by addition of stoichiometric amounts of all-trans retinal. This generates a 565 nm chromophore resulting in the formation of purple membranes (Mukohata et al., 1981). White membrane solutions in 0.1 M NaCl, 0.01 M Hepes, pH 7.0 were titrated with small aliquots of all-trans retinal in 100% ethanol at 20°C. The concentration of the

retinal stock solution was determined spectrophotometrically using a

molar extinction coefficient of 43,400 $M^{-1}cm^{-1}$ at 381 nm. The extent

of reconstitution was determined by taking sequential spectra 10 min

after addition of a retinal aliquot, from 300-700 nm the Aminco DW2

spectrophotometer. When addition of retinal resulted in no additional

increase in 565 nm absorbance, reconstitution was complete. A plot of

$A_{565}$ vs. retinal concentration revealed a linear relationship until a

sharp break point was reached at saturation. The absorbance at this

point and $\varepsilon = 63,000$ $M^{-1}cm^{-1}$ were used to calculate the concentration

of bacterioopsin present in the white membranes.

5. **Chemical modifications of carboxyl residues — Reaction with**
   **water-soluble carbodiimides**

The rationale behind the carbodiimide-nucleophile approach can be

seen from figure 7a (Carraway and Koshland, 1972). The reaction

sequence is initiated by addition of the carboxyl across one of the

double bonds of the diimide system to given an O-acylisourea. The

activated carboxyl group of this adduct can then react by one or two

routes. First an attack by a nucleophile $R-NH_2$ will yield an acyl-

nucleophile product plus the urea derived from the carbodiimide.

Second, the O-acylisourea can rearrange to an N-acylurea via an intra-

molecular acyl transfer. In the special case where the nucleophile is

water, the carboxyl will be regenerated with the conversion of molecule

of carbodiimide to its corresponding urea. Kinetic studies of model

carbodiimide-carboxyl-nucleophile systems have shown that the rearrange-

ment can be made slow compared to nucleophilic attack if the concentra-

tion of nucleophile is sufficiently high. Therefore the coupling

reaction of carboxyl and nucleophile can be driven essentially to

Figure 7. Reactions of Carboxyl Group Specific Modification Reagents.

a) Reaction of carboxyl groups with a water-soluble carbodiimide, EDC. EDC-promoted amide formation proceeds by nucleophile reaction with the o-acylisourea intermediate.

b) Reaction of carboxyl groups with EEDQ, a hydrophobic, highly specific reagent. Formation of an amide product proceeds by reaction of an amine with a mixed carbonic anhydride intermediate.

a) 1-ethyl-3-(3-dimethylaminopropyl) carbodiimide ; (EDC)



(o-acylisourea)

$R_3$-$NH_2$
(nucleophile)

(N-acylurea)

(amide)

$R_1 = CH_2CH_3$

$R_2 = CH_2CH_2CH_2N(CH_3)_2$

$R_3 = CH_2C\overset{O}{\underset{OCH_3}{}}$

b) N-ethoxycarbonyl-2-ethoxy-1,2-dihydroquinoline ; (EEDQ)



$C_2H_5OH + CO_2 +$ (amide)

$R_3$-$NH_2$

(mixed carbonic anhydride)
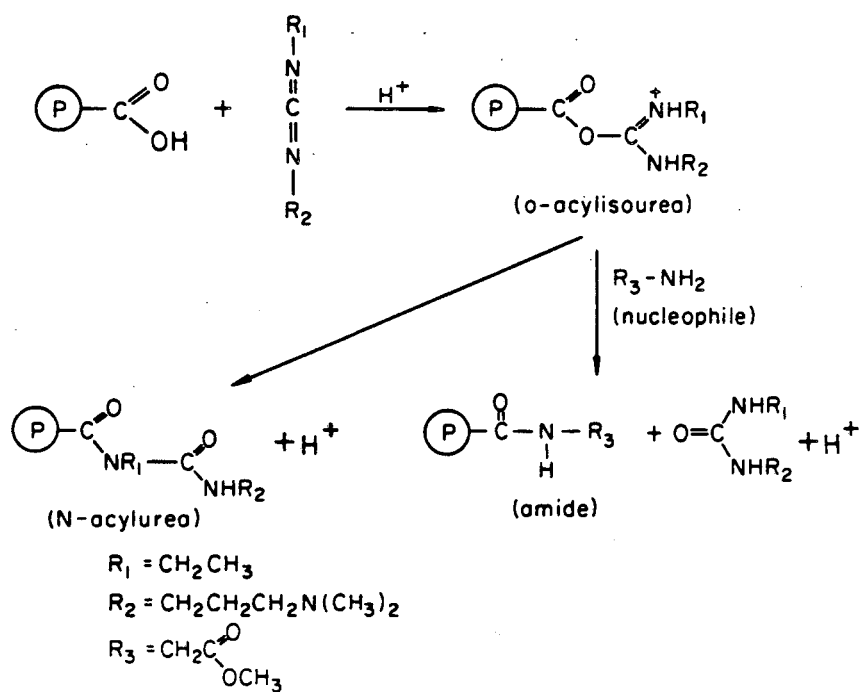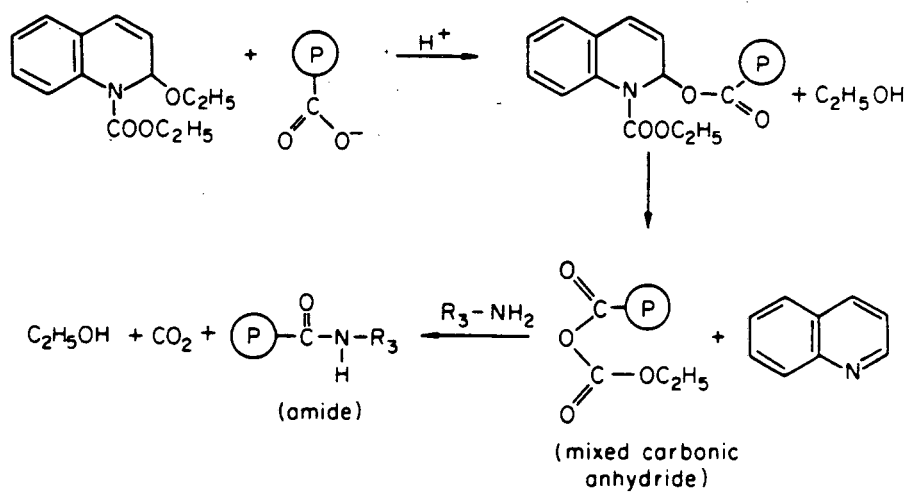
completion in the presence of excess carbodiimide and nucleophilic reagent.

The advantage of the two-stage reaction sequence for modification of protein-carboxyls lies in the versatility of the reaction. By varying the reaction conditions and the two reagents, one can potentially use the basic technique in many diverse ways, as described below.

Purple membranes were treated with one of the folowing water-soluble carbodiimides:

> EDC, 1-ethyl-3-(3-dimethylaminopropyl)carbodiimide HCl;
>
> CMC, 1-cyclohexyl-3-(2-morpholinoethyl)carbodiimide metho-p-toluene sulfonate; and
>
> ETC, 1-ethyl-3-(3-trimethylpropylammonium)carbodiimide iodide.

EDC and CMC were obtained from Sigma Chemical Co. while ETC was synthesized as described in the following section.

a) EDC: purple membranes were washed and resuspended in 0.10 M MES at pH 4.5 at a protein concentration of 1.0 mg/ml. Typically, a 250 mM stock solution of EDC was freshly prpeared before each experiment by dissolving solid EDC in 0.10 M MES at pH 4.5. The carbodiimide solution was added rapidly to a vortexing tube of purple membranes. The samples were placed in a shaking water bath at 25°C. The reaction time was varied for different experiments, and is indicated in each case. Final concentrations for the reactions were also varied (1-50 mM) but typically were 50 mM EDC.

b) CMC and ETC: reaction conditions were similar to those employed for EDC. In some cases, the reactions were carried out at pH 5.6 with 50 mM CMC or ETC for 24 hr at 25°C.

Figure 8.  Structures of Water-Soluble Carbodiimides Employed

in This Study.

l-ethyl-3-(3-dimethylaminopropyl) carbodiimide (EDC)

$$CH_3\,CH_2-N=C=N-CH_2CH_2CH_2\,N\,(CH_3)_2$$
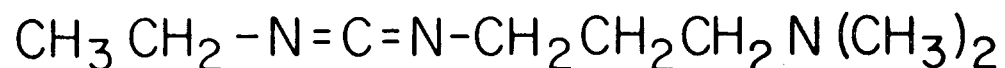
l-ethyl-3-(3-trimethylpropyl ammonium) carbodiimide (ETC)

$$CH_3CH_2-N=C=N-CH_2CH_2CH_2\overset{\oplus}{N}\,(CH_3)_3$$
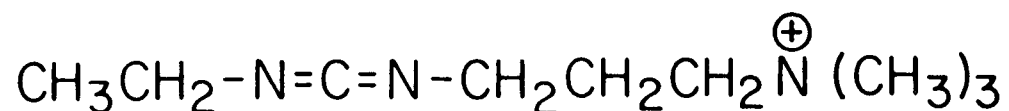
l-cyclohexyl-3-(2-morpholinyl-4-ethyl) carbodiimide (CMC)
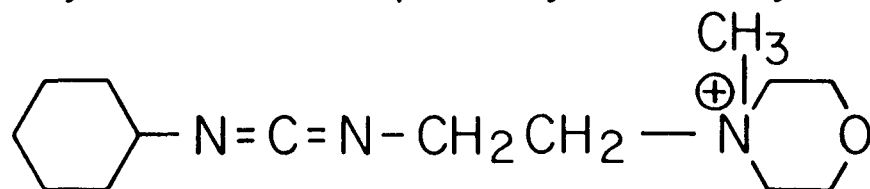
6. **Synthesis of water-soluble quaternary amine carbodiimide reagent: 1-ethyl-3-(3-trimethylpropylammonium)carbodiimide iodide**

The procedure used is an adaptation of the synthesis of Sheehan et al. (1961). 5.0 g (.032 mole) of 1-ethyl-3-(dimethylaminopropyl) carbodiimide hydrochloride was stirred at room temperature into a mixture of 50 ml of 80% saturated $Na_2CO_3$ plus 10 ml of ether. The anhydrous ether is first dried by adding 4 Å molecular sieves and stirring for 1 hr. After stirring for 5 hr, the ether layer which had separated was drawn off with a Pasteur pipette. The aqueous layer was extracted three more times with 10 ml of ether. The combined ether extracts were dried with $CaSO_4$ for 1 hr, and then filtered through glass wool into a solution of 4.01 ml (.0645 mole) methyl iodide in 48 ml ether. The $CH_3I$/EDC molar ratio for the reaction is 2:1. The ether solution was stoppered with a cork, covered with foil, and stirred at room temperature for 18 hr. The ETC-iodide, a white precipitate, was then filtered, washed twice with 20 anhydrous ether, and dried in a vacuum dessicator over $CaCl_2$. The entire sample was dissolved in 20 ml dry acetone, filtered, and then recrystallized by the slow addition of 100 ml anhydrous ether to the stirred solution of ETC in acetone. After filtering the product and drying in a vacuum dessicator, the overall yield was 56%, the melting point was found to be 95-96°C.

7. **Carboxyl group modification by reaction with N-ethoxycarbonyl-2-ethoxy-1,2-dihydroquinoline (EEDQ)**

An investigation of the chemical behavior of EEDQ disclosed that it readily induces the formation of peptide linkages (Belleau & Malek, 1968). As seen in Fig. 7b, experimental evidence was obtained that the mechanism of carboxyl group activation by EEDQ involves the transient formation of a mixed carbonic anhydride intermediate. In the absence

of an amine, the carbonic anhydride intermediate could be isolated and characterized, whereas it was rapidly consumed in its presence. The breakdown products are quinoline, carbon dioxide, and ethanol.

Purple membranes were washed and resuspended in 0.10 M MES, pH 6.0 at 1.0 mg protein/ml. EEDQ stock solutions of either 100 mM or 200 mM were prepared immediately before use in 100% methanol. Appropriate controls were run with methanol alone. The EEDQ solution was added to a rapidly vortexing tube of purple membranes. The reaction was carried out in a shaking water bath for 1 hr (unless indicated otherwise) at 25°C. The final concentraton of EEDQ varied for different experiments. The reaction was terminated by dilution with ice cold 0.10 M NaCl, 0.01 M MES, pH 6.5 and centrifuged immediately at 100,000 x g for 30 min (4°C). Modified samples were washed by the above procedure. The removal of quinoline was followed by taking UV spectra of the wash supernatants on an Aminco DW2 spectrophotometer. Typically, 4-5 washes were required for complete removal of the quinoline product.

## 8. Carboxyl-activating reagent promoted amide formation

A variety of amine-nucleophiles can be coupled to carboxyl residues via an amide linkage as shown in Fig. 7 using either EDC or EEDQ as a carboxyl-activating reagent. This results in the conversion of the carboxyl function to the $R_3$ group of the nucleophile. Depending upon the amine employed, the character of the carboxyamidyl product can be varied considerably. Non-reporter group nucleophiles employed in this study are: aminoethane sulfonic acid, glycine methyl ester, glycinamide, and ethylenediamine. Concentrated stock solutions of the above nucleophiles (1.0-1.25 M) were prepared in 0.10 M MES and adjusted to the appropriate pH with NaOH. Aliquots from the stock solution were

taken to give final concentrations from 1-500 mM. The nucleophile was incubated with purple membranes for a minimum of 10 min prior to addition of the carboxyl-activating reagent at 25°C. The reaction was initiated by the rapid addition and mixing of the carboxyl-activating reagent. The reactions were terminated by dilution with ice cold buffer and washed by centrifugation (as described above) at least three times.

## 9. Chemical Modification of Lysine Residues — Imidoester reaction

Monofunctional imidoesters react with protein ε-amino groups of lysine to form amidine products that retain positive charge, as shown in figure 9. The monofunctional imidoester used to modify BR was ethyl acetimidate (EA from Sigma Chemical Co.). Final concentrations of EA during the reaction varied from 1-200 mM. Purple membranes were suspended in 0.10 M sodium tetraborate, pH 10.0, at 1.0 mg protein/ml. The EA reagent was freshly prepared in 1.0 M NaOH/0.10 M $Na_2B_4O_7$ immediately prior to usage. This is required since imidoesters are unstable and slowly hydrolyze in aqueous solution to the corresponding amide and alcohol (Means and Feeney, 1971). The high alkaline pH favors a rapid and complete conversion to the amidine product, and decreases the likelihood of undesirable side reactions. The reaction was carried out for 30 min at 25°C and then terminated by dilution with ice-cold 0.10 M NaCl, 0.01 M MES at pH 6.5. Samples were subsequently washed by repeated ultracentrifugation and resuspension in the same buffer.

## 10. Fluorescamine assay for primary amino groups

Fluorescamine (Roche Diagnostics) reacts with primary amines to form an intensely fluorescent product (Fig. 10), providing a rapid

Figure 9.   Imidoester Reaction.

The figure depicts the imidoester reaction between the unprotonated form of a protein amino group and a cationic form of the monofunctional imidoester.   Formation of the N-alkyl amidine product from the tetrahedral intermediate is favored at high pH.

# IMIDOESTER REACTION

Protein—NH$_3^{\oplus}$

    Protein—NH$_2$     +     CH$_3$—$\overset{\overset{\displaystyle NH_2^{\oplus}}{\|}}{C}$—OR   ⟶   $\left[ CH_3-\underset{\underset{\displaystyle Protein}{\underset{|}{\underset{\displaystyle NH}{|}}}}{\overset{\overset{\displaystyle NH_2}{|}}{C}}-OR \right]$   H$^{\oplus}$

**PROTEIN AMINO GROUP**          **IMIDOESTER**

                                        **TETRAHEDRAL**
                                        **INTERMEDIATE**

CH$_3$—$\overset{\overset{\displaystyle NH_2^{\oplus}}{\|}}{C}$—NH—Protein    +    ROH                         CH$_3$—$\underset{\underset{\displaystyle Protein}{\underset{|}{\underset{\displaystyle NH^{\oplus}}{\|}}}}{C}$—OR    +    NH$_3$

**N-ALKYL AMIDINE**

                                          **N-ALKYL ACETIMIDATE INTERMEDIATE**
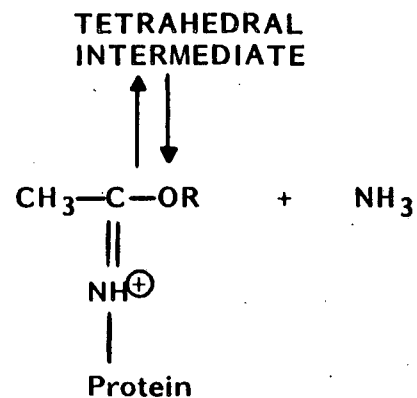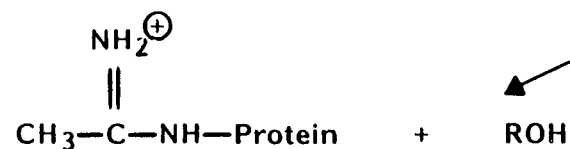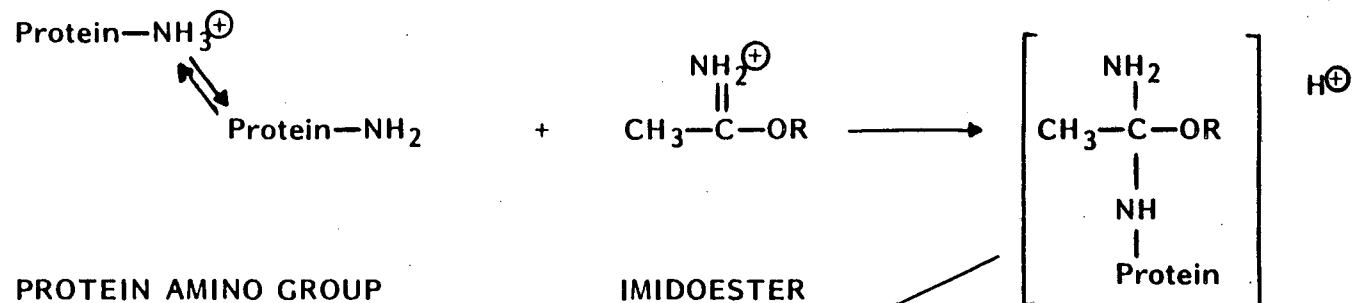
Figure 10.   Fluorescamine Reaction.

The reaction of fluorescamine with amino groups occurs with a $t_{1/2}$ of 100-500 milliseconds producing the fluorophor shown.   Unreacted fluorescamine hydrolyzes with a $t_{1/2}$ of 5-10 seconds to yield non-fluorescent products.

# FLUORESCAMINE REACTION
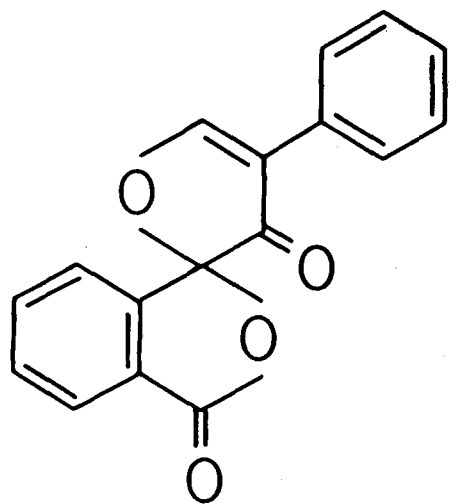


Fluorescamine    Protein amino group    Fluorescent product
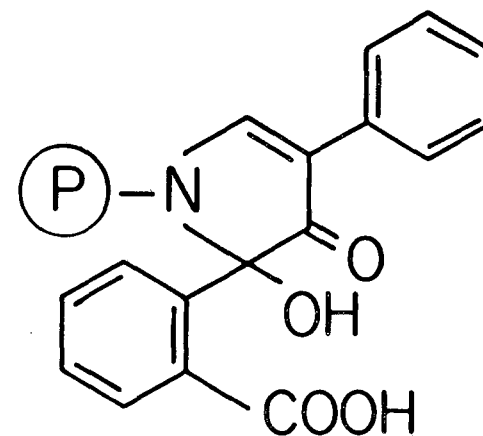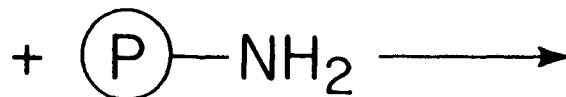
60

and sensitive assay for the free ε-amino group of lysine in BR.
The procedure employed was a modification of Bohlen et al. (1973) using
1% SDS. The BR sample, 0.1 ml, was first denatured by addition of
0.1 ml of 20% SDS and heating, and then suspended in 2.0 ml of 0.1 M
sodium borate, pH 9.2. The reaction was initiated by addition of
0.5 ml of a 0.2 mg/ml fluorescamine solution (made in spectral grade
acetone) to a rapidly vortexing test tube. After 10 min. the fluores-
cence ($\lambda_{ex}$ = 390 nm, $\lambda_{em}$ = 480) was read on a Perkin-Elmer MPF-44A
fluorescence spectrophotometer. Fluorescence values were compared
against a standard curve constructed using fatty acid free bovine serum
albumin and SDS. Protein concentrations were determined by the method
of Lowry et al. (1951).

## 11.  Laser flash photolysis

The laser flash photolysis apparatus, used to obtain the kinetics
of photocycle intermediates, is shown schematically in figure 11. Actinic
illumination was provided by a Phase-R (model DL-1100) pumped dye laser
using Rhodamine 575 (Exciton Chemical Co.) at $1 \times 10^{-4}$ M in 100% ethanol.
The monochromatic flash at 575 nm had a 150 ns risetime, a 1.0-1.5 μs
duration, and a maximum energy of 0.2 J/flash. The measuring beam came
from a General Electric Quartzline lamp (200 mW/cm$^2$ measured at the surface
of the light bulb) and initially passed through a Bausch and Lomb mono-
chrometer (5 nm half-band width) before entering the sample cuvette.
After passing through the sample, the measuring beam passed through an
identical Bausch and Lomb monochrometer. The monochrometers could be
set at 412 nm, 650 nm, or 570 nm depending on the intermediate to be
measured. The light exiting the second monochrometer was detected by

Figure 11.  Schematic of Laser Flash Photolysis Apparatus.

**SCHEMATIC OF LASER FLASH PHOTOLYSIS APPARATUS**
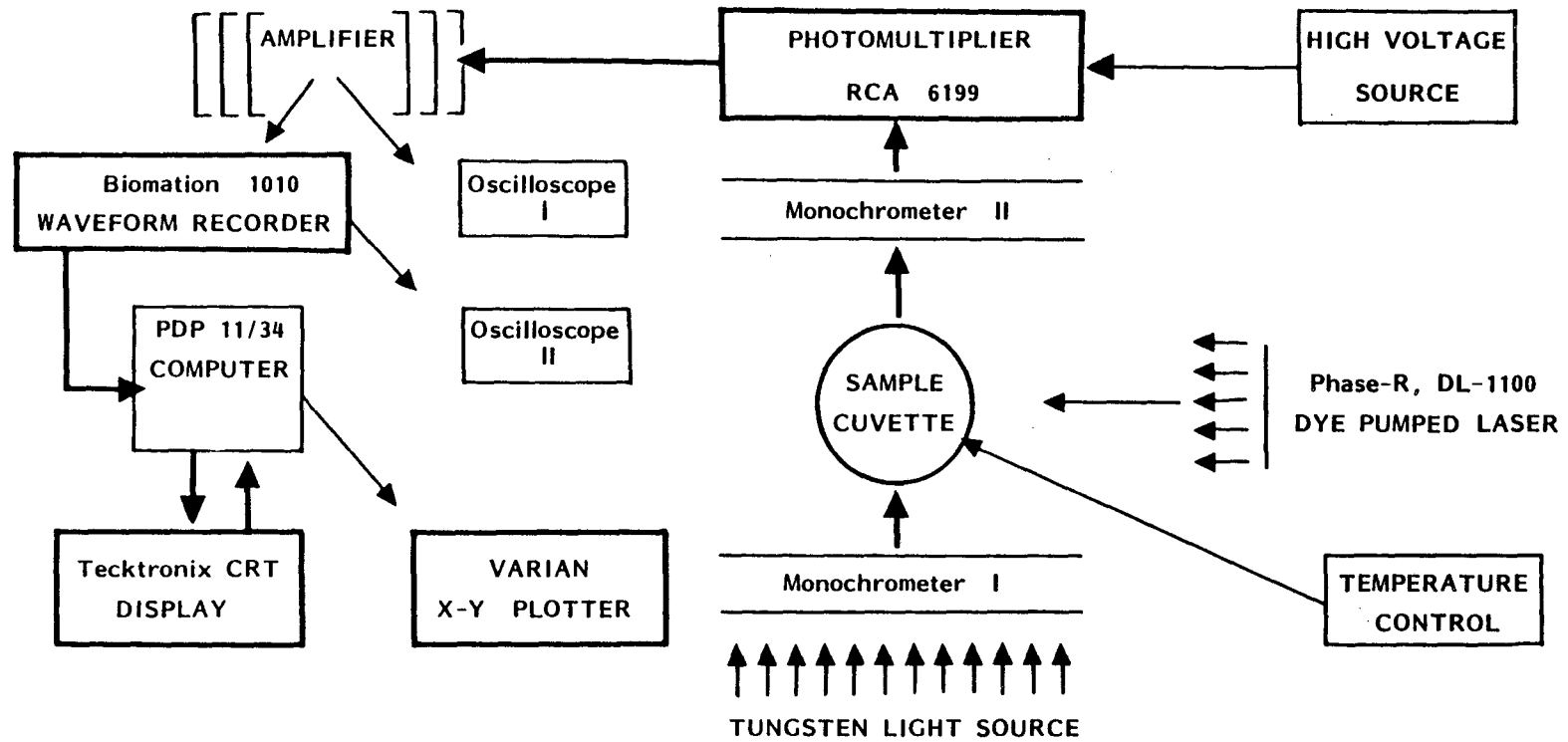


XBL 812-8178

a RCA 6199 photomultiplier tube operated at about -500 V. The signal
was then amplified by a custom built photomultiplier tube current ampli-
fier and sent to a Biomation 1010 Waveform recorder (Gould, Inc.) for
rapid digitization and memory. One analog output from the Biomation
unit went to a Tektronix Type 564 Storage Oscilloscope. A second
output connected the Biomation unit to a Digital PDP-11/34 computer
(Digital Equipment Corp.). Typically, the signal to noise could be
greatly improved by collecting multiple scans (minimum, n = 20) by
accumulating them in the computer buffer. Individual scans were
referenced to each other during data accumulation by collecting a
leading baseline prior to the laser flash and assigning this signal a
"zero" value. Data stored on rko5 discs were analyzed by computer
programs that carried out data averaging, curve fitting of the data,
and calculation of rate constants. Kinetic traces were printed on a
Varian E-80 recorder that was a component of the EPR spectrometer.

## 12.  M-412 photostationary steady-state:

Purple membranes at similar protein concentrations (0.2 mg/ml) were
used for 412 nm photostationary steady-state determination in an Aminco
DW-2 spectrophotometer. Side illumination (120 mW/cm2) was provided
through a Corning 3-67 low wavelength cutoff filter (50% transmission
at 500 nm) and the photomultiplier tube was protected by a Baird
Atomic 412 nm transmission interference filter. Quantitation of the
steady-state level for modified samples was with reference to both the
sample's absorbance at 570 nm and to a control sample run with every
determination. The 570 nm absorbance of modified samples was corrected
for light-scattering (reference = 700 nm) when necessary.

13. <u>Polyacrylamide gel electrophoresis in sodium dodecyl sulfate</u>

SDS gel electrophoresis was carried out in a Bio-Rad Model 220 Dual Vertical Slab Cell using either 1.5 mm spacers and 20 well combs (cross-linking analysis) or 3.0 mm spacers and 10 well combs (trypsin treatment). Gels were made according to the discontinuous Tris-glycine system of Laemmli (1970) using a 5% acrylamide stacking gel and 10% separation gel for analysis of EEDQ and EDC cross-linking products. For analyzing trypsin treatment of BR, a 5% stacking gel and 16% separation gel (acrylamide/bisacrylamide, 30/1.6%) were utilized to achieve resolution of bands of similar, small molecular weight.

Samples for electrophoresis were prepared by mixing purple membrane suspensions ( ≃ 2 mg/ml BR) with an equal volume of solubilization cocktail (8 M urea, 1% SDS, 0.01 M phosphate, pH 6.8, and 1% mercapto-ethanol). Sample mixtures were heated at 100°C for a minimum of 10 min, cooled, and 20-40 µl (10-20 µg BR) applied to the gels. Electrophoresis was carried out at 25 mA while the sample was in the stacking gel, and 40 mA while in the 10% acrylamide running gel, until the tracking dye had migrated to 1.0 cm from the end of the gel.

After completion of electrophoresis, gels were stained for 24 hr with a solution of 0.025% Coomassie Brilliant Blue R250, 25% isopropyl alcohol, and 10% acetic acid, followed by 6-9 hr in 0.0025% Coomassie Brilliant Blue R250, 10% isopropyl alcohol, and 10% glacial acetic acid (Fairbanks <u>et al</u>., 1971). Gels were destained in 25% methyl alcohol, 7.5% acetic acid, and stored in 10% acetic acid. Densitometric tracings of stained gels were made on a Helena Laboratories Quick Scan densitometer. Gels were calibrated for molecular weight using bovine

serum albumin, ovalbumin, chymotrypsin A, myoglobin, lysozyme, and cytochrome c.

## 14. Amino acid analysis

Amino acid analysis was performed according to Spackman et al. (1958) using a Spinco/Beckman 120B amino acid analyzer. Modified samples prepared for amino acid analysis were dialyzed against 4 L of $H_2O$ at 10°C (x 4). A total of 5 mg BR was lyophilized and placed into acid-washed hydrolysis tubes. Then, 0.5 ml of 12 N constant boiling HCl (Pierce Chemical Co.) containing 0.1% phenol was added and the sample repeatedly frozen and thawed while under vacuum in a dry ice/isopropyl alcohol bath. The tube was sealed under vacuum and placed in an oven for 24 hr at 110°C for acid hydrolysis. Samples were loaded on a Beckman A-15 column -- a sulfonated polystyrene ion exchange resin.

The amino acid compositions of BR and its modified derivatives were calculated by assuming the hydrolysate contained the theoretical number of tyrosine (11) and phenylalanine (12) residues, or alanine (29) and phenylalanine (12) residues.

## 15. Tryptophan fluorescence

Fluorescence emission spectra of tryptophan residues in BR and bacterioopsin were obtained using a Perkin-Elmer MPF-44A fluorescence spectrophotometer. The excitation monochrometer was set at 287 nm and the emission wavelength was scanned from 300-450 nm. A slit width of 6 nm was employed. Fluorescence intensity was a linear function of concentration below 0.1 absorbance at 280 nm.

16. **Labeling carboxyl residues with a pH-sensitive chromophoric reporter group: Nitrotyrosine methyl ester (NTME)**

The carboxyl residues of bacteriorhodopsin in purple membranes or bacterioopsin in white membranes were covalently linked to NTME by using EEDQ as coupling agent. NTME was obtained as a gift from Dr. D. Koshland, Dept. of Biochemisty, Univ. of California at Berkeley. Stock solutions of 100 mM NTME were prepared in 100% methanol, since NTME solubility in water is very low. Purple membranes were suspended in 0.10 M MES, pH 6.0, at 1 mg/ml BR protein. Aliquots of NTME were incubated with PM or WM for a minimum of 5 min prior to initiating the reaction with EEDQ. Final concentrations of NTME nucleophile varied from 0.1-10 mM. Stock solutions of EEDQ (100 mM) in 100% methanol were prepared immediately before use. Appropriate BR controls were run with methanol alone. The reaction was initiated by addition of EEDQ to a rapidly vortexing tube, and then placed in a shaking water bath at 25°C for one hour. The reaction was stopped by dilution with ice cold buffer (0.1 M NaCl, 0.01 M Hepes, pH 7) and immediately centrifuged at 100,000 x g for 30 min to pellet the membranes. Modified samples were repeatedly washed by the above procedure and UV-visible spectra of each supernatant were used to determine complete removal of unreacted NTME and quinoline products.

17. **Quantitation of NTME labeling stoichiometry**

The stoichiometry of NTME covalently bound per BR or BO was determined spectrophotometrically essentially according to Malan and Edelhoch (1970). Chemically modified membranes were centrifuged at 100,000 x g for 30 min and the pellet resuspended in 8 M urea, 1% SDS, 0.01 M Hepes, pH 10. The urea-SDS membranes were then heated at 100°C

for 10 min to completely denature the protein. Absorption spectra from 300-700 nm were recorded on an Aminco DW-2 spectrophotometer at pH 10 and pH 3. The absorbance difference between the nitrotyrosyl and nitrotyrosylate chromophores at 436 nm was used to calculate the concentration of NTME present. The extinction coefficient ( $\varepsilon_{436}$ ), and pK for the model compound were determined experimentally for NTME in 8 M urea, 1% SDS, and 0.01 M Hepes. It was found to have a $\lambda_{max}$ = 436 nm at pH 10, $\varepsilon_{436}$ = 5,100 $M^{-1}cm^{-1}$ and pK = 7.6 $\pm$ 0.1.

A value of $\varepsilon_{436}$ = 4,800 $M^{-1}cm^{-1}$ was previously determined by Malan and Edelhoch for nitrotyrosine in 8 M urea, 0.10 M Tris, 0.10 M KCl (1970). The concentation of NTME determined by the above method was then divided by the known concentration of BR or BO to obtain a mole ratio of NTME/BR. Unmodified control samples examined by the same technique described above revealed small absorbance changes at 436 nm due to retinal. The small retinal absorbance difference was used to correct NTME absorbance measurements.

## 18. Visible titration spectra

Absorbance spectra were recorded on an Amino DW-2 spectrophotometer from 300-700 nm (slit width = 3 nm). Purple membranes or white membranes suspended in 0.1 M NaCl, 0.01 M Hepes, pH 7, at 1.0 mg/ml were titrated from pH 7 to pH 11 in small steps, allowing several minutes for mixing and equilibration at each step. Typically, samples were stored at 4°C for 24 hr prior to beginning the backward titration. Changes in pH were measured with a Corning Model 130 pH meter and a Polymark 1885 electrode (Markson Science Inc.). The amount of HCl or NaOH added for titration did not exceed 1% of the sample volume.

## 19. Acid-induced difference spectra

Acid-induced difference spectra were determined in an Aminco DW-2 spectrophotometer. Purple membranes utilized for acid-induced difference spectra were at 0.20 mg/ml to minimize membrane buffering effects. Changes in pH were measured with a Corning Model 130 pH meter and a Polymark 1885 electrode (Markson Science Inc.). Hydrochloric acid (2.0 N and 0.2 N stock solutions) was added gradually with Pipette mann to the sample cuvette. Final added volume did not exceed 1% of the sample volume.

## 20. Spin-labeling of bacteriorhodopsin

BR was covalently spin-labeled by reacting 4-amino-2,2,6,6-tetramethyl-piperidine-N-oxyl (Tempamine) with protein carboxylic amino acid residues using N-(ethoxycarbonyl)-2-ethoxy-1,2-dihydroxyquinoline (EEDQ) as the coupling agent. Purple membranes (2.5 mg/ml BR) suspended in 0.10 M MES, pH 6.0, were incubated with Tempamine for ten minutes prior to addition of EEDQ. Tempamine (200 mM) was present in large excess relative to the concentrations of the carboxyl activating reagent and carboxyl residues on the protein in order to drive the reaction to the amide structure. The molar ratios of the reagents during the 200 mM Tempamine + 10 mM EEDQ reaction were 115 Tempamine: 5.8 EEDQ: 1 protein carboxyl. EEDQ (in 100% methanol) was added to a rapidly vortexing sample and incubated for 24 h in a shaking water bath at 37° C. Appropriate controls were run with methanol alone. The reaction was terminated and samples washed repeatedly by dilution in ice-cold 0.10 M NaCl, 0.01 M Hepes, pH 7.0, and centrifugation at 100,000 x g for 30 min. The ESR signal of the supernatant at very high gain was used to monitor removal of unreacted Tempamine. In final washed

samples, the unreacted Tempamine concentration in the supernatant did not exceed 2% of the protein-bound Tempamine concentration. Tempamine was obtained from Aldrich Chemical Co.; EEDQ from Sigma Chemical Co.

A sequential double chemical modification of BR carboxyl groups was developed in order to spin label only buried residues. BR was first modified by reaction with 250 mM 2-aminoethanesulfonic acid (AES) and 50 mM 1-ethyl-3-(3-dimethylaminopropyl) carbodiimide at pH 4.5 according to a previously described procedure (Herz and Packer, 1981). After extensive washing, the second spin-label modification by 200 mM Tempamine and 10 mM EEDQ was carried out as described above.

## 21. Stearic acid spin labels

The stearic acid spin labels 2-(3-carboxypropyl)-4,4-dimethyl-2-tridecyl-3-oxazolidinyloxyl [5NS], 2-(8-carboxyoctyl)-2-octyl-4,4-dimethyl-3-oxazolidinyloxyl [10NS], and 2-(14-carboxytetradecyl)-2-ethyl-4,4-dimethyl-3-oxazolidinyloxyl [16NS] were obtained from Syva, Palo Alto, California (5NS and 16NS) and Molecular Probes, Junction City, Oregon (10NS). Purple membrane suspensions (10 mg/ml) in 0.10 M NaCl, 0.01 M Hepes, pH 7.0 were labeled by addition of 1% (vol/vol) concentrated spin label solution in ethanol. The final concentration of stearic acid spin label was equivalent to 1.5 moles/mole BR.

## 22. ESR

ESR spectra were recorded on a Varian E-109E spectrometer interfaced to a PDP-11/34 computer. Samples of spin-labeled BR were routinely placed in 50 $\mu$l precalibrated capillaries with an inside diameter of 0.9 mm. ESR spectra were recorded at a frequency of 9.14 GHz (X-band) and at a power setting of 10 mW. A modulation amplitude of 1.25 gauss

was used for 2.0 spin-labeled BR and 1.6 gauss for the spin-labeled stearic acids. The value of the gain is indicated in each figure.

The spin content of labeled BR was calculated from the second integral of the first derivative spectra with reference to a standard curve constructed from different concentrations of Tempamine in buffer solution. The quantitation of the protein spin signal was carried out for both native and denatured labeled BR in order to insure that potential spin-spin interaction did not lead to underestimation of spin content. BR was denatured by addition of 8 M urea, 1% SDS, 10 mM Hepes, pH 7.0 and subsequently boiled for 15 minutes.

Correlation times, $\tau_c$ in seconds, were calculated from ESR spectral data in certain cases using the equation defined by Mehlhorn and Keith (1972):

$$\tau_c = 6.5 \times 10^{-10} \, \Delta H_0 [(h_0/h_{-1})^{1/2} - 1]$$

where $\Delta H_0$ is the width of the midline in gauss and $h_0$ and $h_{-1}$ are the heights of the mid- and high-field lines, respectively. This equation is valid in the fast tumbling range ($\tau_c < 10^{-9}$s) and applies to a homogeneous population of spins.

The motional freedom of the stearic acid spin labels as defined by the approximate order parameter, $S^{app}$, was calculated from the experimental data using:

$$S^{app} = (A_{max} - A_{min})/[A_{zz}^C - 1/2 \, (A_{xx}^C + A_{yy}^C)]$$

according to Griffith and Jost (1976) where it is assumed $A_{max} = \bar{A}_{||}$, $A_{min} \simeq \bar{A}_{\perp}$, and $A_{xx}^C$, $A_{yy}^C$, and $A_{zz}^C$ are the single crystal values (6.3, 5.8, and 33.6G) obtained by Gaffney (1976). The angle of half amplitude of motion, $\gamma$, was then obtained from the calculated value

of $S^{app}$ (23). An estimate of the position of the nitroxide group

of spin-labeled stearic acids relative to the carboxylic head group

was made by dividing the fatty acyl chain into three segments and

assuming an orientation of each segment given by the angle $\gamma$. For a

given segment, a distance, d, was obtained by measurement of a CPK model

and the membrane-perpendicular projection of that segment of the chain

was calculated as $d(\cos \gamma)$. For example, the distance between carbons

10 and 16 (d = 7.5 Å) was used with $\gamma = 45°$, obtained from $S^{app}$

for 16NS to calculate a perpendicular projection of 5.3 Å for that

segment. Since the angle at carbon 16 is greater than that for carbons

10 to 15, this estimate of the projection is a lower limit.

## 23. Trypsin treatment

Trypsin treatment of spin-labeled BR was carried out essentially

according to Gerber et al. (1977). Spin-labeled BR (10 mg/ml) was

treated with 1:100 weight ratio trypsin: BR in 80 mM NaCl, 10 mM $CaCl_2$,

40 mM Tris, pH 8.0 at 37°C and samples were periodically withdrawn.

In the case of continuous ESR kinetic experiments, samples were incu-

bated in the EPR cavity at 37° using the Varian E4540 variable tempera-

ture controller. The trypsin used in experiments had been recrystal-

lized twice, dialyzed and lyophilized (Sigma Chemical Co.).

## 24. Reconstitution of BR into liposomes

BR liposomes were prepared using partially purified asolectin

through a modification of the sonication procedure of Racker (1973).

Phospholipids (40 mg) were dried under a stream of nitrogen in the

dark. To this dried preparation, 1.0 ml of 150 mM KCl, 10 mM phosphate

buffer, pH 7.0 was added and this suspension was sonicated in a bath

type sonicator for 10 min. Immediately after sonication, 2 mg of spin-labeled BR was added to the phospholipid suspension, and the mixture sonicated for an additional 10 min under nitrogen.

## 25. Light-induced proton pumping and volume assays

The internal volume of the vesicles was calculated on the basis of the unquenched internal signal from 1 mM of the spin label, 2,2,6,6-tetramethylpiperdino-N-oxyl (Tempone), in the presence of 60 mM $Na_3Fe(CN)_6$ as described in (Quintanilha and Mehlhorn, 1972). The activity of the reconstituted TA-BR liposomes was tested by measuring pH gradients established by light-induced proton pumping in terms of spin-labeled amine uptake (Quintanilha and Mehlhorn, 1972). ESR spectra of TA-BR liposomes in the presence of 0.5 mM N,N'-dimethyltempamine and 57 mM $Na_3Fe(CN)_6$ show the internal unquenched N,N'-dimethyltempamine signal as clearly resolved narrow lines superimposed on a broad spectrum consisting of ferricyanide quenched spins in bulk water and the spin signal of the labeled protein. The magnitude of the background did not interfere with measurement of changes in height of the $h_{+1}$ (low field) resonance line which were used to calculate the transmembrane pH gradient. Protein was determined by using an $\varepsilon_{570} = 63,000$ $M^{-1}cm^{-1}$ in light-adapted samples.

VIII.  RESULTS AND DISCUSSION

A.  Chemical Modification of Carboxyl Groups

A method for the rapid modification of carboxyl groups in proteins under mild conditions was developed by Hoare and Koshland (1967) using water-soluble carbodiimides. Advantages inherent in this method for modification include: (1) the reaction product is stable and identifiable, (2) the reaction may be used as a quantitative procedure, (3) mild reaction conditions avoid ambiguities caused by denaturation, (4) it allows for the delineation of "buried" and "exposed" residues, and (5) variation in structure of the carbodiimide can affect which carboxyl groups are activated; and variation in charge, size, and chemical and spectral properties of the nucleophile can alter the modification at a specific carboxyl group. The water-soluble carbodiimides have been used to quantitate the number of carboxylate groups in proteins and have been used to locate active-site carboxyls in a variety of enzymes.

1.  Comparative effects of water-soluble carbodiimides

Three different water-soluble carbodiimides have been used to modify BR. All three reagents (EDC, ETC, and CMC) react similarly although differences in reagent size and charge might be expected to alter their reactivity towards certain protein groups. ETC is the quartenary ammonium analogue of EDC, and only differs in its structure by possessing a permanent positive charge at one end (Fig. 8). In this respect, it resembles the quarternary ammonium group of the morpholinyl-ethyl function of CMC.

The effects of carbodiimide modification in the presence and absence of glycine methyl ester (GME) are shown in Table I. In both

TABLE I

COMPARATIVE EFFECTS OF WATER-SOLUBLE CARBODIIMIDES[a]

| Water-soluble carbodiimide (50 mM) | Nucleophile (500 mM) | 570 nm absorbance (% of control) | Rise $t_{1/2}$ (μsec) | 412 nm intermediate Phase of Decay, $t_{1/2}$ (msec) Initial | Second | Photostationary steady-state (% of control) |
|---|---|---|---|---|---|---|
| Control | Control | 100 | 52 | 5.2 | — | 100 |
| EDC | None | 85.7 | 56 | 30 | 210 | 527 |
| EDC | GME | 98.9 | 52 | 6.0 | 12.4 | 108 |
| ETC | None | — | 52 | 13 | 184 | 500 |
| ETC | GME | — | 52 | 12 | 36 | 211 |
| CMC | None | 83.3 | 60 | 20 | 170 | 417 |
| CMC | GME | 96.4 | 52 | 6.0 | 13.2 | 103 |

[a] Reaction at pH 5.6 for 20 hrs; No additions were made to controls.

Figure 12. Kinetics of the decay of the $M_{412}$ intermediate for control

(upper time base) and carbodiimide (EDC) treated purple

membranes (lower time base) illustrating the strongly

inhibited biphasic kinetics of the EDC modified sample.

XBL 7910 - 4290
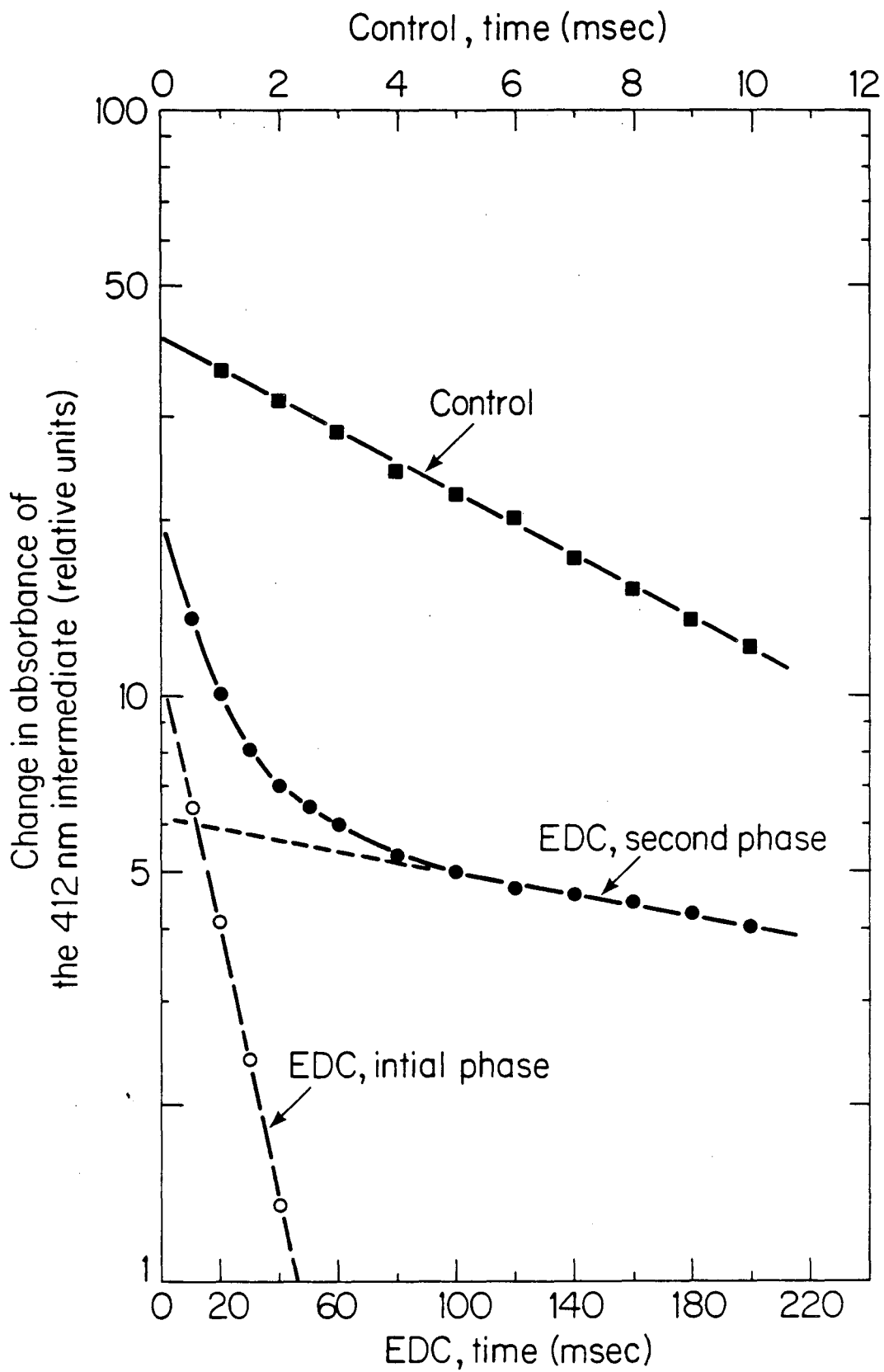
cases, the modified samples show almost no change in UV-visible spectral characteristics. The functional aspects of the modified protein were examined by determining the rise and decay kinetics of the $M_{412}$ intermediate. All modified samples retained photocycling activity and exhibited kinetics for the formation of $M_{412}$ that were similar to a control sample. However, after carbodiimide treatment in the absence of a nucleophile, a strong inhibition of $M_{412}$ decay kinetics was observed. The decay kinetics were markedly biphasic in character. As seen in figure 12, the kinetics for the initial, fast phase were determined by curve fitting the second slower phase, and extrapolating it to zero time. Then, the contribution of second phase was subtracted from the apparent initial phase to generate the corrected initial kinetics. The second phase was maximally inhibited by ETC, approximately fifty times slower than control monophasic kinetics. A striking difference in $M_{412}$ decay kinetics was apparent for samples modified in the presence of a high concentration of GME. The GME + carbodiimide-treated samples showed only a slight inhibition of $M_{412}$ decay kinetics (2-5 fold), and appeared only slightly biphasic.

## 2. Effects of nucleophile charge

Carboxyl groups on BR can be converted into amides by a two-step reaction with a water-soluble carbodiimide and an amine. Depending on the amine employed, the character of the product can be varied considerably. Its ionic character can be similar to that of the carboxyl group replaced (anionic), or it may be converted to a neutral or cationic group as desired (Fig. 13). It was therefore of interest to compare the effects of the glycine methyl ester nucleophile (neutral) on $M_{412}$

Figure 13. Structures of chemically modified carboxyl groups after water-soluble carbodiimide promoted amide formation with nucleophiles of different ionic character.

# WATER-SOLUBLE CARBODIIMIDE PROMOTED AMIDE FORMATION

$(P)-C\!\!\begin{smallmatrix}O\\\\O^-\end{smallmatrix} + NH_2-CH_2CH_2SO_3^- \xrightarrow[\text{pH 4.5-5}]{RN=C=NR'} (P)-C\!\!\begin{smallmatrix}O\\\\NH\end{smallmatrix}\!\!-CH_2CH_2SO_3^-$

Aminoethanesulfonic acid

$(P)-C\!\!\begin{smallmatrix}O\\\\O^-\end{smallmatrix} + NH_2-CH_2C\!\!\begin{smallmatrix}O\\\\OCH_3\end{smallmatrix} \xrightarrow[\text{pH 4.5-5}]{RN=C=NR'} (P)-C\!\!\begin{smallmatrix}O\\\\NH\end{smallmatrix}\!\!-CH_2C\!\!\begin{smallmatrix}O\\\\OCH_3\end{smallmatrix}$

Glycine methyl ester

$(P)-C\!\!\begin{smallmatrix}O\\\\O^-\end{smallmatrix} + NH_2-CH_2-C\!\!\begin{smallmatrix}O\\\\NH_2\end{smallmatrix} \xrightarrow[\text{pH 4.5-5}]{RN=C=NR'} (P)-C\!\!\begin{smallmatrix}O\\\\NH\end{smallmatrix}\!\!-CH_2C\!\!\begin{smallmatrix}O\\\\\overset{+}{N}H_3\end{smallmatrix}$

Glycinamide

$(P)-C\!\!\begin{smallmatrix}O\\\\O^-\end{smallmatrix} + NH_2-CH_2CH_2\overset{+}{N}H_3 \xrightarrow[\text{pH 4.5-5}]{RN=C=NR'} (P)-C\!\!\begin{smallmatrix}O\\\\NH\end{smallmatrix}\!\!-CH_2CH_2\overset{+}{N}H_3$

Ethylenediamine

80

## TABLE II

### EFFECTS OF NUCLEOPHILE CHARGE ON $M_{412}$ KINETICS[a]

| Carbodiimide | Nucleophile | $M_{412}$ decay kinetics, $t_{1/2}$ (msec) | |
| --- | --- | --- | --- |
| | | Initial phase | Second phase |
| Control | Control | 8.0[b] | — |
| None | glycinamide | 7.0 | — |
| EDC | glycinamide | 7.4 | 16 |
| None | aminoethane sulfonic acid | 6.4 | — |
| EDC | aminoethane sulfonic acid | 8.2 | 20 |
| None | ethylene-diamine | 4.6 | — |
| EDC | ethylene-diamine | 3.0 | 28 |

[a] Reaction at pH 5.6 for 20 hrs, no additions were made to control; where present, carbodiimide was 50 mM and nucleophile was 500 mM.

[b] Samples in which only an initial phase is recorded had only monophasic exponential decay kinetics.

decay kinetics with other amine nucleophiles that altered the ionic character of the modified carboxyl group.

Equivalent concentrations of aminoethanesulfonic acid (anionic), glycinamide (positive), and ethylenediamine (positive) were reacted with BR by coupling with 50 mM EDC. The kinetics of formation for the $M_{412}$ intermediate were unaffected as a result of modification. However, the $M_{412}$ decay kinetics were slightly inhibited for all the nucleophile-coupled samples, regardless of the ionic character of the carboxyamidyl product (Table II). The extent of inhibition and biphasic character were similar to that obtained with the EDC + GME modification (Table I). The $M_{412}$ kinetics in the presence of these amine nucleophile are only slightly inhibited relative to the EDC-modified sample kinetics in the absence of nucleophile. Incubation of BR with the nucleophile alone had no effect at all.

### 3. Kinetics and concentration dependence of the EDC reaction

The time course of the EDC reaction was investigated in order to follow the rate at which the $M_{412}$ decay kinetics were inhibited. The results shown in Table III indicate that after only 30 min of reaction, maximal inhibition of $M_{412}$ decay kinetics is observed. A large increase in the photostationary steady-state level of $M_{412}$ accompanies the inhibition of decay kinetics. No effect on the BR chromophore occurs as a result of modification since the $A_{570}/A_{280}$ ratio remains constant. Under these conditions, the concentration of EDC appears saturating with respect to the inhibitory site on BR.

The concentration dependence of the EDC reaction at pH 4.5 (1 hr at 25°C) was examined for its effect on the $M_{412}$ intermediate (Table IV). Laser flash photolysis revealed that concentrations as low as 1 mM

TABLE III

MAXIMAL INHIBITION OF $M_{412}$ DECAY KINETICS

BY EDC REACTION[a]

| Reaction time (min) | $A_{570}/A_{280}$[b] | $M_{412}$ decay[c] $t_{1/2}$ (msec) | 412 nm photostationary steady-state (% of control) |
|---|---|---|---|
| 0 | 1.00 | 7.4 | 100 |
| 30 | 1.03 | 130 | 597 |
| 120 | 1.00 | 136 | 647 |

[a] 50 mM EDC at pH 4.5, 25°C.

[b] Control $A_{570}/A_{280}$ ratio normalized to a value of 1.00.

[c] Samples suspended in 10 mM NaCl, 1 mM MES, pH 6.5. Value of the second phase of the biphasic decay is given for modified samples.

## TABLE IV

### CONCENTRATION DEPENDENCE OF THE EDC REACTION[a]

| EDC (mM) | $M_{412}$ decay[b,c] $t_{1/2}$ (msec) | 412 nm photostationary[c] steady-state (% of control) |
|---|---|---|
| 0.0 | 6.0 | 100 |
| 1.0 | 62 | 484 |
| 5.0 | 110 | 1220 |
| 10.0 | 115 | 1355 |
| 25.0 | 145 | 1400 |
| 50.0 | 185 | 1449 |

[a] Reaction at pH 4.5 for 1 hr at 25°C.

[b] Value of the second phase of the biphasic decay kinetics is given for modified samples.

[c] Samples suspended in 100 mM NaCl, 1 mM MES, pH 6.5.

inhibited $M_{412}$ decay with characteristic biphasic kinetics. EDC con-
centrations resulted in progressively greater inhibition, but appeared
to saturate at the highest concentrations. The second phase of $M_{412}$
decay contributed a larger proportion of the total signal as the decay
time lengthened. The 412 nm photostationary steady-state demonstrated
large increases that paralleled the slower $M_{412}$ decay kinetics.

### 4. Inhibition of $M_{412}$ decay kinetics by a hydrophobic reagent, EEDQ

EEDQ is a hydrophobic, highly specific reagent for the activa-
tion and modification of carboxyl residues (Belleau and Malek, 1968).
It had been previously characterized as behaving like a carbodiimide
(Godin and Schrier, 1970; Pougeois et al., 1978) and its hydrophobic
character may increase its accessibility to buried carboxyls in the
purple membrane interior relative to the water-soluble carbodiimides.
Low concentrations (< 10 mM) of EEDQ had no effect on the position of
absorption maximum or on the extinction coefficient of the 570 nm BR
band. However, higher concentrations resulted in progressive bleaching
of the retinal-protein chromophore.

The effect of EEDQ modification on the $M_{412}$ intermediate was
investigated. Laser flash photolysis of modified samples showed that
almost a 10-fold lower concentration of EEDQ (5 mM) relative to EDC
(50 mM) resulted in a similar strong inhibition of $M_{412}$ decay kinetics
(Table V). Increasing concentrations of either EEDQ or EDC resulted in
a progressively slower, biphasic decay of the $M_{412}$ intermediate (see
Figure 12). The effect saturated at 5 mM for EEDQ and $\simeq$ 50 mM for
EDC. As with EDC modification, the second phase of the decay contributed
a larger proportion of the total signal as the decay time lengthened.

TABLE V

EFFECT OF EEDQ CONCENTRATION ON THE $M_{412}$ INTERMEDIATE[a]

| EEDQ (mM) | $M_{412}$ decay[b,c] $t_{1/2}$ (msec) | 412 nm photostationary[c] steady-state (% of control) |
|---|---|---|
| 0.00 | 4.0 | 100 |
| 0.50 | 44 | 513 |
| 1.25 | 52 | 695 |
| 2.50 | 88 | 709 |
| 5.00 | 88 | 870 |

[a] Reaction in 0.10 M MES, pH 6.0 for 1 hr at 25°C.

[b] Value of the second phase of the biphasic decay kinetics is given for the modified samples.

[c] Samples suspended in 100 mM NaCl, 1 mM MES, pH 6.5.

Large increases in the $M_{412}$ photostationary steady-state were a direct result of the inhibited $M_{412}$ decay kinetics.

### 5. Circular dichroism of modified purple membranes

Circular dichroism (CD) spectra for carboxyl modified BR were recorded to assess whether there were any localized changes in the protein structrue that would affect the chromophore. The major features in the visible region of the CD spectrum (figure 14) are a positive band centered at 535 nm and a negative band centered at 600 nm with a crossover at 575 nm. These bands have been attributed to exciton coupling between the retinyl chromophores in the regular trimeric structure of the membrane (Becher and Cassim, 1977). The positive band is more intense than the negatve band, which indicates that part of the contribution is due to induced optical activity in the retinyl chromophore by the protein environment.

The spectrum for unmodified BR closely resembles spectra already published for this region. The visible CD spectra of 50 mM EDC and 250 mM GME + 50 mM EDC modified samples retain the same bilobed features as the control spectrum. There is an apparent shift of about 5 nm to the red for the EDC and GME + EDC modified samples with no significant differences in the ellipticity values. The very small wavelength shift of the positive band is also evident in the 5 mM EEDQ and 250 mM GME + 5 mM EEDQ treated sample spectra. The different intensities can be attributed to slight variations in the protein concentration of the samples.

### 6. Amino acid analysis

The number of carboxyl residues modified by reaction of EDC with

Figure 14.  Visible CD Spectra of Carboxyl Modified Samples.
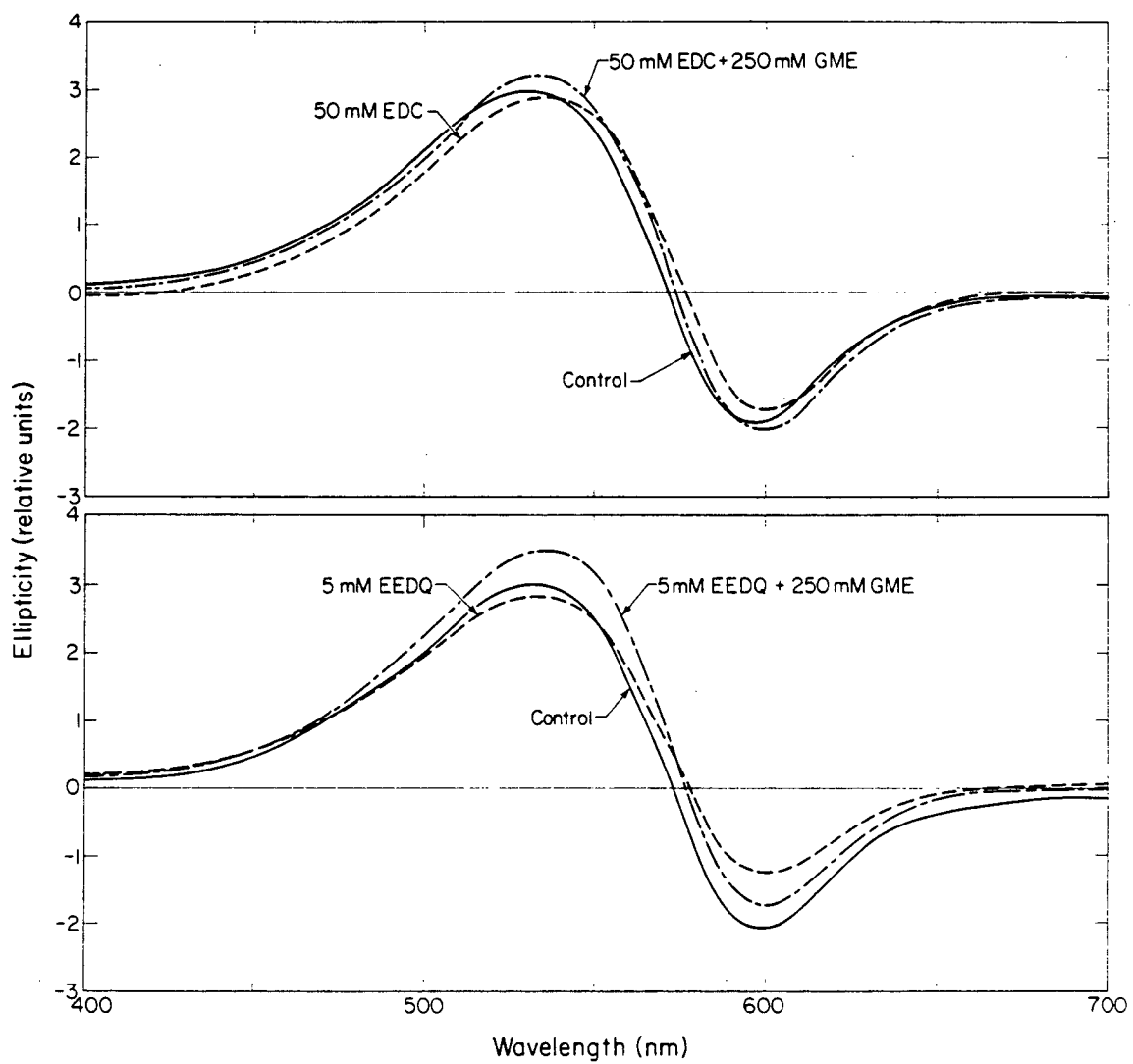
glycine methyl ester can be determined by standard amino acid analysis. The number of modified residues is the difference in the number of glycine residues observed in the reacted and unreacted samples. A summary of the amino acid analysis of a control sample incubated with an equivalent concentration of GME nucleophile and no coupling agent, and 500 mM GME + 50 mM EDC is presented in Table VI. The results are in close agreement with the published compositions from several different laboratories. The number of glycine residues in the unmodified protein (24) was found to be identical with the sample incubated with the nucleophile alone (24). This shows that all unreacted GME was effectively removed prior to analysis. The GME + EDC sample contained 36 glycine residues, 12 residues in excess of the control samples. Thus, 12 carboxyl residues were converted to glycine methyl ester amide products under these defined reaction conditions.

Carbodiimides may also react with either sulfhydryl or tyrosine residues in addition to carboxyl residues (Carraway and Koshland, 1972). The rates of reaction of model sulfhydryl and carboxyl compounds with EDC are approximately equal, while tyrosine reacts more slowly (Carraway and Koshland, 1972). Bacteriorhodopsin contains no sulfhydryl residues and 11 tyrosines. The number of modified tyrosine residue can be quantitated by amino acid analysis since the product is stable to acid hydrolysis (Carraway and Koshland, 1968). The amino acid analysis shows no differences in tyrosine content between control and modified samples, and thus this possible side reaction does not occur.

### 7. Intermolecular cross-linking of BR by carbodiimides

Samples modified by EDC or ETC reactions were subjected to SDS-polyacrylamide gel electrophoresis. Extensive cross-linking between

TABLE VI

AMINO ACID COMPOSITION OF CARBOXYL MODIFIED BACTERIORHODOPSIN[a]

| Amino Acid | Control | + GME | GME + EDC | Expected[b] |
|---|---|---|---|---|
| Aspartic acid | 13 | 14 | 14 | 12 |
| Threonine | 15 | 15 | 16 | 18 |
| Serine | 9 | 9 | 9 | 13 |
| Glutamic acid | 15 | 15 | 15 | 12 |
| Glycine | 24 | 24 | 36 | 25 |
| Alanine | 29 | 29 | 28 | 29 |
| Valine | 20 | 20 | 20 | 21 |
| Methionine | 7 | 7 | 8 | 9 |
| Isoleucine | 13 | 13 | 13 | 15 |
| Leucine | 35 | 36 | 36 | 36 |
| Tyrosine | 10 | 10 | 10 | 11 |
| Phenylalanine | 12 | 12 | 12 | 13 |
| Lysine | 6 | 6 | 6 | 7 |
| Arginine | 7 | 7 | 6 | 7 |
| Histidine | 0 | 0 | 0 | 0 |
| Cysteine | 0 | 0 | 0 | 0 |

[a] Hydrolysis in 6 N HCl at 110°C for 24 hr.

[b] From Khorana et al. (1979).

BR monomers resulted in the loss in intensity of the 26,000 molecular weight band and the appearance of new, higher molecular weight bands that corresponded to dimers, trimers and higher molecular weight oligomers. In addition, some cross-linked material was unable to enter the separation gel, indicative of extremely high molecular weight aggregates. Cross-linking was extensive in samples that had reacted for only 30 minutes, and the pattern did not change substantially with longer reaction time periods.

Addition of an external nucleophile, GME, during the EDC reaction reduced the extent of cross-linking in a concentration dependent manner. Low concentrations of GME were relatively ineffective, while higher concentrations (100-200 mM) almost completely inhibited the formation of higher molecular weight aggregates. Reaction with GME forms a carboxyl-glycine methyl ester amide linkage that prevents cross-linking. In marked contrast to results of the EDC reaction, EEDQ showed no evidence of intermolecular cross-linking.

### 8. Discussion

#### a. Comparative effects of water-souble carbodiimides and nucleophile charge

Three water-soluble carbodiimides used to modify carboxyl groups on BR have been found to exert similar, specific inhibitory effects on the reprotonation phase of the photocycle. Despite differences in reagent size and charge characteristics, they produced nearly identical inhibition of the decay kinetics of the $M_{412}$ intermediate. Nucleophile promoted amide formation of BR carboxyl groups with carbodiimides resulted in a different pattern of inhibition that was also confined to the reprotonation phase of the photocycle. Although carboxyamidyl

modified BR was substantially less inhibited in $M_{412}$ decay than only carbodiimide-treated BR, the amide-coupled samples revealed similar changes regardless of specific carbodiimide employed. The modification's specificity for the inhibitory effect on $M_{412}$ decay kinetics and apparent lack of effect on general protein structure suggest a critical carboxyl residue(s) involved in the photocycle mechanism is modified by all three carbodiimide reagents. The similarities in the pattern of the inhibition by EDC, ETC and CMC suggest they act at a common "inhibitory site" by the same biochemical mechanism.

Conversion of carboxyl groups into amides of different ionic character allowed isolation of the role of carboxyl ionic charge in BR. Substitution of carboxyl residues with aminoethanesulfonic acid retains the gross ionic charge of BR, and the individual anionic loci are merely displaced a few angstroms from the protein. Modification with other amines of identical molecular size and different only in charge (neutral and positive) did not significantly change $M_{412}$ decay kinetics compared to the anionic control modification. The slightly greater inhibition obtained with glycinamide and ethylenediamine may be due to potential cross-linking between the "second" amino group on the nucleophile and a second protein carboxyl group. Thus, the ionic character of the modified carboxyl group(s) are not a determining factor in the decay of the $M_{412}$ intermediate.

### b.  BR structure after modification

To directly correlate carboxyl group modification by carbodiimides or EEDQ with the inhibitory effect on photocycle kinetics, it is necessary to exclude the possibility that modification has caused a non-specific structural change in BR. The retinal-protein chromophore may

be used as an internal reporter group that reflects BR protein structure (Muccio and Cassim, 1979). All carbodiimides tested had no effect on the position of the absorbance maximum or intensity of the retinal-protein absorbance band, indicating no significant perturbations of the protein structure have occurred.

CD spectra provide additional information concerning structural interactions between the chromophore and the protein; as well as general membrane structure in the case of purple membrane sheets. The exciton CD couplet is characteristic of the trimer structure since it has been shown that the monomeric state is characterized by only a positive CD band centered at the absorption maximum (Cherry et al., 1978). It was shown that BR incorporated into phosphatidylcholine vesicles exists in a crystalline lattice below the phase transition temperature, while above the phase transition, the protein molecules are monomeric. Reversible changes in the visible CD accompany changes in the aggregation state of the BR molecules. Similar observations have shown that solubilization of BR in Triton X-100 and octyl-β-D-glucoside leads to formation of protein monomers (Dencher and Heyn, 1978) that have altered visible absorption and CD spectra. The major conclusions that can be derived from the similarity of the control and carboxyl-modified CD spectra are: (1) no significant perturbation of the protein-chromophore environment has occurred as a result of carboxyl modification and, (2) carboxyl modified purple membrane sheets retain the two-dimensional hexagonal lattice of trimers characteristic of purple membrane structure. The retention of crystallinity by the carboxyl modified purple membranes has also been confirmed by analysis of electron diffraction patterns (J. Jaffe and R. Glaeser, personal communication).

## c. Possible locations of modified carboxyl groups

Amino acid analysis was used to show that 12 carboxyl groups are converted to glycine methyl ester-amides by EDC using high reagent concentrations and long reaction times. These extensive reaction conditions suggest that the unreacted groups are determined by constraints of the native BR structure. Since there are 19 carboxyl residues in the protein, 9 aspartate, 9 glutamic, and 1 carboxyl terminus of serine (Khorana et al., 1979), we may infer that 7 carboxyl residues recalcitrant to modification are "buried" residues. Similar chemical modification procedures using EDC promoted amide formation with either glycine methyl ester, glycinamide, or aminoethanesulfonic acid as a nucleophile, showed that unreactive carboxyl residues in lysozyme or trypsin became available to modification under denaturing conditions (Eyl and Inagami, 1971; Lin and Koshland, 1969). In general, the modification studies provided structural information which supported crystallographic findings. The studies were complementary since groups that crystallographic findings placed on the surface were modified, while those located in the enzyme cleft were resistant to modification. The decreased reactivity of seven carboxyls in BR might be due to either a hydrophobic environment or potential steric hindrance of the chemical modification reagents to the reactive site.

The reactive carboxyl group(s) that results in strong inhibition of $M_{412}$ decay kinetics is accessible to both the water-soluble carbodiimides and the hydrophobic EEDQ reagent. The relative higher inhibitory efficacy of EEDQ compared to EDC may be explained by the preferential partitioning of the more hydrophobic reagent into the membrane phase. In this way, the effective concentration of EEDQ in the membrane phase

may be elevated compared to EDC given initially identical bulk aqueous phase concentrations of the two reagents. A possible explanation for the fact that EDC may react in a hydrophobic environment may be given by considering the analogy between EDC and alkyl-trimethylammonium salt (n = 8) molecular structures. If the diimide structure of EDC is considered similar to alkyl carbons in a hydrocarbon chain, then EDC might act as a positively charged ionic amphiphile. It would partition into the purple membrane with the tertiary amine group at the surface and the diimide "alkyl" chain oriented parallel to the lipid alkyl chains. This would place the reactive diimide group about 6 carbon-carbon bond lengths ( ≃7.5 Å) from the surface of the membrane in a hydrophobic environment. Thus, the inhibitory site that is EEDQ and EDC reactive may reside in a relatively hydrophobic environment.

The location of carboxyl group(s) involved in forming intermolecular BR cross-links can be suggested from this and other studies. Similar observations of BR cross-linking by EDC reaction at pH 4.5 were made by Renthal et al. (1979). In addition, it was found that treatment of BR with papain prior to reaction with EDC, resulted in almost no cross-linking. The papain treatment cleaves the C-terminal tail from the membrane, which contains five carboxyl groups: two aspartates, two glutamates, and the terminal carboxyl. Thus, the cross-linking reaction must occur between carboxyls on the C-terminal tail and nucleophilic groups located on the surface of the PM. This study further showed that addition of an external nucleophile strongly inhibited cross-linking. Addition of nucleophile such as GME results in competition with endogenous BR nucleophilic groups for the activated carboxyl, and hence prevents cross-linking reactions from occurring. It is important to note that

the carbodiimide cross-linking reaction that occurred on the membrane surface was not catalyzed by the more hydrophobic EEDQ reagent.

B. Structural Role of Carboxyl Groups in the Photocycle

As shown in the previous section, chemical modification of carboxyl groups by water soluble carbodiimides causes an inhibitory effect on the photoreaction cycle of bacteriorhodopsin. The addition of a nucleophile, regardless of its ionic character, substantially reduced the $M_{412}$ decay inhibition. The mechanism of inhibition and nucleophile reversal was difficult to define since modification resulted in extensive intermolecular cross-linking, as well as possible intramolecular cross-links and N-acylurea products (Carraway and Koshland, 1968). It was therefore of interest to find reaction conditions or other carboxyl modification reagents which eliminated this multiplicity of reaction products. Since EEDQ treatment does not result in intermolecular cross-linking, the role this plays in the inhibition of $M_{412}$ decay kinetics can be ascertained. The concentration dependence of nucleophile promoted amide formation utilizing GME and EEDQ was therefore studied and compared to similar modifications using GME and EDC. The role of intramolecular cross-linking by lysine residues was studied by double modification procedures which first blocked lysyl residues. The effects of carboxyl modification on the $O_{640}$ intermediate and acid-induced blue species were also characterized since carboxyl residues have been hypothesized to be essential for their function.

1. Reversal of inhibition of $M_{412}$ decay kinetics by glycine methyl ester

Treatment of purple membranes with EEDQ resulted in an inhibition of $M_{412}$ decay kinetics with no effect on $M_{412}$ formation, as found previously with EDC treatment (Packer et al., 1979). Addition of a nucleophile (GME) prior to addition of the carboxyl-activating reagents

resulted in partial reversal of the maximal inhibition of $M_{412}$
decay observed after treatment with the carboxyl-activating reagents
alone. The effectiveness of reversal was dependent on GME concentration
(1-250 mM) during the modification reaction. GME was equally effective
when used in conjunction with either EDC or EEDQ reagents (Fig. 15).

The strong biphasic nature of the $M_{412}$ decay is apparent in all
modified samples. Each decay curve was fitted as the sum of two expo-
nential decay processes. Semilogarithmic plots of $M_{412}$ absorbance versus
time showed a straight-line plot for the second, slower phase of the
decay when generated by either computer-programmed routines or by
hand-graphing techniques. It was found that the yield of $M_{412}$ inter-
mediate was independent of the nucleophile concentration employed. The
GME concentration primarily determined the kinetics of the second,
slower phase and its overall contribution to the total $M_{412}$ signal.
The intersection of the extrapolated, dotted lines in Fig. 15 shows
that increasing GME concentrations decreased the contribution of slower
kinetic phase to the $M_{412}$ decay.

2. Effect of lysine modification prior to carboxyl-activating
   reagent treatment

In order to test the idea that $\varepsilon$-amino groups of lysine acted as
an endogenous nucleophile in the EDC or EEDQ reaction, a double modifi-
cation procedure which first blocked lysine residues was developed.
The reaction of lysines with a monofunctional imidoester results in the
conversion of the group to an amidine product (Means and Feeney, 1971)
which is no longer capable of forming an intramolecular cross-linking
product. Purple membranes were first treated with a range of ethyl
acetimidate (EA) concentrations, 1-200 mM, and analyzed to determine

Figure 15. Reversal of Inhibition of $M_{412}$ Decay Kinetics by GME.

$M_{412}$ decay kinetics of samples modified by (a) 10 mM EDC, pH 4.5 for 1 hr and (b) 5 mM EEDQ, pH 6.0 for 1 hr; in the presence of different concentrations (indicated for each curve) of glycine methyl ester nucleophile. Laser flash photolysis conducted at 20°C. Kinetic data obtained from the summation of 20 individual scans for each sample.
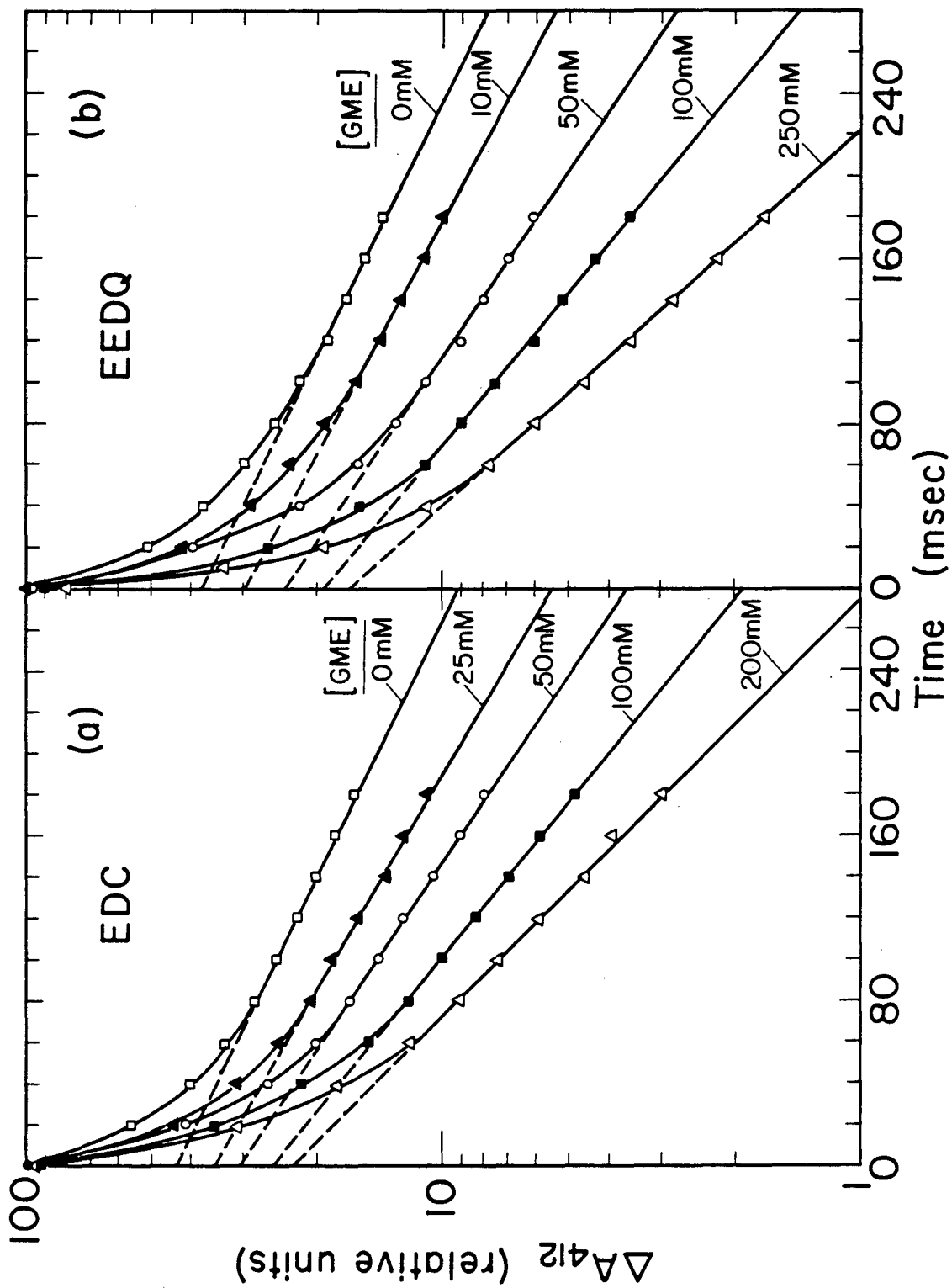
the percentage of free amino groups remaining by the fluorescamine method (Bohlen et al., 1971). The maximal fluorescence obtained in control samples corresponds to six available lysine residues. The results presented in Table VII show the number of lysines modified by increasing concentrations of EA alone and for the 50 mM EDC reaction alone. As shown, 50 mM EDC alone modified 1.2 lysine residues. EDC treatment also modifies a single lysine when the sample has been pre-reacted with 2-5 mM EA which modified up to 2 lysines. Higher EA concentrations (25-200 mM), pre-reacts all available lysines and no additional modification by EDC occurs. In the converse experient, pre-reaction with EDC followed by EA modification, one additional residue is modified below the saturation level. Thus, the EA and EDC reactions are strictly "additive" if less than 3 lysines are modified by the first modification reagent. However, as seen in Table VII, the same level of modification occurred in the 10 mM EA sample (2.7 lysines) as in the 10 mM EA sample that had been pre-reacted with 50 mM EDC (3.3. lysines). Under these conditions, the number of lysines modified (3) was not the sum of the individual reactions (4). When all available lysines (5 of 6) are modified at or above 25 mM EA, no additional lysine modification is possible by subsequent EDC reaction.

The functional consequences of the lysine-carboxyl double modification on the photocycle were determined by studying the $M_{412}$ decay kinetics. In figure 16, the kinetics of the 50 mM EDC reaction alone, 200 mM EA alone, 200 mM EA modification prior to 50 mM EDC treatment, 50 mM EDC treatment prior to EA modification, and the effect of 200 mM GME + 50 mM EDC are compared. As shown previously, when purple membranes were treated with 200 mM ethyl acetimidate, it was found that 5 out

## TABLE VII

### NUMBER OF LYSINES MODIFIED BY EA/EDC AND EDC/EA DOUBLE MODIFICATIONS

| Lysine or carboxyl modification alone | | Prior modification of lysine residues | | Prior modification of carboxyl residues | |
|---|---|---|---|---|---|
| EA(mM) | Number of Lysines Modified | EA(mM)/EDC[a] | Number of Lysines Modified | EDC/EA(mM)[a] | Number of Lysines Modified |
| Control | 0 | Control | 0 | Control | 0 |
| 2.0 | $1.1 \pm 0.1$ | 2.0 | $2.3 \pm 0.1$ | 2.0 | $2.3 \pm 0.2$ |
| 5.0 | 1.8 | 5.0 | $2.9 \pm 0.3$ | 5.0 | $2.9 \pm 0.1$ |
| 10.0 | $2.7 \pm 0.1$ | 10.0 | − | 10.0 | $3.3 \pm 0.2$ |
| 25.0 | $4.1 \pm 0.1$ | 25.0 | $4.4 \pm 0.5$ | 25.0 | − |
| 50.0 | $4.8 \pm 0.1$ | 50.0 | $4.7 \pm 0.1$ | 50.0 | $4.8 \pm 0.1$ |
| 200.0 | $4.8 \pm 0.1$ | 200.0 | $4.9 \pm 0.4$ | 200.0 | − |
| 50 mM EDC | $1.2 \pm 0.4$ | | | | |

[a] EDC concentration in all double-modified samples was 50 mM.

Figure 16. $M_{412}$ Decay Kinetics of Lysine-Carboxyl Double Modified BR.

The $M_{412}$ decay kinetics of 200 mM ethyl acetimidate-treated BR
(EA), EA modification prior to 50 mM EDC treatment (EA/EDC), and 50 mM
EDC treatment prior to EA modification (EDC/EA) are shown. The decay
kinetics of 50 mM EDC alone and 200 mM GME + 50 mM EDC modified samples
are shown for comparison. Laser flash photolysis was conducted on
samples suspended in 0.10 M NaCl, 0.01 MES, pH 6.5 at 20°C.
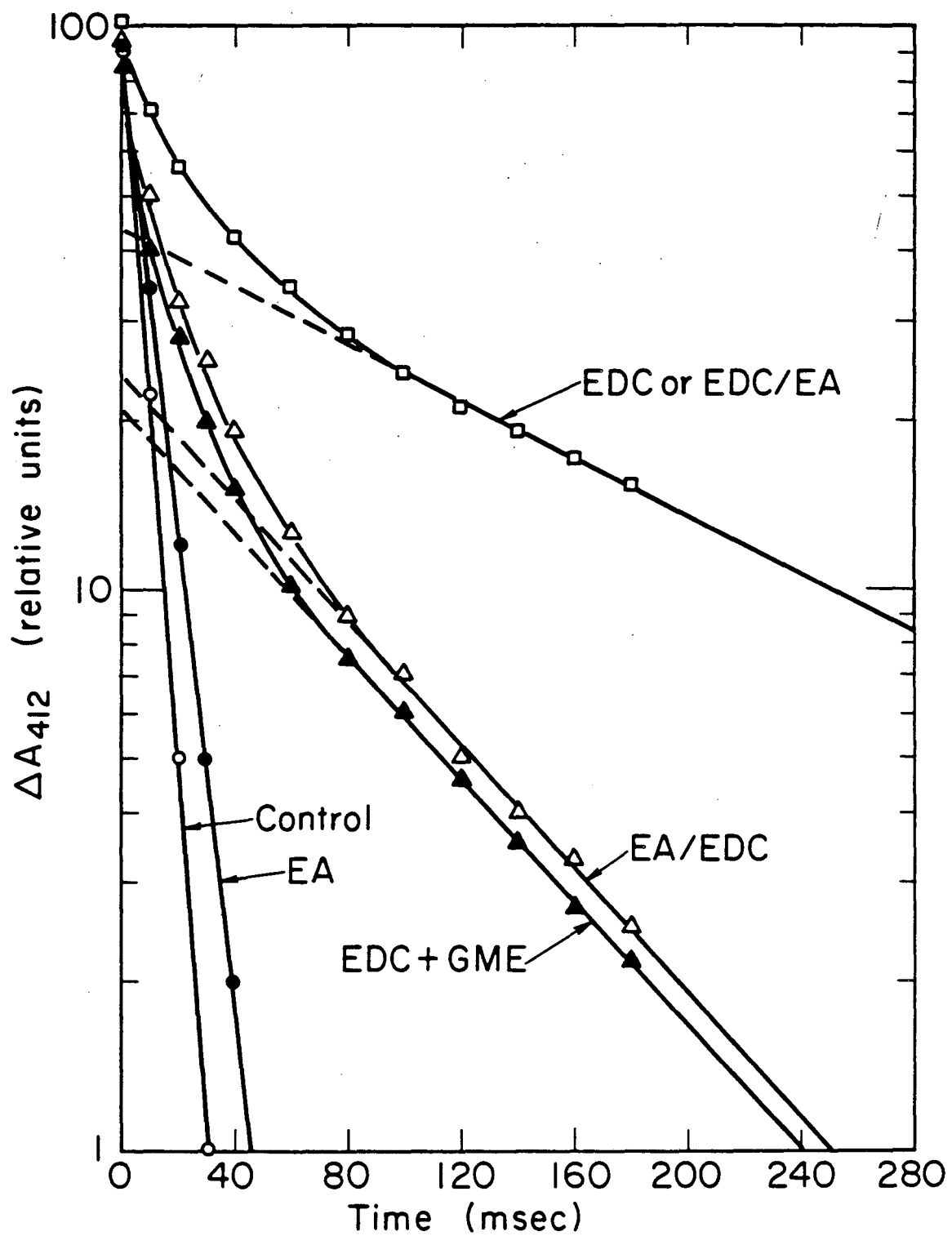
XBL 8010-3790

of 6 available lysines in BR were modified. This represents maximal modification since lysine residues 41 and 216 (which bears the retinyl-lysine Schiff-base linkage) are not reactive (Moore et al., 1980). Flash photolysis revealed a minimal effect of lysine modification on $M_{412}$ decay kinetics. Subsequent treatment of 200 mM EA lysine-modified BR by EDC (50 mM) showed that inhibition of $M_{412}$ decay was greater than only EA treated, but was substantially less than EDC treatment alone. The kinetics of $M_{412}$ decay in the EA/EDC double modification were virtually identical to those obtained with EDC + 200 mM GME. When the order of modification was reversed (EDC followed by EA), no difference was observed compared to EDC treatment alone. When EA modified samples were subsequently modified by EDC + GME, instead of EDC alone, the kinetics of $M_{412}$ decay also did not show any additional significant reversal with respect to EA/EDC treatment (data not shown). Thus, GME was no longer effective in reversing inhibition when lysines were first converted to amidine products by EA. Similarly, EA modification prior to EEDQ treatment also caused partial reversal of $M_{412}$ decay inhibition, although the effect with EDC was more pronounced.

The reversal of inhibition of the $M_{412}$ decay kinetics was correlated with the extent of lysine modification. As seen in Table VIII, the slow, biphasic decay of the 50 mM EDC sample is not greatly affected in the 2 mM EA/EDC or 5 mM EA/EDC samples. However, a large decrease occurs at 10 mM EA/EDC, which does not differ greatly from the value obtained at 200 mM EA/EDC concentrations. Thus, only after the third lysine residue is converted to an amidine product, is there a dramatic decrease (138 msec to 73 msec) in inhibition of $M_{412}$ decay kinetics. $M_{412}$ decay kinetics directly correlates with the concentration of EA

## TABLE VIII

### EFFECT OF EA/EDC DOUBLE MODIFICATIONS ON $M_{412}$ DECAY KINETICS

| BR sample | Fraction of total (6) lysines modified | $M_{412}$ Decay $t_{1/2}$ (msec) | |
|---|---|---|---|
| | | Initial phase | Second phase |
| Control | 0 | 4.3 | — |
| 200 mM EA | 0.80 | 6.0 | — |
| 50 mM EDC | 0.20 | 25 | 165 |
| 2 mM EA/EDC[†] | 0.38 | 12 | 145 |
| 5 mM EA/EDC | 0.48 | 12 | 138 |
| 10 mM EA/EDC | — | 13 | 73 |
| 50 mM EA/EDC | 0.78 | 6.0 | 85 |
| 200 mM EA/EDC | 0.82 | 9.9 | 54 |

[†] Final concentration of EDC for all double modified samples is 50 mM.

that is required to compete with EDC for reaction with a single lysine residue.

### 3. Apparent absence of photointermediate $O_{640}$ and kinetics of reformation of $BR_{570}$

The effects of carboxyl modification on the $O_{640}$ intermediate were studied since it has been suggested that a carboxyl group(s) is responsible for formation of this transient photocycle chromophore (Fisher and Oesterhelt, 1980). At 650 nm, control purple membranes (pH 6.5, 20°C) showed the typical pattern for the $O_{640}$ intermediate of an initial negative absorbance change which is quickly reversed and yields a positive peak followed by a slow decay (Fig. 17). The magnitude of the initial negative absorbance is apparently a contribution from the large negative change in absorbance that occurs at 570 nm. This was visualized by computer subtraction of the flash photolysis signal at 560 nm from the signal obtained at 650 nm. The magnitude of the sub-tracted signal is based on the relative absorbance at the two wavelengths. The corrected flash photolysis kinetics are true kinetics for the 'O' intermediate (data not shown).

Carboxyl-modified samples exhibited an entirely different pattern at 650 nm from controls. In both EEDQ and EEEQ + GME modified prepara-tions analyzed at 20°C, an initial negative transient absorbance response appeared, but it was followed by a gradual increase in absorbance towards the baseline and no further. Kinetic analysis of these traces at longer time periods confirmed that positive absorbance at 650 nm did not develop. Increasing the temperature to 40°C, which normally substantially favors $O_{640}$ intermediate formation (Moore et al., 1978), revealed a positive absorbance at 650 nm in the modified samples.

Figure 17.  Effect of EEDQ Carboxyl Modification on the Photocycle

of M (410 nm), O (650 nm), and BR (560 nm) Intermediates.

The effect of temperature on the kinetics of control and EEDQ-
treated samples are shown illustrating the apparent absence of the 'O'
intermediate in the EEDQ sample at 20°C.
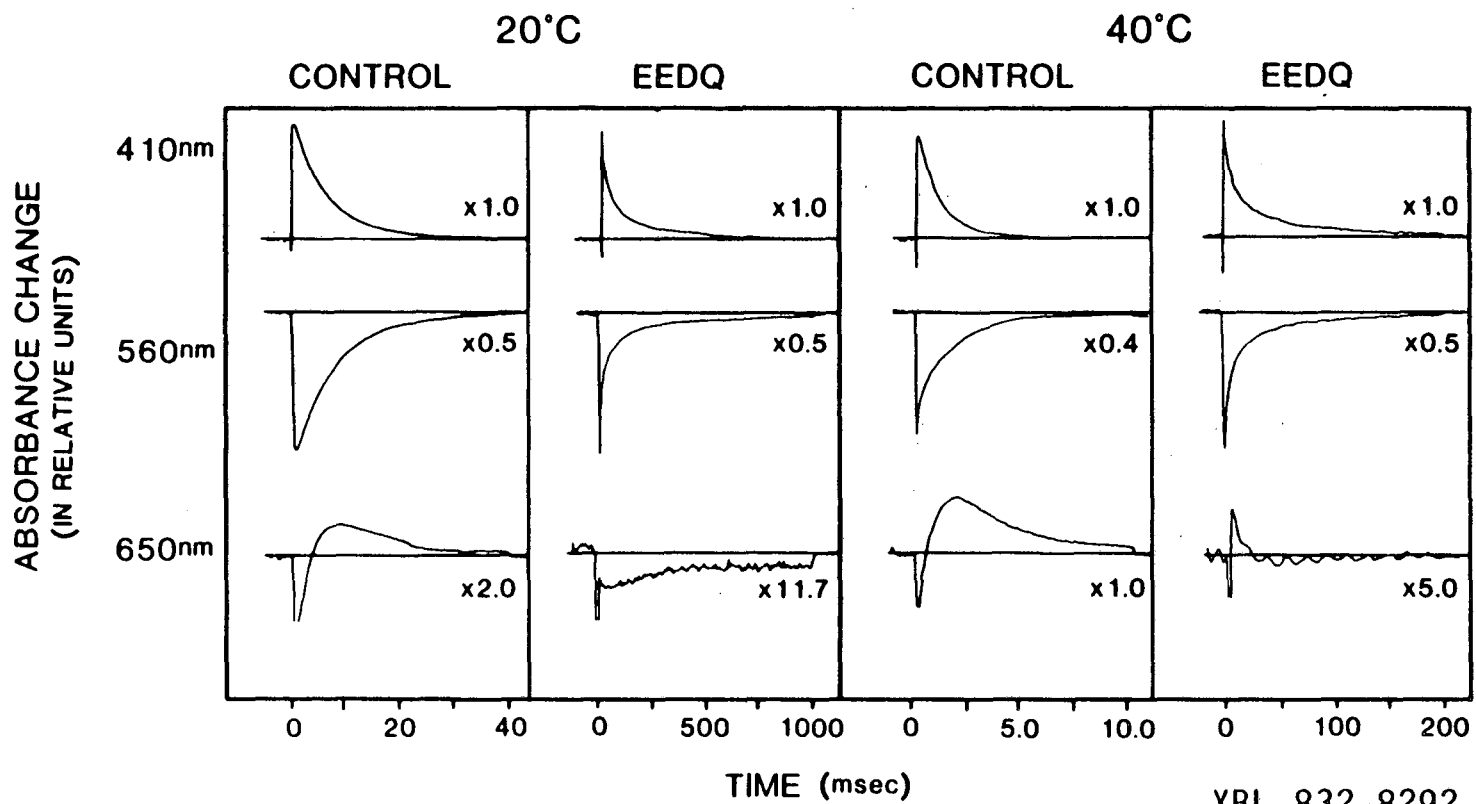
XBL 832-8292

Figure 18.  Effect of EDC and GME + EDC on the Photocycle Kinetics

of M (410 nm), O (650 nm), and BR (560 nm) Intermediates.

The apparent absence of the $O_{650}$ intermediate is seen in the
carboxyl modified samples at 20°C.
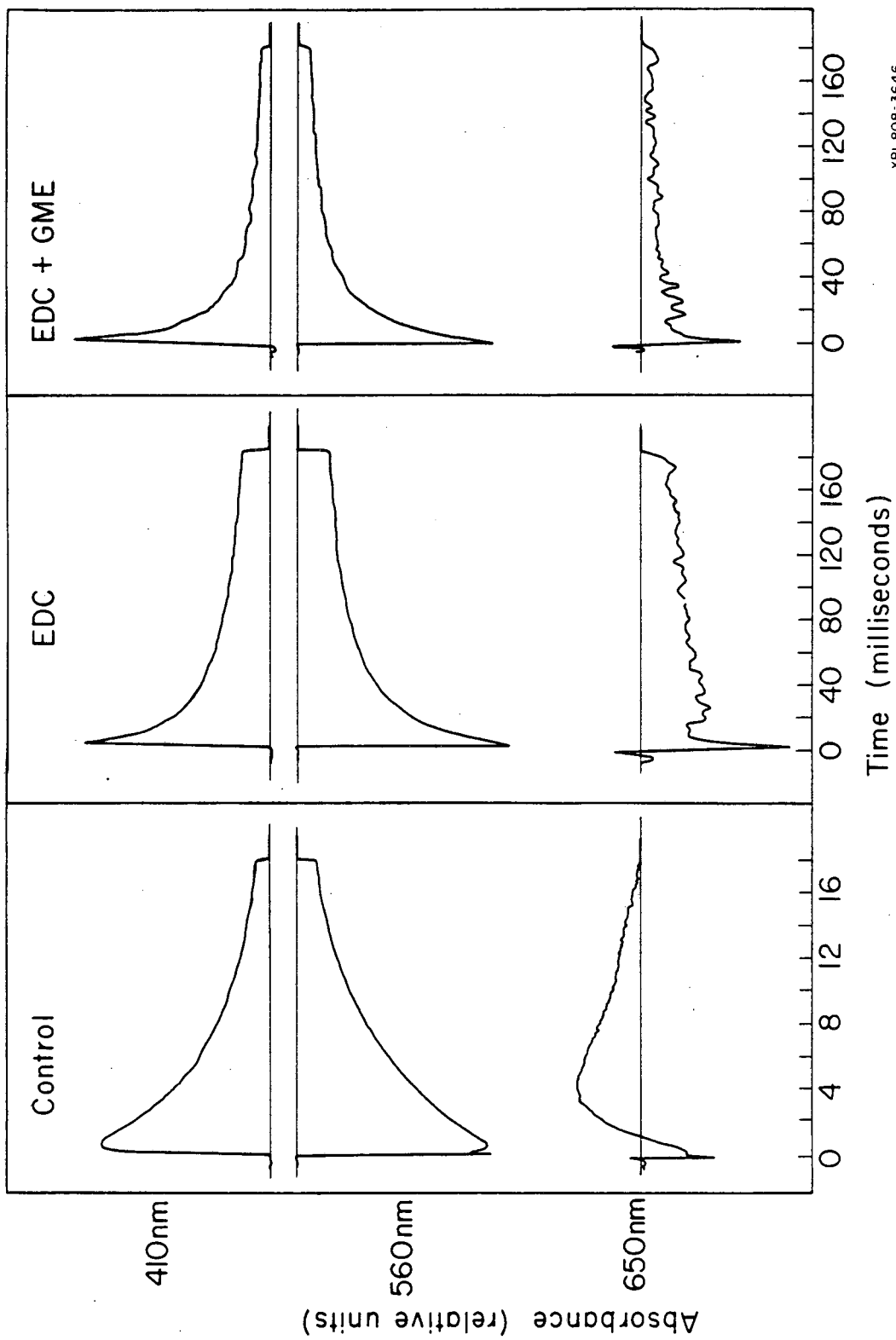
XBL 808-3646

This positive absorbance appeared in the same time domain as the signal from control samples at 40°C indicating the kinetics of the $O_{640}$ intermediate are substantially unaltered.

The apparent kinetics of the increase in absorbance at 650 nm were similar to both the kinetics of the second phase of $M_{412}$ decay and reformation of $BR_{570}$ for all carboxyl modified samples. The results obtained from EDC and EDC + GME modified samples also revealed the absence of positive absorbance at 650 nm and similar kinetic parameters for $M_{412}$ decay and $BR_{570}$ reformation (Fig. 18).

Flash photolysis conducted on samples at pH 3.0 showed that the overall shape of the control response was similar to that obtained at neutral pH, although the magnitude of the response at 650 nm is increased and the decay process is greatly slowed. However, EDC modified samples photolyzed at pH 3.0 showed no positive absorbance at 650 nm, but a complex negative absorbance response.

4. Effects of carboxyl-modification on the formation of the acid-induced species

In order to examine the possible relationship between the $O_{640}$ intermediate, the acid-induced species, and protein carboxyl groups; the formation of the $O_{640}$ intermediate was studied in modified membranes. Acid titration of purple membranes is known to induce a red shift in the absorption spectrum, leading to formation of an acid species absorbing maximally at 600-610 nm. This effect is reversible since the original spectrum can be regenerated by addition of base (Moore et al., 1978). Difference spectra of control purple membranes at pH 7.0 (25°C) and samples at various acid pH values revealed a substantial decrease in absorbance at about 550 nm and a concommitant absorbance increase of

Figure 19. Difference Spectra of the Blue, Acid-Induced BR Chromophore.

   a) Acid titration of control purple membranes. The inset
shows that the pK = 3.5 for the transition.

   b) Acid titration of 50 mM EDC modified purple membranes.
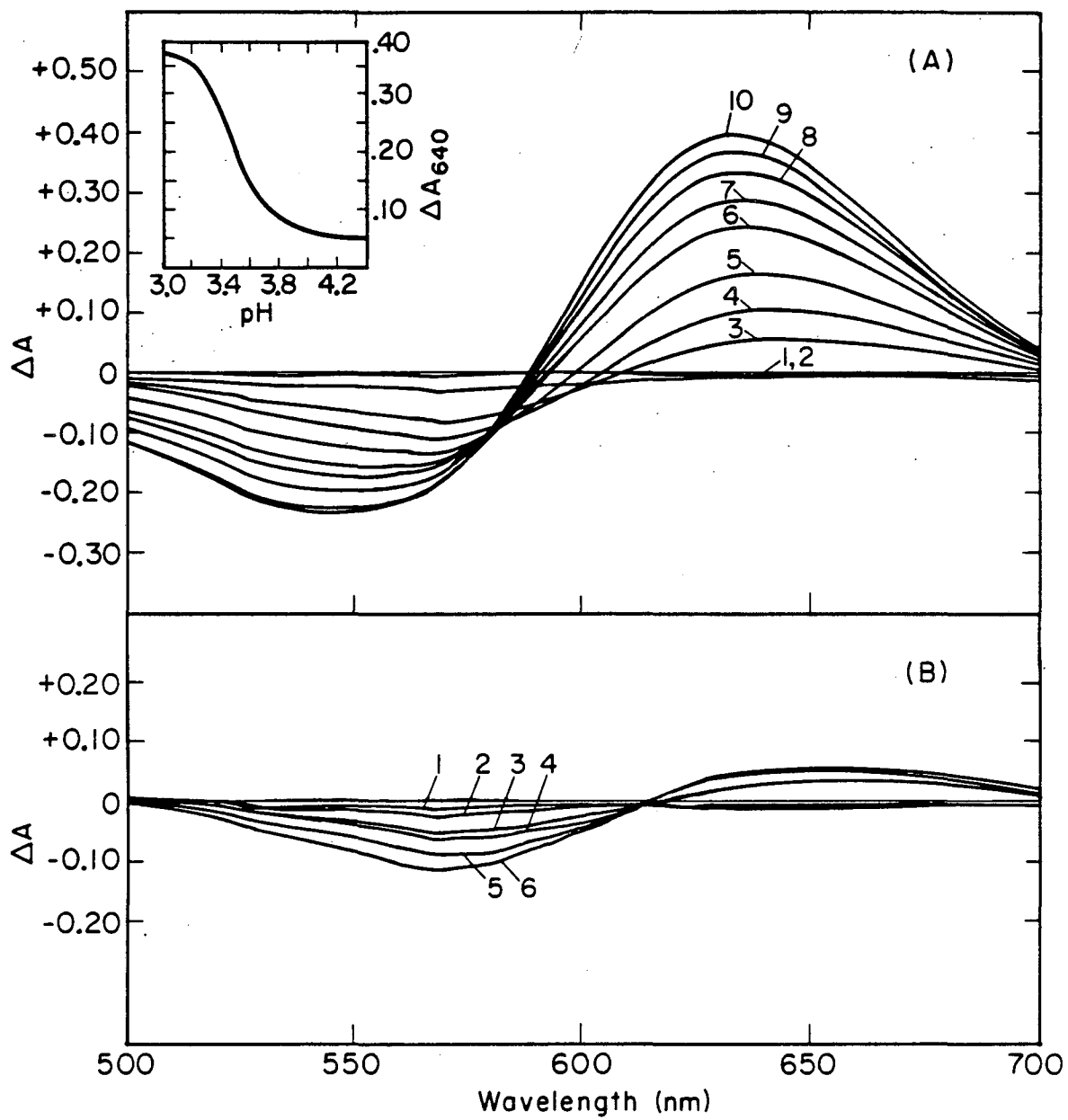
XBL808-3644

a broad band centered at 640 nm (Fig. 19a). A plot of $A_{640}$ vs. $\Delta pH$ revealed that the 640 nm peak had a pK = 3.5 (inset), in agreement with the results of obtained by Tsuji and Rosenheck (1979). Below pH 3.0, some membrane aggregation was observed, although reversal of aggregation by addition of NaOH was still effective. Acid titration of carboxyl-modified purple membranes showed substantial differences in their spectral behavior relative to controls. Samples modified by EDC, EDC + GME, EEDQ, and EEDQ + GME treatment consistently did not show the formation of a spectral species absorbing at 600-610 nm at acid pH up to pH 3.0 (Fig. 19b). However, the modified preparations revealed a decrease in 570 nm absorbance with increasing acidity. Carboxyl-modified samples appeared purple at pH 3.0 while control purple membranes appeared blue. Difference spectra of EDC modified BR showed a negative peak with an absorbance maximum at 570 nm and a very small, broad, positive band centered at 650 nm.

## 5. Discussion

A structural role for a carboxyl residue in the BR photocycle has been found by analyzing the kinetics for the decay of the $M_{412}$ intermediate. The results indicate that one "zero-length" carboxyl-lysine cross-link occurs as a result of carboxyl-activating reagent modification that strongly inhibits the reprotonation phase of the photocycle. This suggests that a carboxyl-lysine pair is in close proximity in the native membrane, and is probably interacting ionically.

### a. Role of an endogenous BR nucleophilic group in the carboxyl-modification reaction

This study has shown that increasing concentrations of an exogenous nucleophile provide increasing protection against inhibition of $M_{412}$

117

decay kinetics induced by carboxyl activating reagents alone. The strong similarity in the protection conferred by GME to both EDC and EEDQ treated samples indicates that the mechanism of protection is the same. The GME concentration dependence of the protection further suggests that GME competes with an endogenous BR nucleophilic group for an activated protein carboxyl group. Potential nucleophilic groups on BR that could react with carboxyl groups to form intramolecular cross-links are the $\varepsilon$ - amino groups of lysine and the phenolic groups of tyrosine. Since amino acid analysis shows that tyrosines are not modified, the role of lysine residues as endogenous nucleophiles was investigated.

b. Evidence for lysine-carboxyl interactions from double modification studies

A double chemical modification procedure, which first blocked lysine residues prior to carboxyl modification was developed. If the $\varepsilon$ -amino groups of lysine were reacting with activated carboxyls, prior blocking should prevent this reaction. Quantitation of lysine groups using the fluroescamine method showed this to be the case for EA, EDC, and EA/EDC modified samples. It was found that one lysine residue per BR molecule was involved in a cross-linking reaction after EDC modification. However, the data also indicate that EA and EDC compete for the modification of a single lysine residue. The critical lysine residue that reacts with EDC is modified by EA only when the EA concentration is equal to or greater than 10 mM. The same level of modification occurred in the 10 mM EA sample (2.7 lysine) as in the 10 mM EA sample that had been pre-reacted with 50 mM EDC (3.3 lysines). If the EA and EDC reactions were modifying different lysine residues, the

double modified sample would be expected to contain 4 modified lysines, i.e., the sum of the lysines modified by the individual reactions. This indicates that the third lysine residue modified at 10 mM EA is the lysine residue which reacted with an EDC-activated protein carboxyl group.

The functional consequences of the lysine-carboxyl double modification on the BR photocycle were directly correlated with modification of the third lysine. If at least three lysines were modified, subsequent EDC modification produced only mild inhibition of $M_{412}$ decay kinetics. The kinetics obtained in such samples closely coincided with the values of $M_{412}$ decay obtained in carboxyl-nucleophile modified samples when the nucleophile was present at high concentration (i.e., 10 mM EDC + 200 mM GMF).

The inhibition of $M_{412}$ decay kinetics obtained by reaction with either EDC or EEDQ, and the reversal of inhibition obtained by reaction in the presence of GME can be attributed to a common cause. In the absence of added nucleophile, EDC or EEDQ results in an intramolecular cross-link between a carboxyl group and lysine residue that creates maximal inhibition of $M_{412}$ decay kinetics. In the presence of GME, the added nucleophile competes with the lysine residue for the activated carboxyl group. Reaction of GME with the carboxyl residue results in glycine methyl ester amide formation and prevents the cross-linking reaction, yielding minimally inhibited kinetics. Lysine-carboxyl double modification experiments further support this idea because lysines that are first modified by EA are unavailable for subsequent reaction with carboxyls activated by EDC or EEDQ and cannot form intramolecular cross-links.

Thus, it is clear that the cause of maximal inhibition of $M_{412}$

decay kinetics can only be attributed to intramolecular cross-linking in EDC- or EEDQ-treated samples. An intramolecular cross-link between a carboxyl and lysine residue in BR may act to constrain conformational changes that take place during the photocycle, which are particularly important for the decay of the M intermediate. It has been shown that intramolecular cross-linking by bifunctional imidoesters resulted in inhibition of $M_{412}$ decay kinetics although the effect was smaller than in the present study (Konishi et al., 1979). Carbodiimides and EEDQ are "zero-length" cross-linkers (Klein et al., 1980), whereas the bifunctional imidoesters have 8-11 Å flexible bridges between their functional groups. Thus, a cross-link that forms as a result of carboxyl-activating reagent treatment must occur between a lysine and carboxyl residue that are in very close proximity to each other and probably interacting ionically.

c. Correlation of photocycle intermediate $O_{640}$
and the acid-induced species

Available data has led to the suggestion that the formation of both the $O_{640}$ intermediate and the acid-induced species chromophores may be due to retinal-carboxyl group(s) interactions. The flash photolysis data shows the apparent absence of $O_{640}$ in both EDC- and EEDQ-treated samples (in the absence and presence of a nucleophile). One interpretation is that carboxyl group(s) that are required for $O_{640}$ formation are blocked. However, careful consideration of $O_{640}$ kinetic traces shows that part of the kinetics measured at 650 nm in the modified samples at 20°C represent changes of the $BR_{570}$ species whose broad absorption band extends out to 700 nm. Typically, in the BR absorbance spectrum, the value at 640 nm represents 10% of the absorbance at

570 nm peak value. Flash photolysis kinetic traces of modified samples at 650 nm (20° and 40°C) are therefore the composite of the fast $O_{640}$ intermediate changes superimposed upon slow changes of the regeneration of $BR_{570}$.

The results obtained are consistent with a scheme where $M \xrightarrow{k_1} O \xrightarrow{k_2} BR$ and $k_2 \gg k_1$ at 20°C but $k_2 \simeq k_1$ at 40°C as is the case in control samples at 20°C. In the series reaction, the slow reaction is the rate limiting step and dominates in the kinetic control of the overall process. When $k_2 \gg k_1$, the photocycle has a slow conversion of $M_{412}$ to $O_{640}$, and is followed by a rapid reaction of $O_{640}$ to $BR_{570}$. In this case, the concentration of $O_{640}$ remains low throughout the course of the reaction, and $BR_{570}$ appears essentially as $M_{412}$ disappears. Thus, the apparent absence of $O_{640}$ at 20°C and its appearance at 40°C are explained solely by the changes in the kinetic parameters of the photocycle that result from modification.

Previous studies have suggested that an acid-induced species may represent a stabilization of the 'O' intermediate (Moore et al., 1978; Fisher and Oesterhelt, 1979). The structure of the acid species studied by CD spectra in the ultraviolet region show that the α-helical content of BR is not significantly altered at pH 3.0 ($\leq$ 10%) (Tsuji and Rosenheck, 1979). Schreckenback et al. (1977, 1978) report the existence of a pH-dependent equilibrium between the planar and nonplanar conformations of retinyl in the BR binding site. Ring-chain planarization was found to require the deprotonated form of a group with pK of 3.8, which supports the existence of a carboxyl group in the chromophore environ-ment. Thus, the red spectral shift for $O_{640}$ and the acid species probably results from small changes in the structure of the chromophore

environment and/or protonation of groups in the vicinity of the chromophore.

In carboxyl-modified BR, it is clear that the $O_{640}$ intermediate is capable of forming in samples in which the acid-induced species is not. This may indicate that two distinct groups are responsible for the observed spectral transitions. The group responsible for the shift to longer wavelengths in $O_{640}$ formation may undergo transient changes in its protonation state during the reprotonation phase of the photocycle. The second group responsible for formation of the acid species may not initially be in contact with the retinal chromophore, but moves into contact during a local rearrangement in the vicinity of the chromophore induced by acid titration. Alternatively, a single carboxyl group may be responsible for both spectral species and one mechanism for formation may be preferentially inhibited. In this case, a carboxyl residue which is necessary for $O_{640}$ formation would not be modified in this study, and intramolecular cross-linking may be responsible for preventing formation of the acid-induced species.

C. Carboxyl Group Interaction with the Retinal-Protein Chromophore

There is considerable support for the suggestion that electrostatic

interactions between the retinal chromophore and charged or dipolar

groups on bacterioopsin are responsible for regulation of the absorption

maximum (Honig et al., 1979; Sheves et al., 1979; Warshel, 1979).

These external point-charge models for wavelength regulation have postu-

lated the existence of carboxyl residues in the immediate chromophore

environment. This study has used chemical modification procedures

developed for carboxyl groups to attempt to identify such residues.

A pH-sensitive chromophoric reporter group, nitrotyrosine methyl ester

(NTME), has been attached to a carboxyl group in order to monitor the

protein environment at the "active site" (Fig. 20). The spectral and

ionization properties of the reporter group have been studied in bac-

teriorhodopsin and bacterioopsin. The influence of the reporter group

on the kinetics of the photocycle is also described.

1. Spectral and ionization properties of the model compound

The UV-visible titration spectra of NTME in 0.1 M NaCl is shown in

figure 21. In acidic solution, the fully ionized form has an absorbance

maximum at 355 nm ( $\varepsilon$ = 2,980 $M^{-1}cm^{-1}$) and a strong UV peak at 277 nm.

Upon, alkalinization, the 355 nm peak is shifted to 428 nm ( $\varepsilon$ =

4,310 $M^{-1}cm^{-1}$) and exhibits an isosbestic point at 381 nm. The pK for

the transition was found to be 6.60. In these respects, the ionization

and spectral behavior of NTME is very similar to nitrotyrosine which

shows an $\varepsilon_{428}$ = 4,300 $M^{-1}cm^{-1}$ in 0.10 M Tris, 0.10 KCl (Malan and

Edelhoch, 1970).

Figure 20.  Summary of the NTME Labeling Reaction for Carboxyl

   Residues.

   Summary of the reaction of nitrotyrosine methyl ester, a
pH—sensitive reporter group, with carboxyl residues of bacteriorhodop-
sin.  EEDQ was employed as a hydrophobic reagent to activate carboxyl
residues.

(EEDQ) + (Protein) + (NTME) →

$P$—C—N—C—CH$_2$—〈NO$_2$, OH〉 + 〈quinoline〉 + C$_2$H$_5$OH + CO$_2$
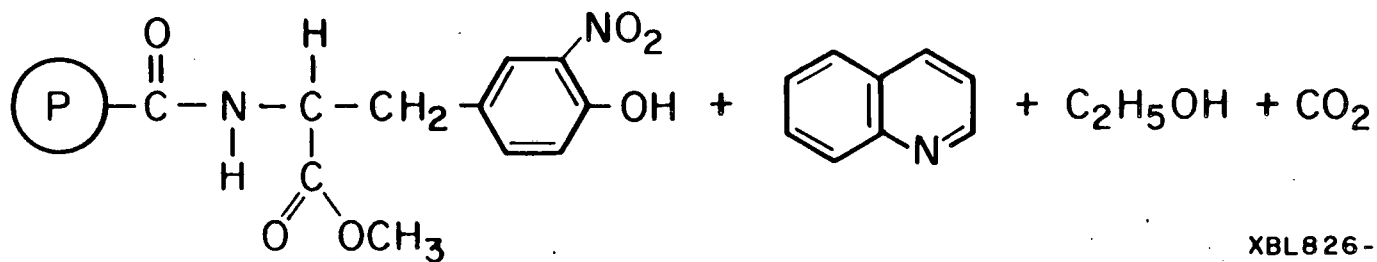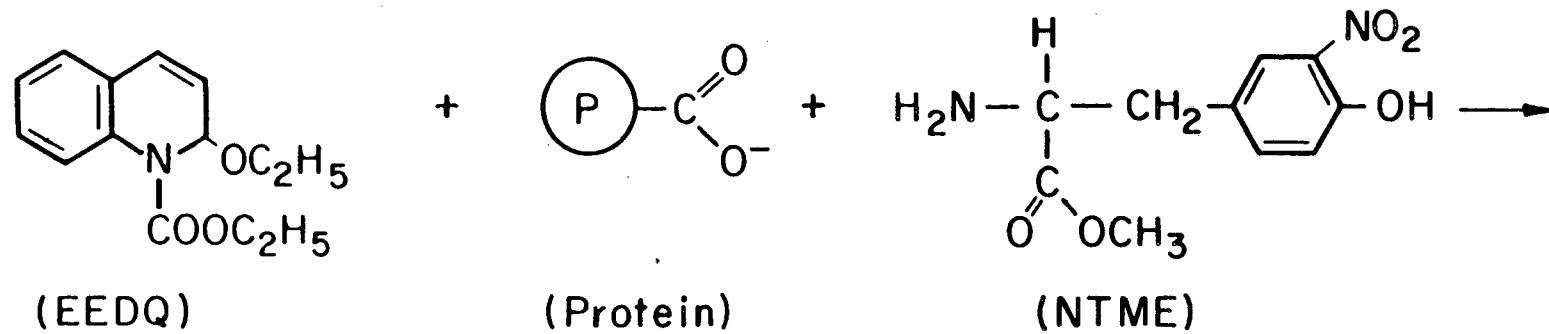
Figure 21. Spectral and Ionization Properties of the NTME Model

Compound.

Ultraviolet-visible spectra of the titration of nitrotyrosine methyl ester model compound in 0.1 M NaCl, 0.010 M Hepes. The inset shows the pK determined from the absorbance changes at 428 nm.
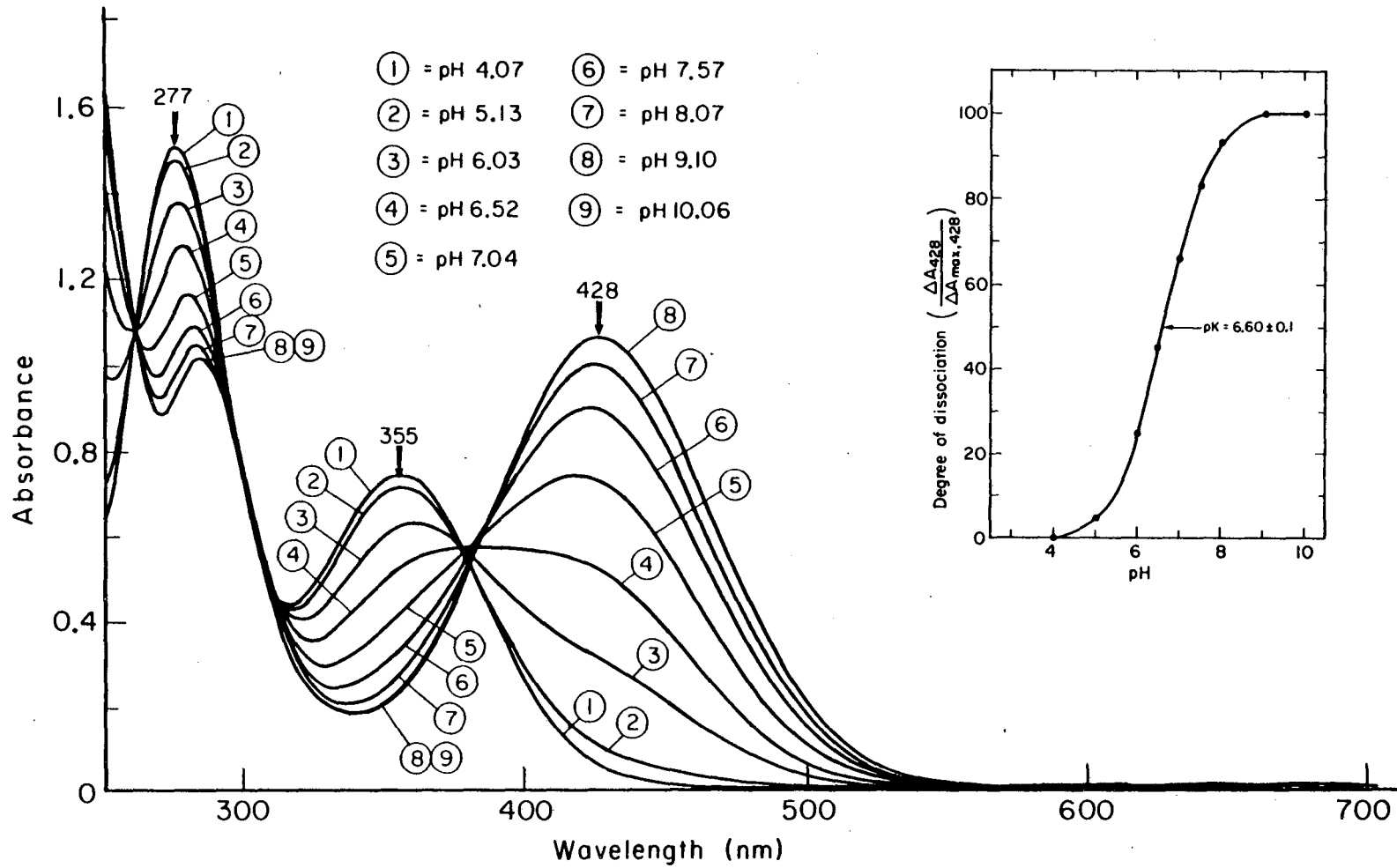
## 2. Stoichiometry of NTME labeling of BR in purple membranes

The stoichiometry of the labeling reaction was controlled by varying either the concentration of the carboxyl-activating reagent, EEDQ, or the concentration of the nucleophile, NTME (Table IX). Utilizing a constant concentration of 1 mM NTME present in small excess over the available protein carboxyl residues, increasing concentrations of carboxyl-activating reagent produced higher stoichiometries of coupling. The converse experiments utilizing 5 mM EEDQ (EEDQ: COOH = 13:1), exhibited a bell-shaped curve since higher nucleophile concentrations resulted in less coupling. Thus, a combination of short reaction times and low reagent concentrations allowed identification of samples with a stoichiometry of almost 1 mole NTME/mole BR. NTME has proven to be the most efficient nucleophile yet employed in the carboxyl coupling reaction, since much higher concentrations of glycine methyl ester, aminoethane-sulfonic acid, or a spin-labeled amine were required to obtain a similar coupling stoichiometry (Herz et al., 1981; Herz et al., 1983).

## 3. Reporter group-protein chromophore interactions in purple membranes

The absorption spectra (300-700 nm) for the alkaline forward titrations of control and NTME-modified BR in purple membranes are shown in figures 22 and 23a (upper half), respectively. The spectral region examined covers the visible absorption bands of BR that arise from retinal-protein interactions, as well as the spectral region of the reporter group. The spectrum at pH 7.0 differs from unmodified BR in that a large elevation in the broad absorption band from 300-500 nm is seen, although no new peaks are evident. The absorption maximum of the

## TABLE IX

### STOICHIOMETRY OF NIME LABELING OF BR IN PURPLE MEMBRANES

I.  Effect of variable concentration of carboxyl-activating reagent,
    EEDQ, NIME = 1.0 mM: reaction time = 0.5 hr.

| EEDQ (mM) | mole ratio<br>NIME : EEDQ : COOH | NIME per BR |
|-----------|-------------------------------|-------------|
| 0.0 | 2.6 : 0.0 : 1 | 0.00 |
| 0.1 | 2.6 : 0.26 : 1 | 0.16 |
| 0.5 | 2.6 : 1.3 : 1 | 0.31 |
| 1.0 | 2.6 : 2.6 : 1 | 0.74 |
| 5.0 | 2.6 : 13.0 : 1 | 2.83 |

II. Effect of variable concentration of nucleophile, NIME, EEDQ =
    5.0 mM; reaction time = 1.0 hr.

| NIME (mM) | mole ratio<br>NIME : EEDQ : COOH | NIME per BR |
|-----------|-------------------------------|-------------|
| 0.0 | 0.0 : 13 : 1 | 0.00 |
| 0.5 | 1.3 : 13 : 1 | 3.80 |
| 1.0 | 2.6 : 13 : 1 | 5.00 |
| 2.5 | 6.5 : 13 : 1 | 3.90 |
| 5.0 | 13.0 : 13 : 1 | 2.64 |
| 10.0 | 26.0 : 13 : 1 | 1.44 |

main retinal-protein 570 nm peak is unaffected at pH 7.0. Acid titra-
tion from pH 7.0 to pH 3.0 results in no changes in the 300-500 nm region
of the spectra. This is unusual since a peak at 360 nm characteristic of
the nitrotyrosyl chromophore is expected to be evident. Spectra of
samples incubated with only NTME and no EEDQ (in which no coupling is
detected), are unchanged from control samples.

Alkaline titration from pH 7.0 to pH 11.0 results in dramatic
changes in the reporter group and retinal-protein regions of the spec-
tra. The formation of a new peak at 428 nm characteristic of the
nitrotyrosinate ion occurs concomitantly with a large decrease in the
extinction coefficient of the 570 nm band, exhibiting an isosbestic
point at 480 nm. In addition, there is a general decrease in absorbance
in the 300-380 nm region. Control purple membranes titrated from pH
7.0 to pH 11.0 show only a small decrease in the absorbance maximum
at 570 nm and at pH 11.0, 82% of the original absorbance remains
(Fig. 22). No changes occur in the 300-450 nm spectral region and no
isosbestic points are present. As seen in figure 23b, the absorbance
changes at NTME-PM at 428 nm were used to obtain a pK for the spectral
transition of the reporter group associated with the forward titration.
The protein-bound NTME residue is found to have a pK of about 10-11,
at least 3 pK units higher than the model compound in solution.

The backward (acidic) titration of the same sample after 24 hr
under alkaline conditions reveals a new pattern of spectral changes
(Fig. 23a, lower half). The decrease in absorbance at 428 nm is no
longer coupled to absorbance changes at 570 nm. Instead, a new isos-
bestic point between a small peak at ≈360 nm characteristic of the
nitrotyrosyl and the 428 nm nitrotyrosinate chromophores appeared.

Figure 22.  Visible Spectra of the Alkaline Titration of Control Purple

Membranes.

Membranes suspended in 0.10 M NaCl, 0.01 M Hepes.  1, pH 7.0;
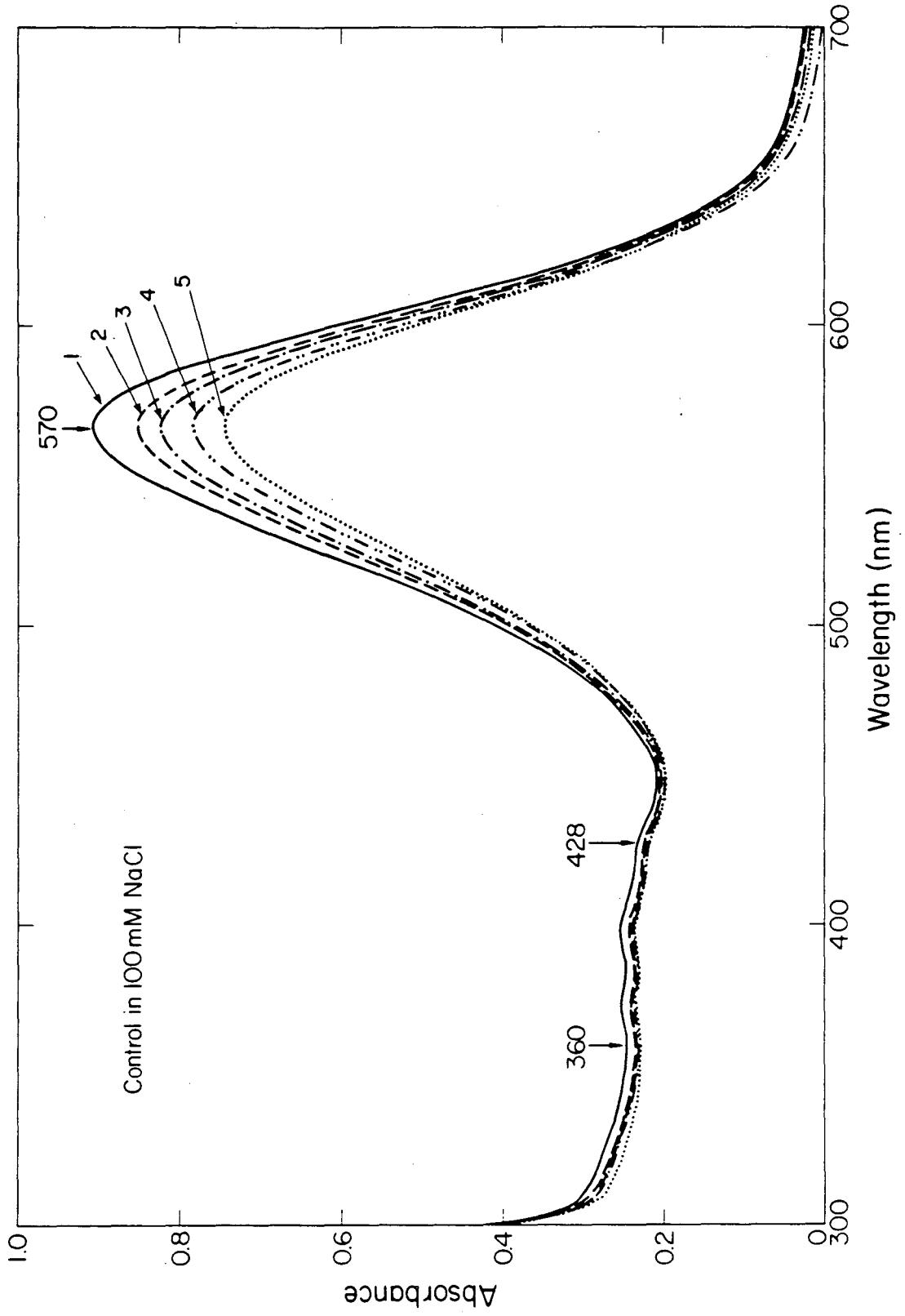
2, pH 8.0; 3, pH 9.0; 4, pH 10.0; 5, pH 11.0.

XBL 832-1271

Figure 23.    Spectral and Ionization Properties of NTME Modified

Purple Membranes.

a)   Visible spectra of the forward alkaline titration (pH 7.0-

11.0) of NTME-BR in purple membranes (upper) and backwards, acidic

titration (pH 11.0-5.0, lower).   The increase in absorbance at 428 nm

during the forward titration occurs concomitantly with a decrease in

the 570 nm peak and decrease in the 360 nm region of the spectra.

The absorbance at 428 nm decreases during the backward titration as

the 360 nm region increases.   Purple membranes suspended in 0.1 M NaCl,

0.01 M Hepes.

b)   Changes in the pK of the NTME reporter group associated with

the forward and backward titrations of NTME modified purple membranes.

5.0 mM NTME + 10 mM EEDQ in 100 mM NaCl
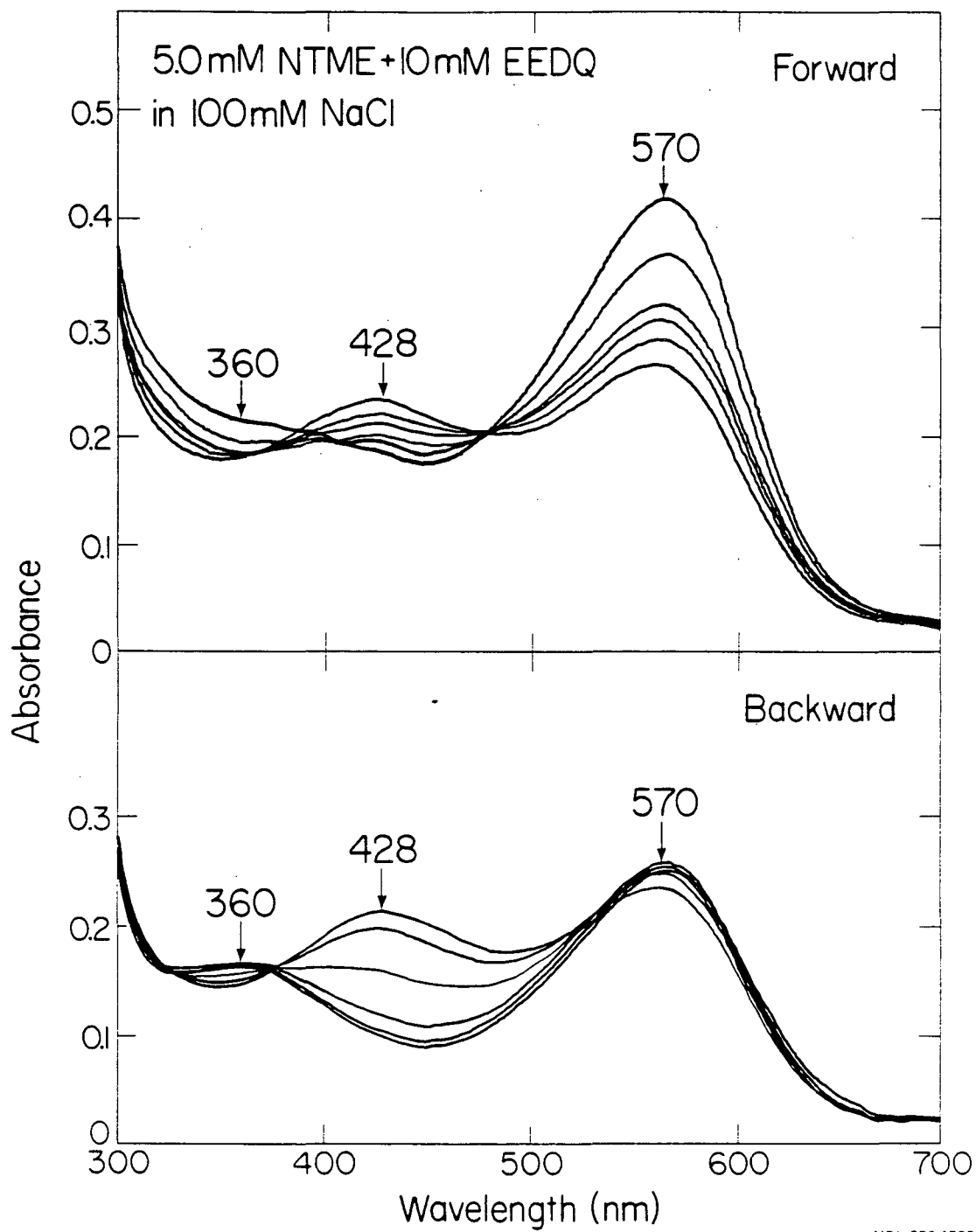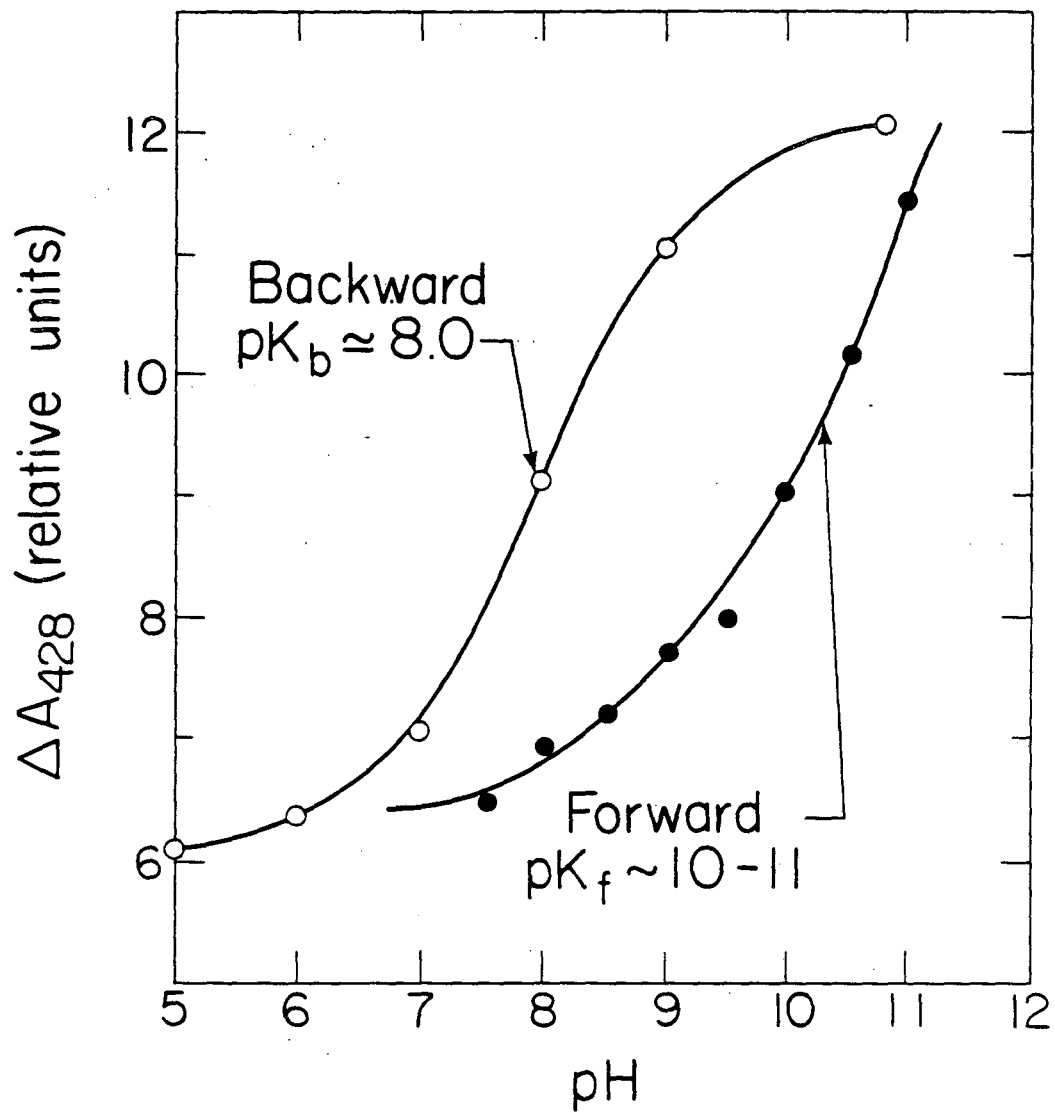
XBL 826-1502

XBL 826-1503

The backwards titration also demonstrates a new, substantially lower

pK = 8.0 (Fig. 23b) for the reporter group.

Circular dichroism spectra (300-700 nm) of NTME-BR at pH 7.0 (data

not shown) show an exciton couplet band with a positive peak at 530 nm

and a negative band at 605 nm, as well as a sharp negative peak at

320 nm. These CD spectral features are characteristic of control BR

(Muccio and Cassim, 1979). Alkaline titration of NTME-BR resulted in a

small gradual decrease in the exciton coupling band until about 75 percent

of the 530 nm peak remained at pH 11.0.

### 4. Reporter group properties in the apoprotein—Bacterioopsin in white membranes

It was of interest to determine whether the unusual spectral and

ionization behavior of the NTME residue bound to BR was caused by

retinal-NTME interactions. A chemical bleaching procedure for BR

using NH₂OH produces a retinaloxime species (Oesterhelt et al.,

1974) which is not desirable since it remains bound to the membrane

and absorbs in the same spectral region as NTME. We used white membrane

(WM) isolated from R₁mW, a mutant strain of H. halobium deficient in

retinal synthesis, that has been carefully characterized by Mukohata et

al. (1981). The major protein component of this membrane is

bacterioopsin which appears in the form of hexagonally close packed

trimers. The addition of stoichiometric amounts of retinal generates

a 565 nm chromophore, and forms purple membranes. The regenerated WM

also displays a characteristic bilobed visible CD spectra characteristic

of PM. Visible spectra of WM are featureless except for a small peak

at 414 nm which is due to small amounts of a contaminating respiratory

pigment.

Figure 24.  Spectral and Ionization Properties of NIME Modified

   White Membranes.

a)  Difference spectra of the forward alkaline titration (pH 7.0–
11.75) and backwards, acidic titration (pH 11.8–5.5) of NIME-BO in
white membranes (upper half).  The increase in absorbance at 438 during
the forward titration is coupled to a general decrease at about 320 nm.
The decrease at 440 nm during the backward titration is coupled to the
formation of the 369 nm peak.  The 417 nm peak is due to a small amount
of a contaminating respiratory pigment.

b)  Changes in the pK of the reporter group associated with the
forward and backward titrations of NIME modified white membranes.

1.0 mM NTME + 5 mM EEDQ in 100 mM NaCl

Forward

Backward
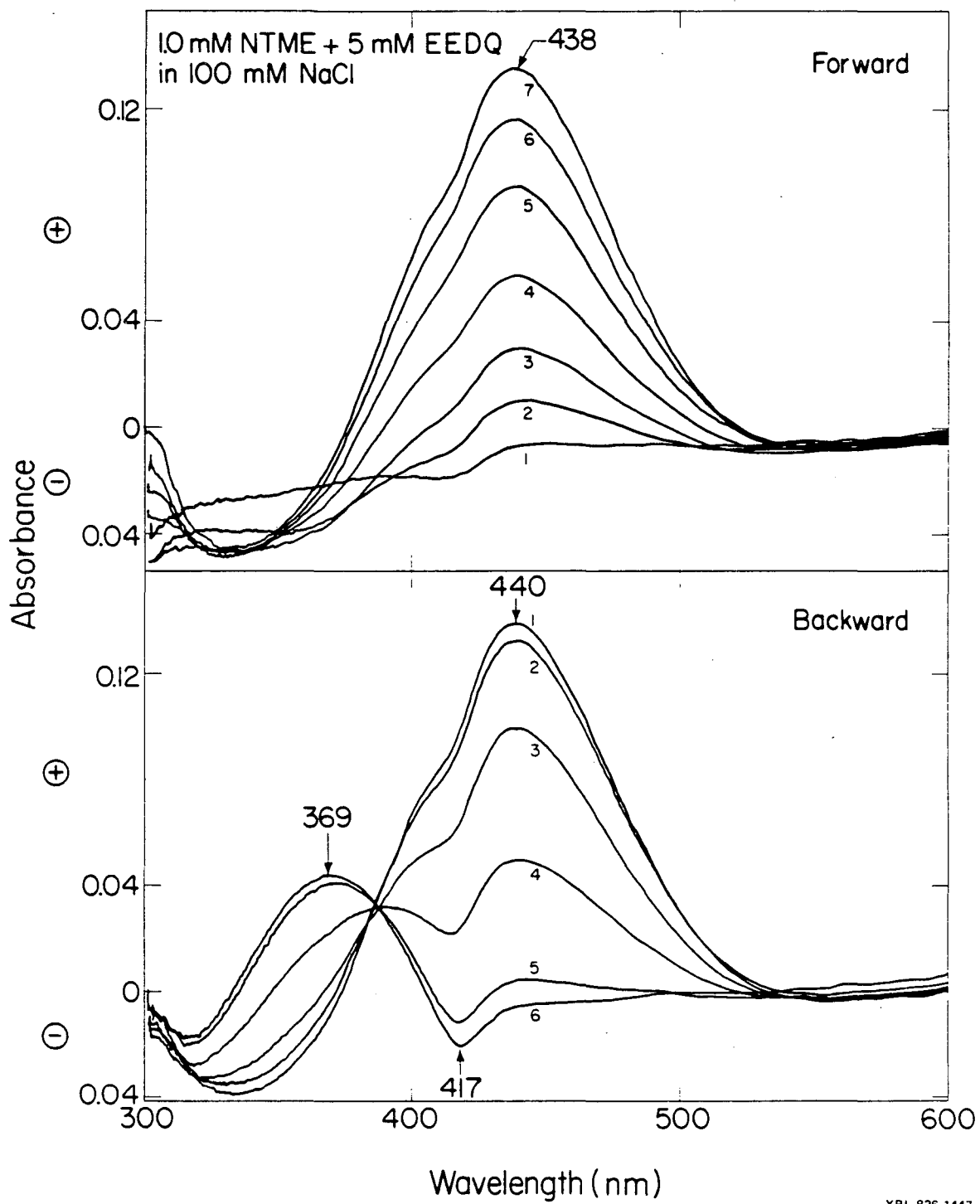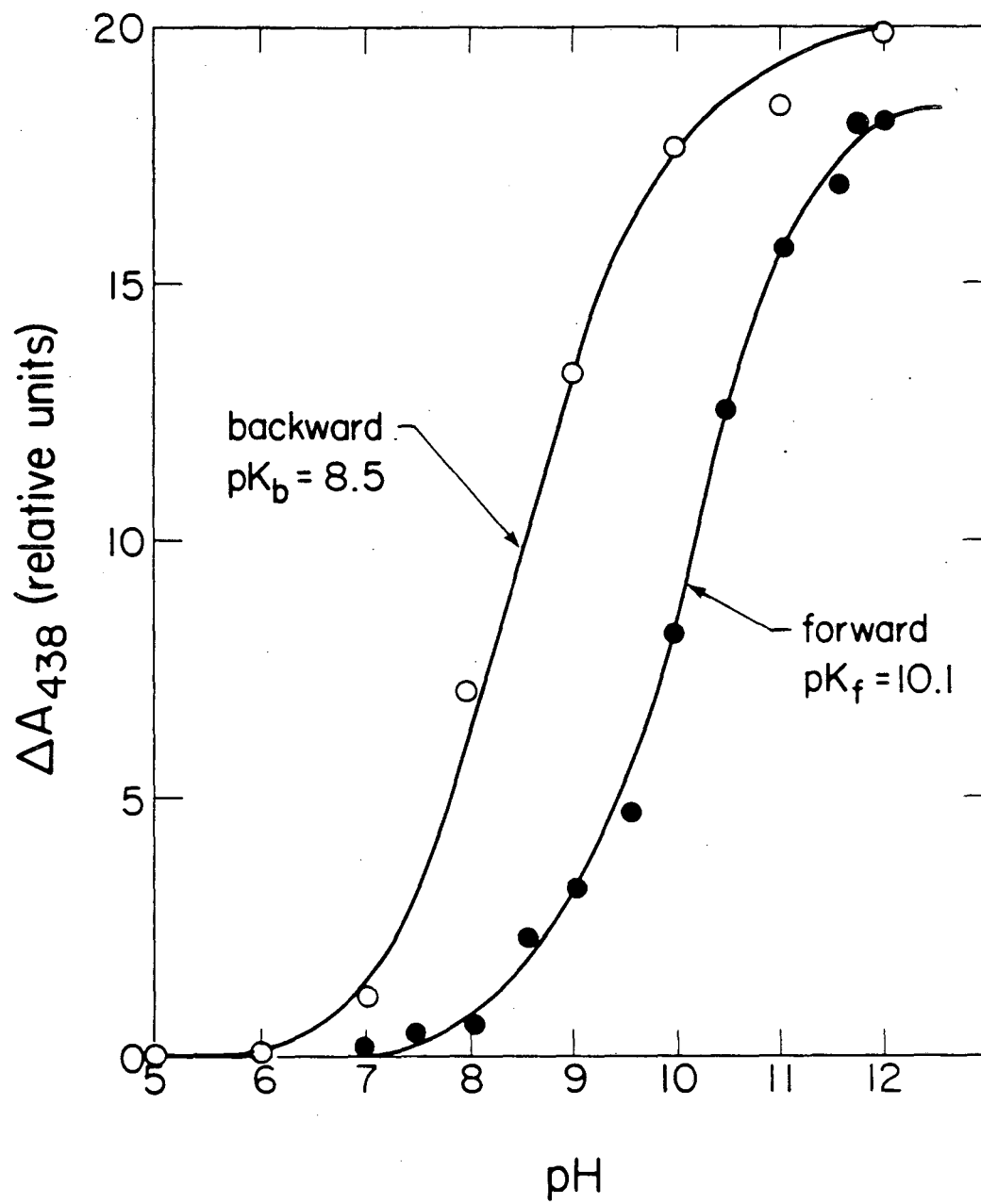
XBL 826-1447

XBL 826-1449

White membranes were chemically modified with NTME using the same procedures developed for purple membranes. The spectral and ionization behavior of the bound NTME residues were determined from difference spectra of alkaline and acidic titrations (Fig. 24a). Formation of the nitrotyrosinate ion resulted in formation of a peak at 438 nm with a pK = 10.1 (Fig. 24b). A small decrease in absorbance at 320 nm accompanied this change, but the transition did not show a clear isosbestic point. However, the backward titration demonstrated a clear isosbestic point at 385 nm as a result of conversion of the 438 nm nitrotyrosinate ion to a 369 nm absorbance peak characteristic of the nitrotyrosyl chromophore. As in the case of NTME-modified PM, the backward titration of NTME-WM exhibited a decreased pK = 8.5. Thus, both NTME-PM and NTME-WM exhibit essentially identical spectral and ionization behavior for the reporter group that accompanies forward and backward titrations.
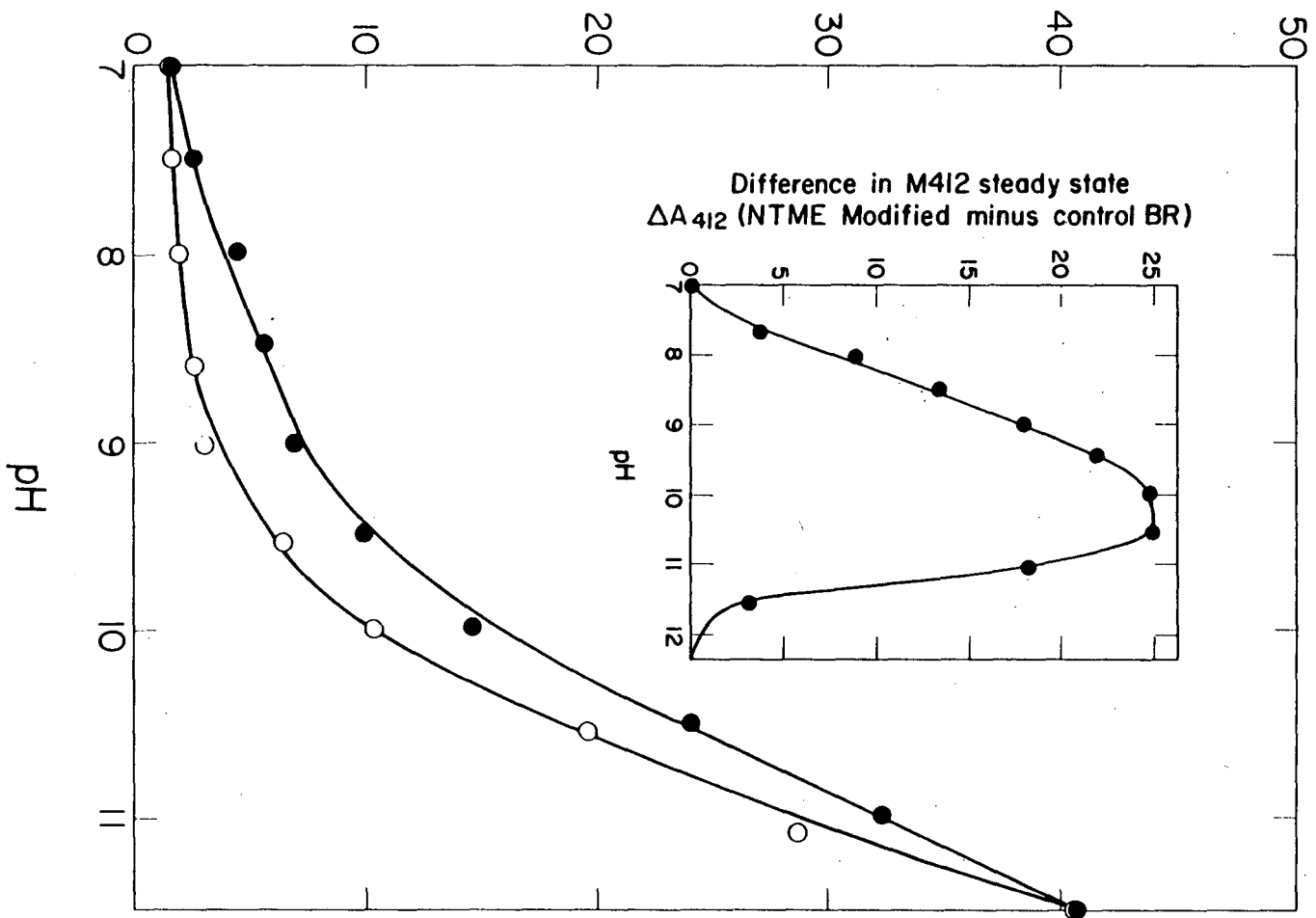
### 5.  pH dependent steady-state levels of $M_{412}$ intermediate

Since retinal-protein chromophore interactions with NTME were evident from the isosbestic point of the titration spectra, we sought to identify effects of the NTME group on activity of BR. The formation and decay of the $M_{412}$ intermediate is closely linked to changes in the protonation state of the Schiff base (Lewis et al., 1974) and the release and uptake of protons from the purple membranes (Govindjee et al., 1980). The activity of BR as a function of pH in the region of the pK of protein bound reporter group should be a sensitive measure of NTME effects on the photocycle.

Alkaline titrations of control and NTME-BR were carried out to quantitate the steady-state level of the $M_{412}$ intermediate. Previous

Figure 25.  pH Dependence of the $M_{412}$ Steady-State Following NTME Modification of Purple Membranes.  Samples were suspended in 0.1 M NaCl, 0.01 M Hepes at 25°C.  O, control (unmodified) purple membranes; ●, 1.0 mM NTME + 5.0 mM EEDQ modified purple membranes.  The inset shows the difference between the control and NTME modified samples.

M4I2 steady state absorbance (relative units)

Difference in M4I2 steady state
$\Delta A_{4I2}$ (NTME Modified minus control BR)

pH

XBL 826·1448

141

studies (Sherrer et al., 1981) have shown a strong pH dependence of
the decay kinetics of $M_{412}$, and a tyrosine residue has been implicated
in the mechanism. The pH dependence of $M_{412}$ levels was compared
by normalizing the NTME values to the control value at pH 7.0 in order
to correct for initial differences in protein concentration and steady-
state levels. Since the group of interest has a pK = 10-11, this will
not affect comparison of the NTME pH-dependent effects on activity.
Figure 25 shows that NTME modified samples show an elevated level of
the $M_{412}$ intermediate throughout most of the alkaline pH range.
The inset in figure 25 shows that the largest difference in activity
is in the region of pH 10-11. This suggests that NTME attached to BR,
which has a pK of 10-11, causes the increased levels of $M_{412}$ in the
steady state.

Steady state levels of $M_{412}$ measured during the backward titration
of NTME-BR were different from both the NTME-BR forward and control
forward titration. A plot (data not shown) of the difference in steady
state values vs. pH as in Fig. 25 showed a bell-shaped curve shifted to
lower pH values by $\simeq 1.5$ pH units relative to the forward titration.
The $M_{412}$ pH dependent shift is slightly smaller than the pK shift found
for the NTME residues by reporter group spectra.

### 6. Decay kinetics of the $M_{412}$ intermediate

To further investigate the increased steady-state levels, laser
flash photolysis was used to determine the kinetics of the rise and
decay of the $M_{412}$ intermediate. Kinetics for formation of $M_{412}$ in
control and NTME-modified BR were the same. At pH 7.0, figure 26
shows that the decay kinetics for NTME-BR were slightly inhibited. The
control sample exhibits a monophasic decay with a $t_{1/2}$ = 6 msec at 20°C

Figure 26.  M$_{412}$ Decay Kinetics of NTME-Modified Purple Membranes.

Semilogarithmic plots of data obtained from computer accumulated scans show a single exponential decay for control membranes at pH 7, and a slightly slower, biphasic M$_{412}$ decay kinetics for the NTME-modified sample.  At pH 10, both decay times are substantially longer, although the NTME sample is greatest affected.  Laser flash photolysis was performed on samples suspended in 0.1 M NaCl, 0.01 M Hepes at 20°C.

KINETICS OF M412 DECAY

NTME MODIFIED BR

CONTROL

XBL 832-8070
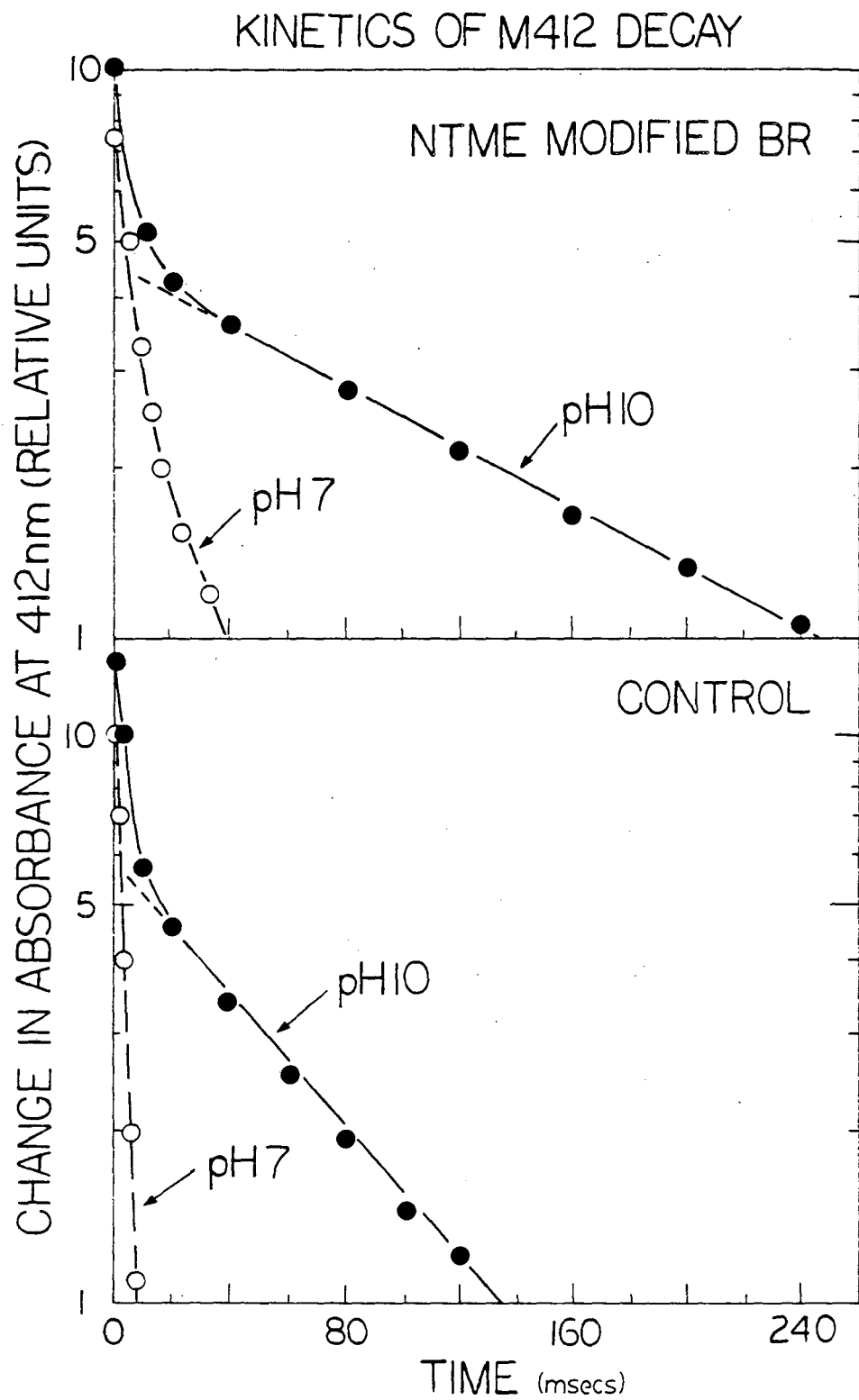
while the NTME-BR appeared slightly biphasic, with the dominant fast phase $t_{1/2}$ = 9.3 msec, and the second slower phase $t_{1/2}$ = 20 msec. This indicates that the protonated NTME species introduces only a slight perturbation to the overall photocycling mechanism. The decay kinetics were also determined at pH 10.0 where the $M_{412}$ steady-state levels showed the greatest difference between control and modified samples. As expected, the control sample showed slower $M_{412}$ decay kinetics (fast phase $t_{1/2}$ = 7.5 msec and $t_{1/2}$ = 55 msec for the second slow phase) which were strongly biphasic. The difference between the decay kinetics for the NTME-BR sample at pH 7.0 and 10.0 was even greater, $t_{1/2}$ = 125 msec for the second, slow phase. The ratio of the half time for $M_{412}$ decay in the control sample at pH 10 versus pH 7 is 9.17, while the same ratio for the NTME-modified BR is 13.4. Comparison of the pH dependent effects on $M_{412}$ kinetics shows that the modified sample's decay kinetics are increased a factor of 1.5 relative to the increase the control sample shows. Since the $M_{412}$ steady state level is determined by the ratio of the kinetics of $M_{412}$ decay to $M_{412}$ rise kinetics, these changes should be reflected in the steady state level. Comparison of the steady-state values at pH 10 (Fig. 24) shows that the increase is very close to a factor of 1.5. Clearly, the protonation of the reporter group influences the photochemical cycle by determining the decay kinetics of the $M_{412}$ intermediate.

## 7. Discussion

The NTME chromophore appears to be a sensitive probe to monitor changes in BR's microenvironment near the retinal binding site. The results suggest that the NTME chromophore bound to a carboxyl group resides in a hydrophobic membrane domain in the native state.

### a. Implications of chemical modification for the microenvironment of the retinal binding site

The unusual absorption spectra of NTME in native PM that is evident at neutral pH is correlated with the unusually high pK of 10-11 for the residue. These spectral and ionization properties may be due to either an electrostatic interaction with a nearby group or a change in the polarity of the environment. A decrease in the polarity of the environment around any group will result in a smaller extent of ionization, regardless of its charge type (Kokesh and Westheimer, 1971). The pK of 2,6-di-tert-butylphenol is increased 2-3 units relative to that of phenol presumably because the adjacent, bulky hydrophobic tert-butyl groups hinder solvation of the anion (Cohen and Jones, 1963). Examples of nitrotyrosine pK changes, as well as theory, demonstrate that a change to a more hydrophobic environment will increase the pK of nitrotyrosine residues.

The backwards (acidic) titration demonstrates an irreversible hystersis that produces a lower pK = 8.0, closer to that of the model compound in solution. In addition, the protonated peak at 360 nm characteristic of the model compound in solution appears with an isosbestic point between the two NTME species. The elevated pK of NTME residue at the membrane surface could possibly be explained by the large negative surface potential of purple membrane sheets (Carmeli et al., 1981). In accordance with Guoy-Chapman Theory (McLaughlin, 1977), at low ionic strength the surface pH will be more acidic than that of the bulk aqueous phase, and the intrinsic ionization of a surface group will occur at a lower pH than that measured in the bulk phase. However, since the pK of NTME-BR is essentially identical in 0.01 M NaCl and 1 M NaCl (data not shown) where the surface charge is completely

screened, we may exclude surface charge effects on the experimentally determined pK values.

These results suggest that the NTME chromophore resides in a hydrophobic membrane domain in the native state. Exposure to high alkaline pH results in a change in pK which may be explained by a localized configurational change that transfers the NTME chromophore from a buried hydrophobic membrane domain into a more aqueous environment. Numerous examples of irreversible configurational changes as evidenced by titration curves of water-soluble globular proteins have been reported (Tanford, 1962). The decrease in the pK of two anomolously high pK carboxyl groups of β-lactoglobulin has been ascribed to a similar mechanism. In this case, the transfer of two buried carboxyl groups from a hydrophobic region to the surface occurs as the result of an alkaline titration-induced conformational change (Basch and Timesheff, 1967). Muccio and Cassim (1979) reported that alkaline titration of BR results in a small decrease in the 570 nm absorbance band that was reversible up to pH 10.0. Between pH 10.0-11.8, the spectral changes at 570 nm are increasingly less reversible. However, the secondary structure of the membrane protein monitored by far-ultraviolet circular dichroism was invariant over the pH 7.0-11.8 regions (Muccio and Cassim, 1979). This indicates that the pH range that BR was exposed to is not expected to alter the overall protein conformation, and therefore, the extent of the NTME-BR configuration change is small. This is supported by the fact that large BR conformational changes (induced by exposure to pH $\geq$ 12.0 or to charged detergents) result in the release of retinal from its binding site, forming a 364 nm spectral peak with an $\varepsilon = 50,400$ $M^{-1}cm^{-1}$ (Muccio and Cassim,

1979). The forward titration spectra clearly show the absence of any absorbance increase at 364 nm, demonstrating that retinal remains in its binding site. Furthermore, Muccio and Cassim (1979) found only a 5° increase in the orientation of the transition dipole of the retinal chromophore in linear dichroic studies of oriented membrane films at pH 11.5. These facts point to a small, configurational change that specifically affects the reporter group distance from retinal, while leaving the retinal binding site intact.

The CD spectra of NTME-BR found in this study retains the bilobed visible band previously described for bacteriorhodopsin. Part of the origin of this bilobed band has been ascribed to excitonic interactions of dissymetrically arrayed retinal chromophores within the membrane (Ebrey et al., 1977). Since the excitonic interactions among chromophores have been correlated with rigid purple membrane organization (Cherry et al., 1978), no significant change has occurred in this property of the modified membrane. Furthermore, the presence of the bilobed band in modified membranes indicates that the presence of the reporter group(s) results in a minimal perturbation of the protein and chromophore structure, since other chemical modification procedures which affect the chromophore result in the loss of this feature (Lam and Packer, 1983; Herz and Packer, unpublished observations). In addition, the alkaline titration CD spectra for modified membranes exhibit a small decrease in intensity for the bilobed band that closely resembles the changes reported for control membranes (Muccio and Cassim, 1979). Thus, the stability of the membrane has also not been affected by the carboxyl modification.

To determine if NTME interactions with retinal "per se" were responsible for either the unusual spectral or ionization behavior, we examined these properties in NTME-labeled WM (lacking retinal). The alkaline titration of NTME-WM showed spectral and pK properties nearly identical to that found in PM. The acidic titration after alkaline conditions also demonstrated an irreversible hysteresis that shifted the reporter group to a lower pK and caused a return to the model compound spectral properties. The extreme similarity between reporter group properties in PM and WM allows us to conclude the NTME-retinal interactions are not responsible for the unusual ionization and spectral properties found in PM and these properties must only reflect the protein microenvironment in the vicinity of the reporter groups.

The absorption spectra of NTME-BR during alkaline titration are quite similar in appearance to the alkaline titration spectra of nitrated BR observed in two studies (Lemke and Oesterhelt, 1981; Katsura et al., 1982). Both reports found elevated pK's of 9-10 for the modified nitrotyrosine residues and unusual spectral properties associated with the chromophore in the 300-500 nm spectral region, as in this study. Katsura et al. (1982) observed an isosbestic point at 475-480 nm that was correlated with an absorbance decrease of a 540 nm peak (a blue-shifted retinal-protein chromophore). These spectral characteristics have been interpreted as identifying a tyrosine residue(s) that interacts with retinal in the chromophore binding site.

There is considerable support for the suggestion that electro-static interactions between the retinal chromophore and charged or dipolar groups on bacterioopsin are responsible for wavelength

regulation of the red absorption band of the purple membrane complex (Nakanishi et al., 1979; Warshel, 1978; Yoshihara et al., 1981). The models predict a shift in the absorption maxima if a new charge is introduced into the chromophore environment. A carboxyl group located in the same hydrophobic environment as the NTME reporter group would also be expected to have a pK shifted to higher values. The β-carboxyl of an aspartic acid side chain or the γ-carboxyl of glutamic acid side chain which have a pK in aqueous solution of 4.5 (Tanford, 1962) would be shifted to a pK of 7.5-8.5. The replacement of the protonated carboxyl group at neutral pH by the protonated nitrotyrosine residue (pK 10-11) would lead to no change in the charge environment of retinal. However, alkaline pH would create a negative charge which shifts the absorption maxima to the 440 nm region where it overlaps with the absorbance of the nitrotyrosinate ion. Although a negatively charged carboxylate group is converted to a negatively charged nitrotyrosinate group as a result of chemical modification, the pK and the distance of the charge from existing protein functional groups and retinal are substantially altered.

b. Location of a carboxyl residue at the retinal
   binding site

Calculations utilizing chromophore models as well as studies of synthetic model compounds demonstrate that charge effects on absorption maxima are highly dependent on the geometry and distance of the negative charge from the conjugated system (Sheves et al., 1979). A small blue shift was found to occur in model compounds when a negatively charged carboxylate group was positioned 3 Å from the Schiff base linkage. However, a larger red shift occurred when the charge was placed 3 Å

from the conjugated polyene system. A low dielectric medium around the NTME and retinal chromophores could increase the distance through which they are capable of interacting (Inouye et al., 1979). Given the current lack of knowledge concerning the three-dimensional structure and functional group composition of the "active site" of BR, it is not possible to accurately specify the distance and geometry of the reporter group with respect to retinal in the binding site.

Nevertheless, the location of the modified carboxyl in the primary sequence can be suggested by reference to current models of BR secondary and tertiary structure (Huang et al., 1983; Agard and Stroud, 1981; Engelman et al., 1982). The pK changes observed by spectral titration infer that the modified residue is buried in a hydrophobic domain in the native state, but accessible to the aqueous membrane interface after a small configurational change. Of seven possible buried carboxyl residues, only four residues are situated within approximately 15 Å of extracellular surface of the membrane. In order to place the modi-fied carboxyl group within 10 Å of the retinal chromophore, it is reasonable to assume the residue is either on the same helix or an adjacent helix to helix G that bears the retinal-lysine (Lys 216) Schiff base linkage (Katre et al., 1981; Bayley et al., 1981). Although the complete assignment of helical segments (A-G) to specific rods of density (1-7) in the electron density map of BR is not definitive, experimental data places helix F adjacent to helix G (Trewhella et al., 1983), and most patterns assign helix A a position adjacent to helix G (Agard and Stroud, 1982). The retinal chromophore has been found to be inclined at an angle of about 23° from the plane of the membrane using linear dichroism measurements (Bogomolni et al., 1977).

In a recent study, Huang et al. (1983) used a retinal photoaffinity label to identify Glu-194 on helix F as a residue adjacent to the $\beta$-ionone ring of retinal. Given these constraints on structure and the above assumptions, the modified carboxyl group in the chromophore environment is most likely to be Glu-194 (helix F) since it is the closest to the retinal chromophore. Two other groups, Glu-204 (helix G) and Glu-9 (helix A) are also candidates for the modified site. The identification of the modified residues in the primary sequence should serve to further define the structure of BR in the purple membrane as well as elucidate the role of carboxyl residues in the BR chromophore structure.

## D. Topography and Mobility of Spin-labeled Carboxyl Residues

An additional method that would make it possible to draw a more detailed and precise picture of the arrangement of the BR polypeptide in the purple membrane is the chemical modification of selected functional groups by the introduction of spin-label reporter groups (Morrisett, 1976). Although lack of site specificity can be an inherent limitation in functional group modification (Glazer et al., 1976), useful structural information can still be obtained if the complex ESR spectrum can be deconvoluted by biophysical and biochemical methods (Likhtenstein, 1976). This approach allows the study of the local topography and mobility of different domains of the membrane protein in the vicinity of the covalently bound labels.

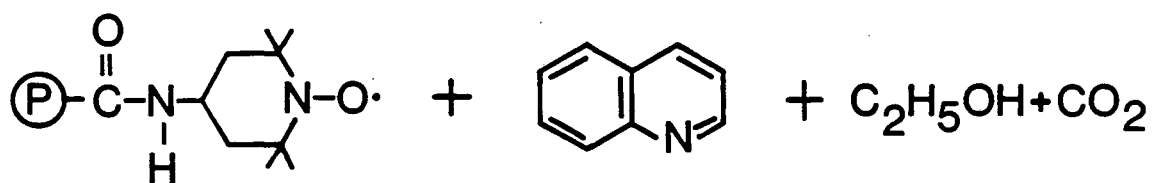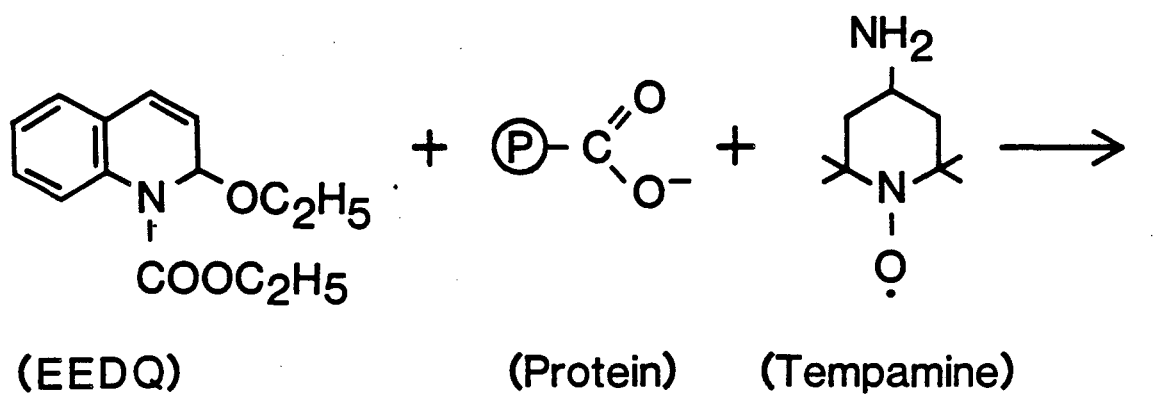### 1. Stoichiometry of the spin-labeling reaction

BR was covalently spin-labeled by reacting 4-amino-2,2,6,6-tetramethyl-piperidino-N-oxyl (Tempamine) with protein carboxylic amino acid residues using N-(ethoxycarbonyl)-2-ethoxy-1,2-dihydroxyquinoline (EEDQ) as the coupling agent (Fig. 27a). The amount of spin label covalently coupled to BR was found to depend on the concentration of the carboxyl activating agent, EEDQ, present during the reaction. The concentration dependence of EEDQ on the spin-labeling reaction was studied using a large excess of Tempamine nucleophile (200 mM). EEDQ concentrations $\leq$ 1.0 mM produced insignificant labeling, while higher concentrations (10 - 30 mM) yielded progressively increased levels of nucleophile coupling (2.0 - 4.25 TA per BR). Only a few of the 19 carboxyl residues found in BR were modified by this procedure. ESR spectra clearly revealed an increase in the immobilized spin content of samples that was correlated with higher stoichiometries of

Figure 27.

    a)   Summary of Spin-labeling Reaction for Carboxyl Residues

        of Bacteriorhodopsin.

    b)   Increase in the Immobilized Spin Content Correlated with

        Higher Stoichiometries of Labeling.

        ESR spectra of BR labeled by reacting 200 mM Tempamine with

        15-30 mM EEDQ. Washed samples, resuspended at 10 mg/ml

        TA-BR and ESR spectra recorded at the same gain.

# SPIN–LABELING CARBOXYL RESIDUES OF BACTERIORHODOPSIN



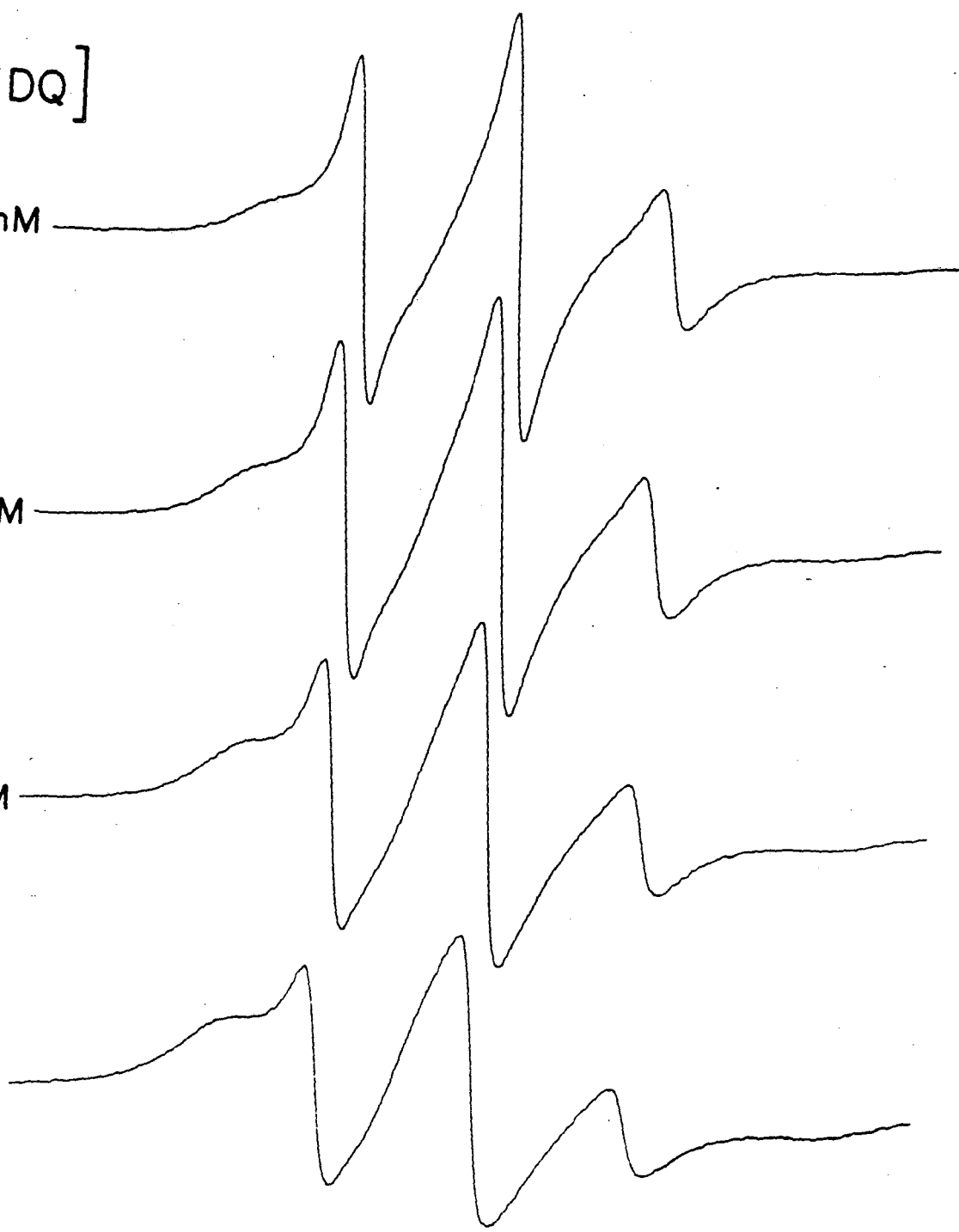(EEDQ)        (Protein)        (Tempamine)

[EEDQ]

15 mM

20 mM

25 mM

30 mM

XBL834-901

spin-labeling (Fig. 27b). Higher stoichiometries of labeling resulted in a broadening of the central line width ($\Delta H_0$), growth of the low field shoulder of the $h_{+1}$ peak, and the appearance of two new extrema with a maximum splitting of 68.4 G characteristic of a strongly immobilized signal. In order to quantitate spin content, computer double integration of the first derivative ESR spectrum was carried out for both "native" and SDS-urea-heat denatured samples to preclude underestimation due to spin-spin interaction. Although the ESR spectra of denatured BR showed much greater mobility than the "native" sample, no significant differences in spin content for the 10 mM EEDQ sample were observed.

Higher stoichiometries of labeling also resulted in bleaching of the 570 nm retinal-protein chromophore. The 4.25 TA-BR sample was completely bleached, exhibiting a 370 nm spectral peak characteristic of free retinal. To avoid changes in protein structure that might accompany extensive modification, and to work with spin-labeled BR that retained its functional properties, all further work was carried out with 200 mM TA + 10 mM EEDQ-modified BR which contained an average of 2.0 spins per BR molecule (2.0 TA-BR).

## 2. Properties of 2.0 TA-BR

Spin-labeled 2.0 TA-BR was found to have slightly altered visible spectral characteristics. A shift in the $\alpha$-band 570 nm absorbance peak to 555 nm occurred as well as a reduction in the apparent molar extinction coefficient, from 63,000 to 43,100 $M^{-1}cm^{-1}$. No 360-370 peak, characteristic of unbound retinal, was seen as a result of modification. Accompanying this change in the $\alpha$-band was a general increase in absorbance in the $\beta$-band between 300 and 500 nm. The modified membranes appeared slightly redder than control purple membranes. Despite these

differences, many other spectral responses and functions were retained. TA-BR exhibited light-dark adaptation. Control purple membranes kept in the dark showed an absorption maximum at 558 nm and illumination caused a 10 nm red shift in this absorption maximum and a 14% increase in absorbance. The 2.0 TA-BR dark adapted protein had an absorption maximum at 548 nm which shifted to 555 nm upon illumination with an absorbance increase of 4%. Acid titration resulted in a red-shifted chromophore in TA-BR as in the case of control BR.

The 2.0 TA-BR sample retained photocycling activity and exhibited slightly slower kinetics for decay of the $M_{412}$ intermediate. Chemical bleaching of TA-BR by hydroxylamine and light produced a retinaloxime species absorbing at 365 nm, as in the case of control BR, indicating no modification of retinal had occurred. The bleached membrane was reconstituted by addition of all-trans retinal and yielded a 555 nm retinal-protein chromophore. These characteristics indicated that the structure and function of BR were not substantially affected by the 2.0 tempamine spin-label chemical modification.

### 3. Effects of denaturing agents

To demonstrate the sensitivity of TA-BR to large structural changes, we tested the effects of denaturation on the ESR spectra. Previous studies with other spin-labeled proteins have demonstrated a transition from a moderately immobilized to a sharp, highly mobile ESR spectrum that correlated with loss of α-helical structure measured by circular dichroism (Morrisett and Broomfield, 1971). The latter technique also demonstated a large loss in α-helical structure when BR was solubilized in SDS in the absence of urea or heating (Huang et al., 1981).

In the absence of any chemical denaturing agents, heating resulted

Figure 28.  TA-BR Conformational Changes Caused by Denaturation.

a)  Changes in ESR spectra of 2.0 TA-BR caused by addition of SDS-urea at indicated concentrations and heat (100°C for 10 minutes).  All spectra recorded at 5 x $10^8$ gain.

b)  Progressive low field line height increase as a function of SDS-urea concentration.

TA-BR Protein conformational changes
caused by Denaturation
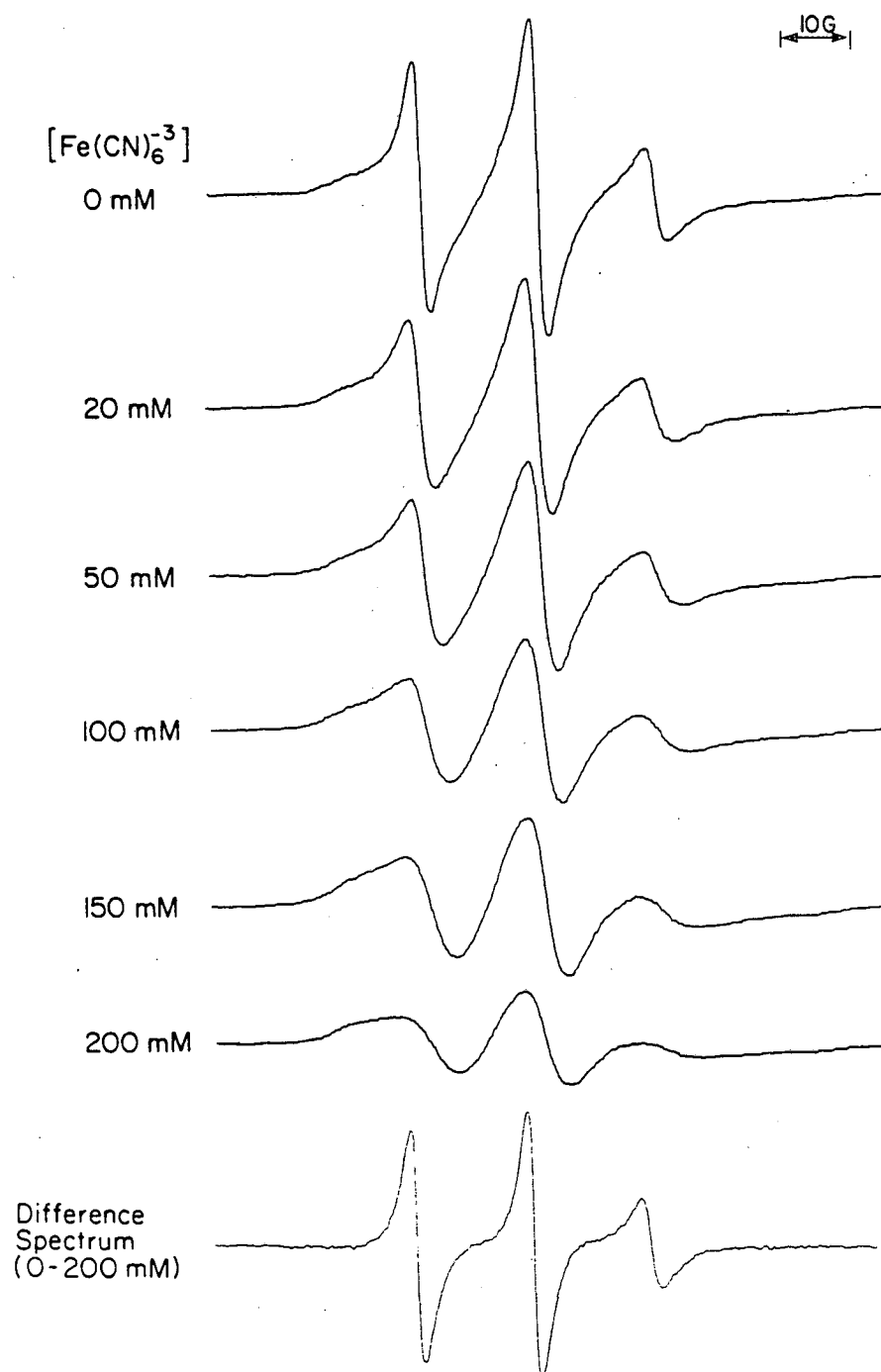
Denaturant: 8M Urea, 1% SDS

XBL 822-83
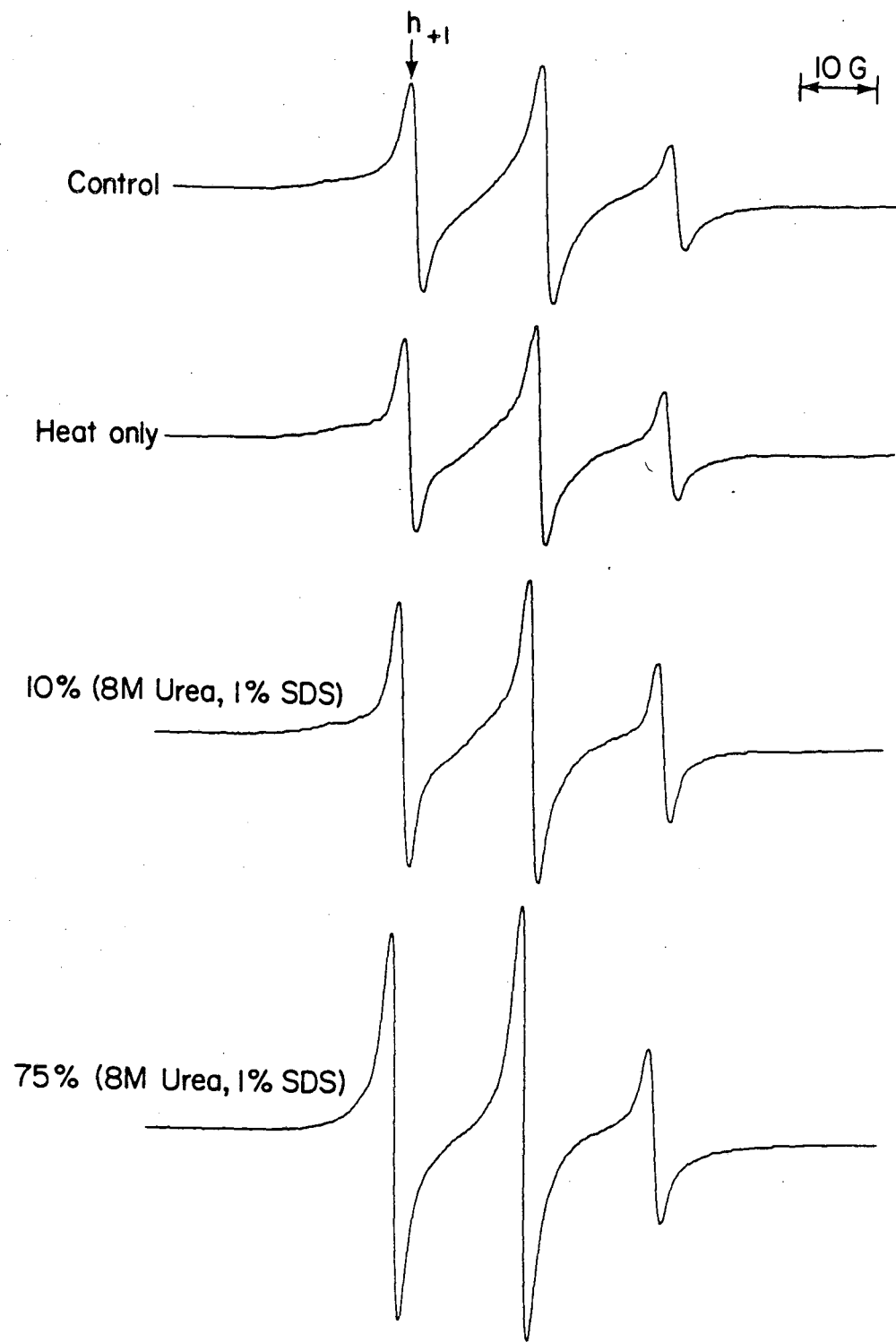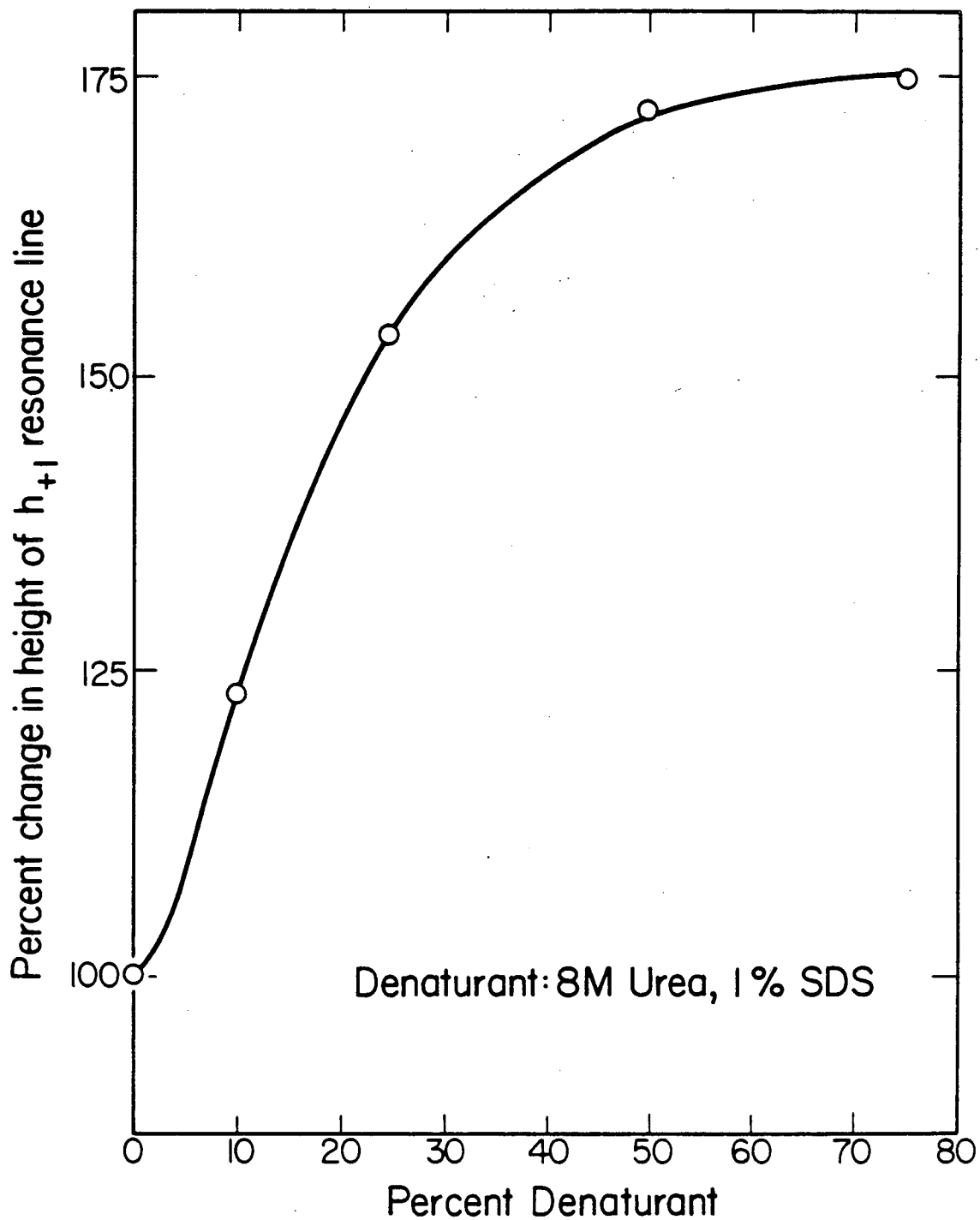
in loss of the 555 nm chromophore, and a significant change in mobility of protein bound spin labels. The heat-denatured sample showed an increase in all resonance line heights, a narrowing of the central line width, but the shoulder of the $h_{+1}$ peak remained (Fig. 28a). Thus, the overall ESR spectrum of the spin labels showed more mobility than the control, but a large immobilized component remained. The change in mobility of the protein bound spin labels as a function of SDS-urea concentration is shown in Figure 28b. As the concentration of SDS-urea was increased, there were substantial increases in the resonance line heights, a decrease in $\Delta H_O$, and loss of the $h_{+1}$ shoulder. The $h_{+1}$ line height increased to a maximum of 175% of the control value when the concentration reached 4 M urea and 0.5% SDS. The ESR spectrum of TA-BR at high concentrations of SDS-urea appeared as a homogeneous population of spins possessing high mobility ( $\tau_c = 7.61 \times 10^{-10}$ s), indicative of the release of previously immobilized labels.

### 4. Accessibility of spin-labeled bacteriorhodopsin to paramagnetic broadening agents

As seen in figure 29, the control ($0$ mM $Fe(CN)_6^{-3}$) spectrum appears to be composed of at least two components of different mobility as evidenced by the broad low field shoulder adjoining the sharp $h_{+1}$ peak. In order to distinguish spectral components located at the protein surface from other labeled sites, the spin exchange broadening between protein bound spin labels and paramagnetic ions in solution (presumed to require direct contact between colliding paramagnetic species; Keith et al., 1977) was used to deconvolute the complex ESR spectrum. Sodium ferricyanide ($Na_3Fe(CN)_6$) and nickel chloride

Figure 29. Paramagnetic broadening of 2.0 TA-BR by increasing

concentrations of $Fe(CN)_6^{-3}$. Difference spectrum at

bottom obtained by computer subtraction of 200 mM $Fe(CN)_6^{-3}$

from 0 mM spectrum. 2.0 TA-BR (10 mg/ml) was suspended in

150 mM KCl, 10 mM phosphate, pH 7.0. All ESR spectra

recorded at $5 \times 10^3$ gain.

Paramagnetic Broadening of TA-BR Spin Labeled
Bacteriorhodopsin by $Fe(CN)_6^{-3}$

$\overleftrightarrow{10G}$

$[Fe(CN)_6^{-3}]$

0 mM

20 mM

50 mM

100 mM

150 mM

200 mM

Difference
Spectrum
(0-200 mM)

XBL 822-117A

(NiCl$_2$) were employed as paramagnetic broadening agents since they possess similar relaxation-rate constants for interactions with a nitroxide radical in water but differ in charge characteristics (Likhtenstein, 1976). These compounds are extremely water soluble, presumably chemically inert with respect to functional groups of BR, and do not contribute an ESR signal of their own.

Titration of spin-labeled native BR with Na$_3$Fe(CN)$_6$ resulted in the progressive broadening of the spin signal until only a highly immobilized signal remained at high (200-273 mM) Fe(CN)$_6^{-3}$ concentrations (Fig. 29). Low concentrations of Fe(CN)$_6^{-3}$ selectively quenched the more mobile components of the spectrum, while the immobilized components were not affected. ESR spectra showed a significant loss of the $h_{+1}$ peak that occurred in the 0-200 mM Fe(CN)$_6^{-3}$ concentration range while the underlying $h_{+1}$ shoulder was not affected. In addition, computer subtraction of Fe(CN)$_6^{-3}$ quenched spectra from control TA-BR spectra revealed high mobility difference spectra (e.g., bottom of Fig. 29). The amplitude of these high mobility ESR difference spectra was found to increase as the Fe(CN)$_6^{-3}$ concentration increased. At 200 mM Fe(CN)$_6^{-3}$, only strongly immobilized spin signals remained and higher Fe(CN)$_6^{-3}$ concentrations produced only slight additional changes in the quenched ESR spectra.

The presence of a large immobilized ESR signal that remained at high Fe(CN)$_6^{-3}$ concentrations suggested the existence of buried spin label residues in the native membrane-protein structure. Denaturation is expected to open the BR structure and increase the accessibility of Fe(CN)$_6^{-3}$ to previously buried protein domains. The ESR spectra in Figure 30 show that Fe(CN)$_6^{-3}$ was substantially more

Figure 30. Effects of paramagnetic broadening agent charge, concen-
tration and BR protein conformation on quenching effective-
ness. 2.0 TA-BR was 10 mg/ml in native samles and 5 mg/ml
in denatured samples. Denatured samples contained 5 M
urea, 0.5% SDS, and were heated at 100°C for 10 min prior
to addition of paramagnetic ion. Gains are indicated in
figure.

# EFFECTS OF QUENCHER CHARGE AND PROTEIN
# CONFORMATION ON SPIN-LABELED BACTERIORHODOPSIN
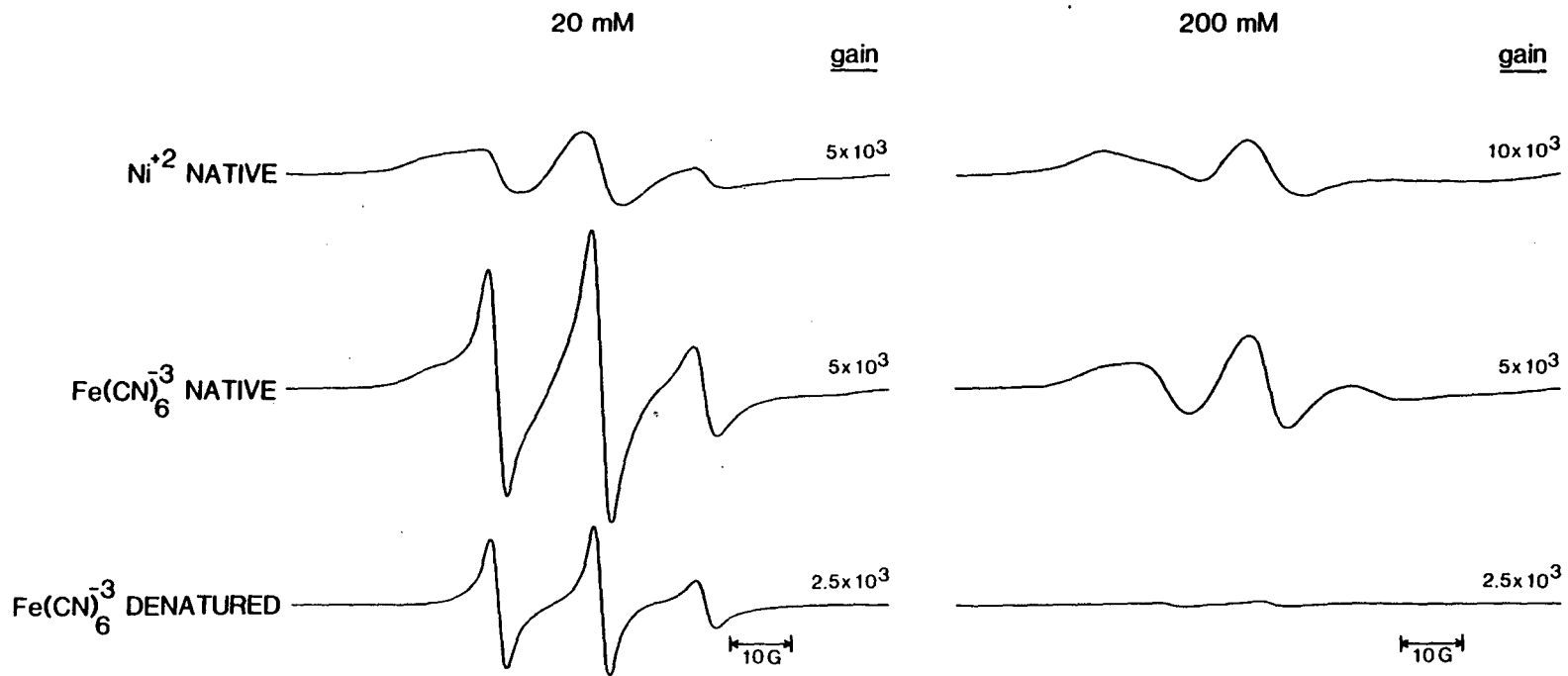
XBL 821-7775

effective in quenching the SDS-urea treated signal at equivalent concentrations of probe. At 20 mM $Fe(CN)_6^{-3}$, the decrease in the $h_{+1}$ line height for the SDS-urea treated sample was 61% compared to 25% for the native sample. At 200 mM $Fe(CN)_6^{-3}$, the SDS-urea TA-BR signal was completely broadened while a strongly immobilized spectrum remained in the native TA-BR sample.

Paramagnetic broadening by $Ni^{+2}$ was also found to remove the mobile components of the complex TA-BR spectrum. Figure 4 also shows that a large immobilized signal remained at high concentrations of $Ni^{+2}$ which appeared more strongly immobilized than the corresponding $Fe(CN)_6^{-3}$ broadened spectrum. This may be due to the fact that $Ni^{+2}$ showed a much greater line broadening efficacy than $Fe(CN)_6^{-3}$ at equivalent concentrations. Substantial quenching of native TA-BR occurred at 20 mM $Ni^{+2}$ while effects of 20 mM $Fe(CN)_6^{-3}$ were minimal. Moreover, 40 mM $Ni^{+2}$ and 245 mM $Fe(CN)_6^{-3}$ produced nearly identical ESR spectra.

The substantial differences in the concentration dependence between positively charged $Ni^{+2}$ and negatively charged $Fe(CN)_6^{-3}$ suggested the important influence of the negatively charged surface potential of purple membrane sheets. To corroborate this interpretation, the effect of ionic strength on quenching was investigated by increasing the concentration of NaCl while keeping $Fe(CN)_6^{-3}$ constant at 40 mM. Increased concentrations of NaCl resulted in a decreased $h_{+1}$ intensity that was 50% of its original intensity at 2.0 M, a 100% increase in $\Delta H_0$, and saturation of the changes at high NaCl concentration. The 2.0 M NaCl spectrum in the presence of 40 mM $Fe(CN)_6^{-3}$ appeared similar to 120-160 mM $Fe(CN)_6^{-3}$ in the absence of salt.

### 5. Paramagnetic broadening of stearic acid spin labels in purple membranes

The paramagnetic broadening of a series of stearic acid spin labels (Fig. 31a) bound to purple membranes was studied in order to: (i) verify that the accessibility of $Fe(CN)_6^{-3}$ and $Ni^{+2}$ quenching agents was limited to the purple membrane surfaces, and (ii) to employ them as an empirical molecular ruler to estimate the depth of the buried TA-BR spin label. The second goal was achieved by examining the paramagnetic broadening of the stearic acid spin labels by $Cu^{+2}$, which is capable of acting at a distance by a through-space dipolar interaction (Hyde et al., 1979).
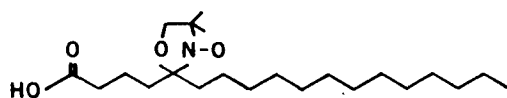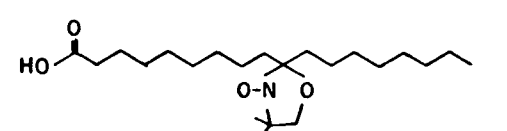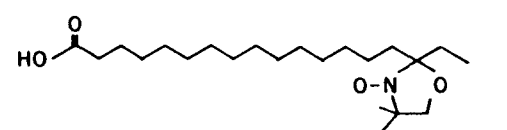
The effects of $Fe(CN)_6^{-3}$, $Ni^{+2}$, and $Cu^{+2}$ on the spectra of 5, 10, and 16-doxylstearic acid spin labels were compared. As seen in Figure 5, the ESR spectra of 5NS bound to purple membranes exhibited a strongly immobilized spectrum plus a small contribution from an aqueous mobile component. The 5NS signal was found to have a maximum hyperfine splitting $(2\ A_{||})$ of 63.1G, as previously described by Chignell and Chignell (1975). The apparent order parameter, $S^{app}$, was calculated to be 0.91 and the half amplitude of motion, $\gamma$, was 21°. The nitroxide moiety was calculated to be 5.9Å from the membrane surface. The amplitude and shape of the spectra were unaffected by the presence of 10-100 mM $Fe(CN)_6^{-3}$ except for the loss of the small, aqueous mobile component. However, $Ni^{+2}$ decreased the amplitude of the 5NS spectra without altering the lineshape (data not shown). Only 51% of the central line $(h_0)$ height remained in the presence of 20-200 mM $Ni^{+2}$. The 10NS label was also found to have a large hyperfine splitting $(2\ A_{||} = 61.0G)$ and its spectrum closely resembled that of the 5NS label (data not shown). Calculations gave $S^{app} = 0.84$, $\gamma = 31°$ and a distance of

Figure 31.

    a) Structures of the spin-labeled stearic acids employed in this study.

    b) Paramagnetic broadening of 5NS and 16NS stearic acid spin labels bound to purple membranes. BR (8 mg/ml) was suspended in 0.1 M NaCl, 0.01 M Hepes, pH 7.0 and contained 1.5 moles of either 5NS or 16NS/mole BR.

# Structure of Spin Labeled Stearic Acids

| Designation | Structure | Nitroxide distance from carboxyl group |
|---|---|---|
| 5 NS |  | 6.3 Å |
| 10 NS |  | 12.6 Å |
| 16 NS |  | 20.1 Å |

XBL8211-1306

171

# Paramagnetic Broadening of Stearic Acid Spins Labels Bound to Purple Membranes
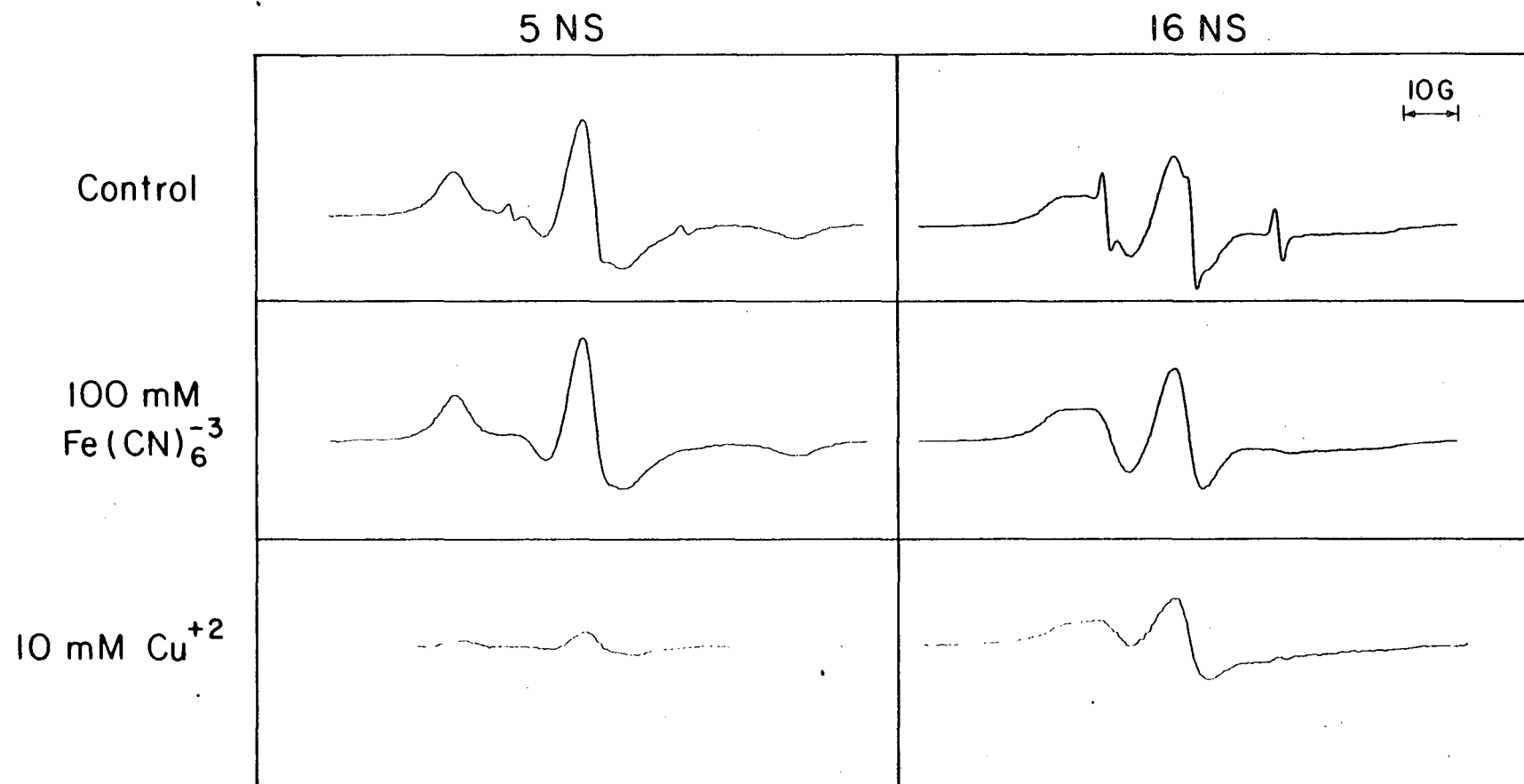
the nitroxide moiety of 11.3 Å from the surface.

In contrast to the strongly immobilized 5NS and 10NS spectrum, the 16NS spectrum is only moderately immobilized (2 $\bar{A}_{||}$ = 56.8G, $S^{app}$ = 0.59, $\gamma$ = 45°). This orientation gives a calculated distance of 16.6 Å for the 16NS nitroxide from the surface. The presence of a larger aqueous mobile signal superimposed on the membrane signal is due to increased partitioning of 16NS into the aqueous phase. As in the case of 5NS, high concentrations of $Fe(CN)_6^{-3}$ had no effect on the 16NS ESR spectra other than to broaden the aqueous mobile component. In the presence of 100 mM $Ni^{+2}$, the amplitude of the 16NS $h_0$ line was essentially unchanged (92% of the control).

The paramagnetic broadening of 5NS, 10NS, and 16NS by $Cu^{2+}$ exhibited even greater differences when compared to the effects of $Fe(CN)_6^{-3}$ (Fig. 5). The 5NS signal was almost completely broadened by 10 mM $Cu^{+2}$, with only 16% of the $h_0$ line height remaining. No additional broadening was observed at higher $Cu^{+2}$ concentrations ($\leq$ 200 mM). The more deeply buried 10NS and 16NS nitroxides were also broadened, but to a lesser extent. At 10 mM $Cu^{+2}$, 55% of the 10NS $h_0$ line height remained and 62% remained for 16NS. Stearic acid spin-label spectra that were reduced in amplitude retained the same lineshape as the control sample and did not show an increased central linewidth ($\Delta H_0$). At low concentrations of $Cu^{+2}$, the low field $Cu^{+2}$ ESR signal did not significantly contribute to the ESR signal in the nitroxide region. A small sloping baseline was observed in the presence of 100-200 mM $Cu^{+2}$, but did not interfere with quantitation of nitroxide ESR spectral parameters.

To determine if divalent cations without paramagnetic broadening

properties affected the mobility of the 5NS and 16NS labels, ESR
spectra were recorded in the presence of equivalent concentrations of
$Ca^{+2}$. For both the 5NS and 16NS stearic acid spin labels, $Ca^{+2}$ had
no effect on spin mobility, but caused a small increase in the parti-
tioning of the label into the membrane. At 10 mM $Ca^{+2}$, the extent
of this change was so small that no increase in the immobilized $h_0$ line
height was measurable.

### 6. Selective labeling of buried carboxyls by prior blocking of surface groups

As a biochemical approach to further corroborate the results
obtained with paramagnetic quenching agents, a sequential double
modification procedure was developed to selectively prereact and thereby
block surface carboxyl residues so that spin-labeling of only buried
residues occurred. In order to block surface residues, the first
carboxyl modification used a permanently charged non-spin label nucleo-
phile, aminoethanesulfonic acid (AES). After extensive washing, the
second modification using EEDQ and Tempamine was carried out under
identical conditions employed as in the single step modification (200
mM TA + 10 mM EEDQ). The stoichiometry of the double modified samples
prepared by this procedure contained an average of 0.4 spins per BR
molecule.

ESR spectra of the AES/TA double modified BR showed predominantly
a strongly immobilized spin signal with a central line width of 7.6 G
and a maximum hyperfine splitting of 68.7 G (Figure 32). A very small
amount of unremoved free tempamine remains observable in the control
spectrum which is broadened in the $Fe(CN)_6^{-3}$ spectrum and can also
be removed by additional washing. The strongly immobilized ESR signal

Figure 32. Interactions of paramagnetic broadening agents and AES/TA

Double Modified BR. AES/TA-BR (8 mg/ml) was suspended in

0.1 M NaCl, 0.01 M Hepes and $Fe(CN)_6^{-3}$ or $Cu^{+2}$ was

added to give the indicated concentrations. All spectra

recorded at $2 \times 10^4$ gain. Notice that the $Cu^{+2}$ spectra

retains the same lineshape as the $Fe(CN)_6^{-3}$ sample and is

only slightly decreased in intensity.

Paramagnetic Broadening of Double Modified Carboxyl
Spin – Labeled Bacteriorhodopsin

AES / TA – BR
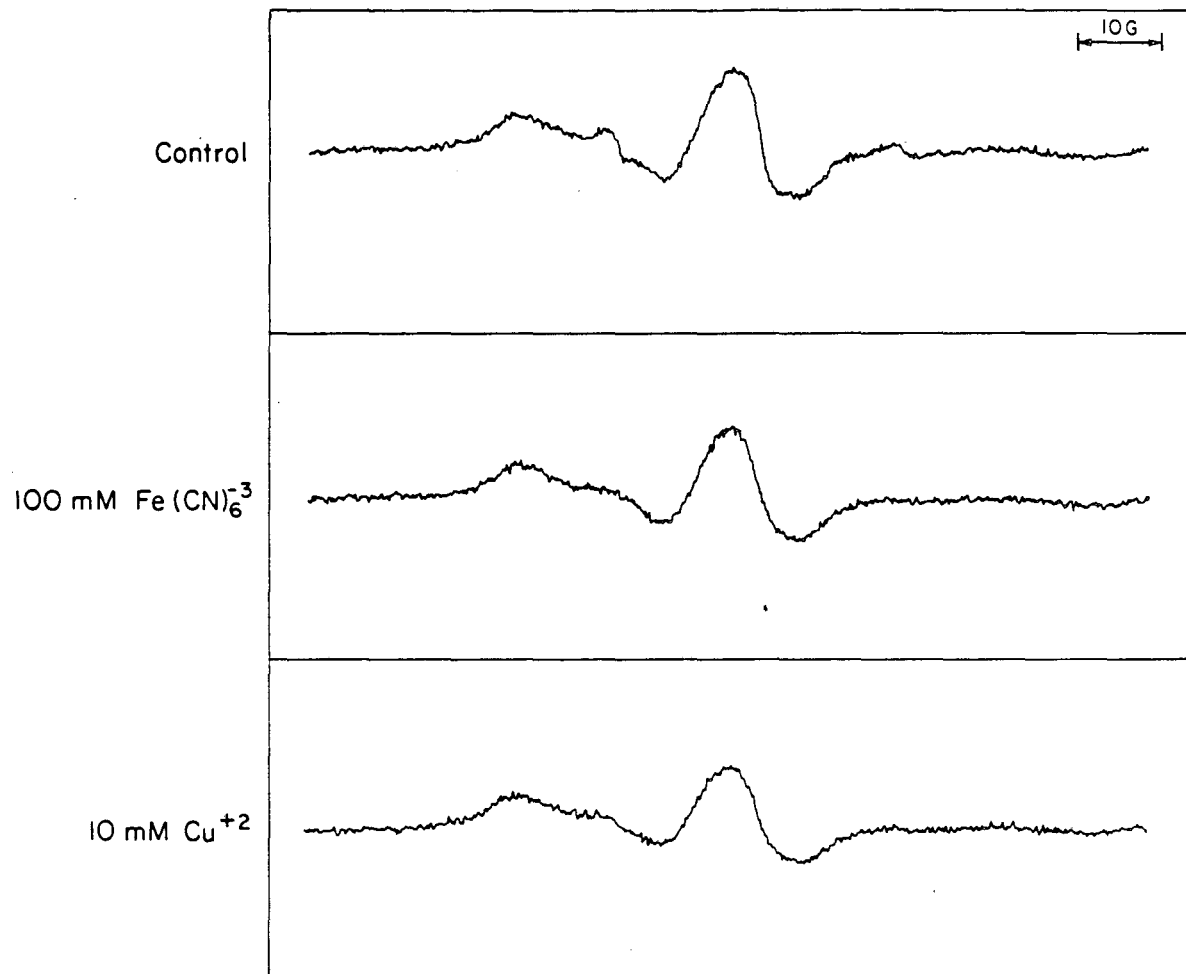


XBL 8211-1305

was not broadened by high concentrations of $Fe(CN)_6^{-3}$ as expected for
a buried spin residue. Paramagnetic interactions of the AES/TA-BR
spin label with $Cu^{+2}$ were also examined in an attempt to estimate
its depth from the membrane surface. The interaction of 10 mM
$Cu^{+2}$ and AES/TA-BR resulted in only a moderate decrease in amplitude
(75% of control remained) with no apparent broadening. Higher $Cu^{+2}$
concentrations caused no further decreases in the amplitude and
lineshape of the AES/TA spin label spectra. The observed reduction
in amplitude without apparent line broadening is consistent with a
dipolar interaction between $Cu^{+2}$ and the immobilized protein-bound
nitroxide (Leigh, 1970).

### 7. Trypsin treatment

To further resolve which surface groups had been labeled, 2.0
TA-BR was treated with trypsin. Trypsin treatment of BR has been
shown to cleave at a single site and release the C-terminal tail from
the membrane (Gerber et al., 1977). The tail is composed of 20 pre-
dominantly polar amino acid residues and contains 5 carboxyl groups.
Trypsin treatment of 2.0 TA-BR resulted in the progressive increase in
the mobile components of the total spectrum. The kinetics of this
change were monitored by either recording sequential ESR spectra or by
following the increase in magnitude of $h_{+1}$ peak (Fig. 33b). The 200%
increase in line height of the $h_{+1}$ resonance line was almost complete
in 5 hours. SDS-polyacrylamide gel electrophoresis showed only the
loss of a 1500 M.W. fragment from the 26,000 M.W. spin labeled protein
and yielded a single new band of the expected molecular weight. The
trypsin-treated TA-BR membranes were centrifuged (100,000 x g, 30 min)
to separate the membrane protein from the soluble peptides. As seen

Figure 33.  Changes in ESR Spectra Due to Cleavage of C-Terminal Tail

by Trypsin Treatment.  Trypsin treatment was in 40 mM Tris,

pH 8.0, 80 mM NaCl, 10 mM $CaCl_2$ at trypsin:TA-BR weight

ratio of 1:100.

a)  ESR spectra of TA-BR (5 mg/ml) before trypsin addition and

after 4 hr incubation at 37°C.  The soluble tail and trypsinized membrane

were separated by centrifugation, and ESR spectra of the supernatant

and pellet (after resuspension) were recorded at identical gain at 37°C.

b)  Kinetics followed by ESR recording of $h_{+1}$ resonance line using
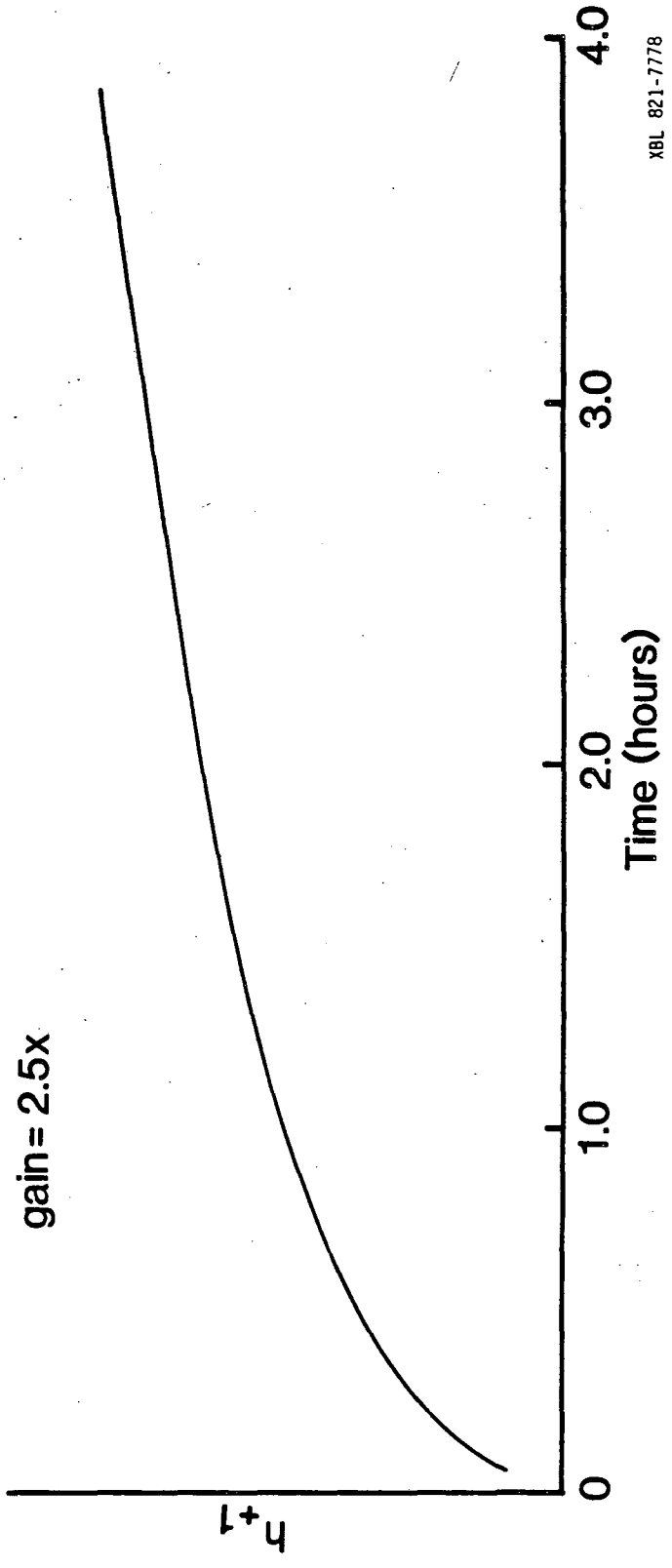
2.5x higher gain than in (a) at 37°C.

# TRYPSIN TREATMENT OF CARBOXYL SPIN-LABELED BACTERIORHODOPSIN



XBL 821-7779

180
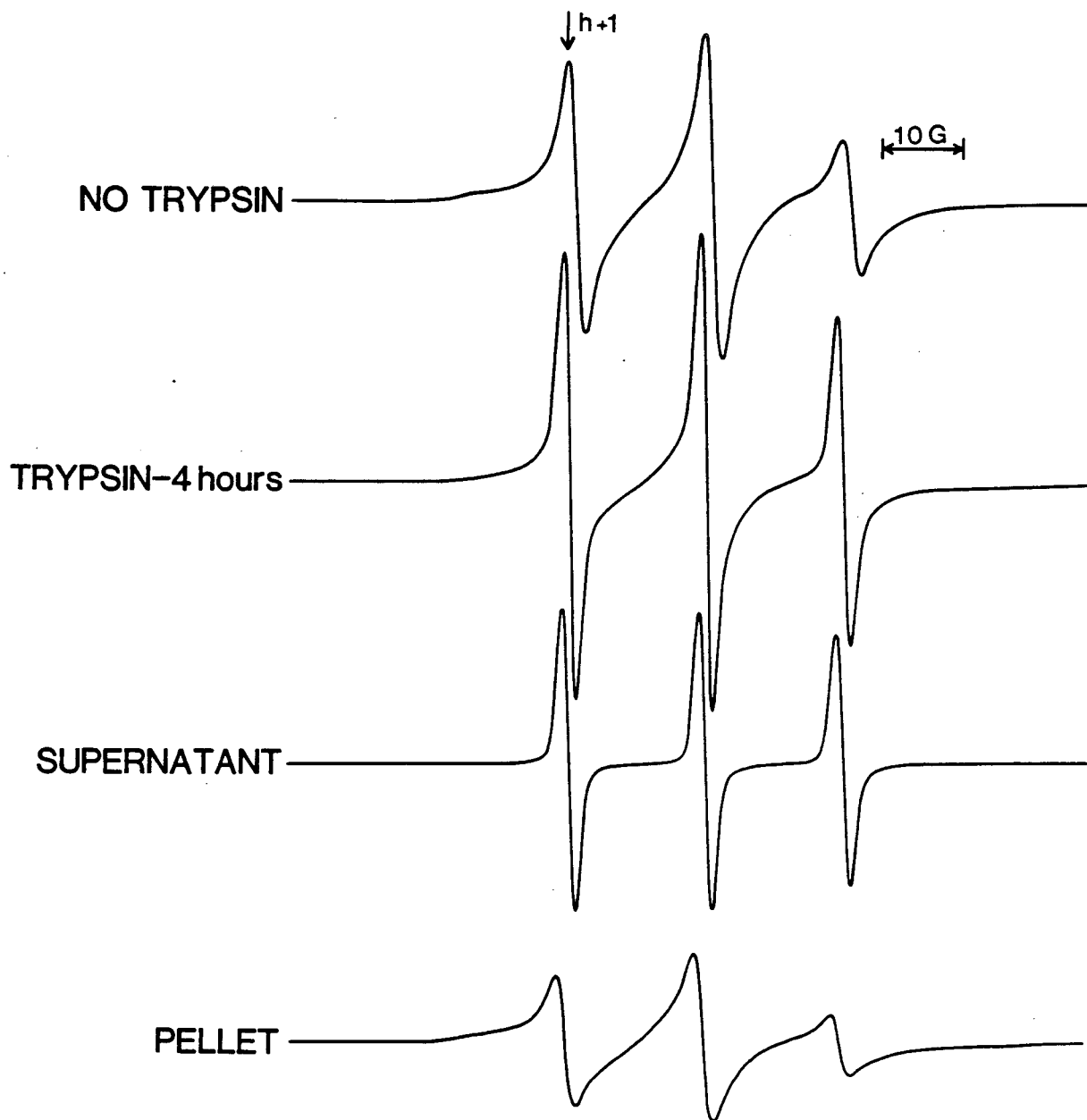


KINETICS OF TRYPSINIZATION
gain = 2.5x

h+1

Time (hours)

XBL 821-7778

in Figure 33a, ESR spectra of the clear supernatant fraction showed only a highly mobile spin population which was calculated to have a $\tau_c = 1.65 \times 10^{-10}$ s. The ESR signal of this fraction was completely quenched by a low concentration of $Fe(CN)_6^{-3}$ (20 mM). The trypsin-treated TA-BR membrane pellet was washed and resuspended at the same concentration as before trypsin treatment. ESR spectra showed the loss of most of the more mobile components compared to the untreated TA-BR spectrum. However, a significant mobile feature remained after trypsin treatment. A large immobilized signal remained in the presence of high concentrations of $Fe(CN)_6^{-3}$.

8. Proton pumping activity of spin-labeled BR studied in
   reconstituted liposomes

To obtain information on the sidedness of the surface labeled sites, 2.0 spin-labeled BR was incorporated into liposomes by a procedure shown to produce unilamellar liposomes (Swanson et al., 1980). It had been shown previously through proteolytic digestion experiments that essentially all (95%) BR incorporated into unilamellar liposomes is oriented with the C-terminal tail (cytoplasmic face) facing outwards (Huang et al., 1980). Such "inside-out" orientation results in light-induced proton pumping to the liposome interior and internal acidification. The incorporation and functional integrity of TA-BR liposomes were verified by measuring internal liposome volume and light-dependent proton pumping. An ESR volume measurement with Tempone gave a volume of 0.75 μl/mg lipid. Light-induced proton pumping, assayed by quanti-tating the distribution of N,N'-dimethyl-tempamine, resulted in internal acidification and a pH gradient of 0.6 units. Hence, the gross orientation and function of BR were preserved after spin-labeling. To

Figure 34.   ESR spectra of $Fe(CN)_6^{-3}$ quenched 2.0 TA-BR in purple

membrane sheets and in reconstituted liposomes.  Samples

were suspended in 150 mM KCl, 10 mM $PO_4^-$, pH 7.0.  Note

the sharp inflections in the $Fe(CN)_6^{-3}$ quenched liposome

spectra that are absent from the corresponding quenched

purple membrane sheets.

$Fe(CN)_6^{-3}$ Quenching of spin-labeled Bacteriorhodopsin in Purple Membrane sheets and Liposomes

TA-BR in
Purple Membrane Sheets

TA-BR in
Reconstituted Liposomes

$Fe(CN)_6^{-3}$

0mM

100mM

200mM

10 G
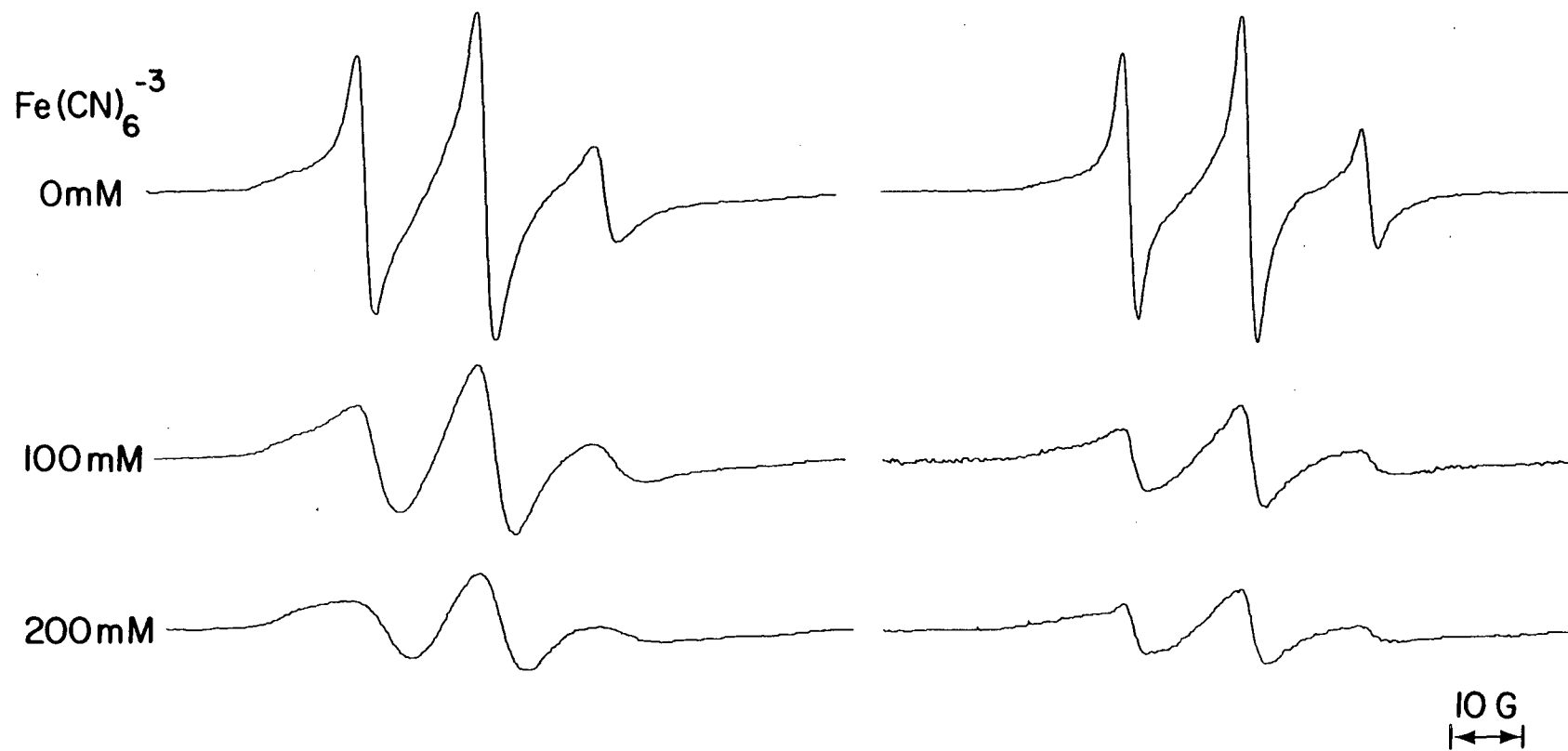
XBL 822-85

permit comparison with digestion of TA-BR in purple membrane sheets, liposomes containing TA-BR were also trypsin treated. At room temperature, a substantial increase in the low field peak height occurred over a period of 8 hours with kinetics similar to those obtained in TA-BR purple membrane sheets. An ESR spectrum of the supernatant after centrifugation showed the presence of highly mobile spins, as in the case of trypsin treatment of TA-BR purple membrane sheets.

Quenching of TA-BR in purple membrane sheets and in liposomes was compared under conditions of identical ionic strength and buffer composition. Incorporation of TA-BR into liposomes resulted in a small increase in the overall mobility of the ESR spectrum. Quenching in liposomes by $Fe(CN)_6^{-3}$ resulted in the loss of most of the mobile spectral components whereas all of the mobile components were quenched in the TA-BR purple membrane sheets. The sharp inflection in the $h_0$ line and small peak in the $h_{+1}$ line that remained in the quenched liposome spectra were absent in the 200 mM $Fe(CN)_6^{-3}$ purple membrane sheet spectra (Fig. 34). The quenched components can be ascribed to spins on the cytoplasmic purple membrane surface facing the liposome exterior. The mobile component that remains in the $Fe(CN)_6^{-3}$-quenched liposomes may be due to a small number of spins on the extracellular surface of purple membranes, although fractional misorientation cannot be excluded.

## 9. Discussion

A combination of analytical procedures for spin labeled membrane proteins has been applied to definitively show that at least two classes of carboxyl groups exist in bacteriorhodopsin: a strongly immobilized, buried membrane group and a weakly immobilized, surface set that includes

carboxyls on the C-terminal tail. There is considerable theoretical interest in whether or not carboxylic amino acids, which are normally charged in aqueous solution, can be accommodated within stable hydrophobic membrane domains (Honig and Hubbell, 1983). Although models of bacteriorhodopsin structure have suggested the presence of buried carboxyl residues, this study provides the first evidence for such residues deep within hydrophobic domains of the protein. By utilizing paramagnetic ion interactions with spin-labeled stearic acids to measure molecular distances, we show that one or more of these carboxyls is $\geq 16$ Å away from the aqueous interface.

The introduction of bulky nitroxide groups into a protein structure raises legitimate concerns about the integrity of the chemically modified protein. To assure that 2.0 TA-BR was not structurally or functionally compromised, we showed that the spin-labeling process did not significantly alter spectral characteristics, photocycling kinetics, bleaching properties or proton-pumping activity. It was also shown that the 2.0 TA-BR was sensitive to structural perturbation by demonstrating that substantial ESR spectral changes resulted when the protein was denatured with chemical agents and heat treatment. The amide linkage resulting from the EEDQ-Tempamine reaction provides excellent sensitivity to the carboxyl's microenvironment since it is very short in length and possesses limited flexibility (Fig. 27). This is an important consideration since experiments with spin-labeled proteins have demonstrated that the sensitivity of ESR spectra to the microstructure of proteins is strongly dependent on the structure of the "leg" linking the nitroxide to the protein backbone (Cornell and Kaplan, 1978). Hence, the 2.0 TA-BR preparations were deemed representative of the native BR protein.

a. <u>Interpretation of ESR data for localization of carboxyl residues</u>

The principal approach for defining the topography of carboxyl groups in the protein was to examine paramagnetic interactions between ions in the aqueous phase and covalently attached nitroxides on the carboxyl groups. Two types of paramagnetic interactions were employed: the spin exchange interaction and the dipole interaction. The former arises when electrons of two paramagnetic molecules or ions share orbitals and requires that there be an appreciable overlap of their electronic wavefunctions. This requirement is generally considered to be equivalent to the occurrence of direct collisions between the paramagnetic species (Keith <u>et al.</u>, 1977). Spin exchange results in line broadening of affected nitroxides. The occurrence of such broadening implies direct contact of spin-labeled groups with the aqueous phase, and these groups are considered to be surface residues. On the other hand, dipole interactions occur over much larger distances and can be used, in principle, to determine the distance of buried spin labels from to the aqueous phase. Some transition metals, such as $Cu^{+2}$, $Mn^{+2}$, and $Gd^{+3}$, are capable of a large through-space dipolar interaction with spin labels (Hyde <u>et al.</u>, 1979). This interaction varies as the inverse of the sixth power of the distance and has been used to estimate the distance between two spins (Taylor <u>et al.</u>, 1969; Burley <u>et al.</u>, 1972). The theoretical treatment of this problem developed by Leigh (1970) demonstrated that the ESR signal of an immobilized spin label covalently bound to a protein was not broadened, but only decreased in amplitude as a result of a dipolar interaction with a paramagnetic ion at a fixed distance. Hyde and Rao (1978) extended this type of calculation in order to consider a situation in

which a number of metal ions could interact with each free radical. A main conclusion of their analysis was that even though there is a wide range of distances, observed magnetic interactions will be determined primarily by the distance of closest approach.

We tested paramagnetic ions employed in this study to determine if they could be utilized as either good surface or good dipole agents in the purple membrane preparations. Although it is a fairly straightforward matter to estimate the relative magnitudes of exchange interactions and dipole interactions between paramagnetic ions and nitroxides in aqueous solutions (Salikhov et al., 1971), these properties can be markedly altered as a function of chelation or binding of the paramagnetic ions. Therefore, we used a series of spin-labeled stearic acids bound to these membranes as an empirical molecular ruler to assess the extent to which a given paramagnetic ion interacts with intramembrane nitroxides as a function of their distance from the membrane surface. The results showed that $Fe(CN)_6^{-3}$ could be used to identify surface spin labels. We observed the absence of any paramagnetic interactions between $Fe(CN)_6^{-3}$ and spin-labeled stearic acids bound to purple membranes. We would not expect $Fe(CN)_6^{-3}$ to bind significantly to membranes because of charge repulsion. On the other hand, nickel and other divalent cations have been shown to bind to phospholipid vesicles (Wagner et al., 1980). The low, effective concentration for broadening suggests binding also occurs in purple membranes. It has been observed that $Cu^{+2}$ and $Ni^{+2}$ are effective dipole reagents in aqueous solutions (Hyde and Sarna, 1978), and they were found to interact with nitroxides within hydrophobic membrane domains.

$Cu^{+2}$ was found to be a strong dipolar agent since its interactions

with the spin-labeled stearic acids extended to the depth of the 16NS nitroxide. One characteristic of the stearic acid spin-label spectra in the presence of the $Cu^{+2}$ was a decreased amplitude without apparent line broadening. The decrease in amplitude followed the pattern, 5NS > 10NS > 16NS, which is correlated with the depth of the nitroxide moiety from the membrane surface. $Ni^{+2}$ was found to be a weak dipolar agent since its interaction with spin-labeled stearic acids resulted in line height reduction of spins (5NS) located near the membrane interface, while deeply buried spins (16NS) were unaffected. These observations resemble previous data on $Ni^{+2}$ interactions with the 5NS and 16NS spin labels in sarcoplasmic reticulum vesicles (Champeil et al., 1980).

The effects of paramagnetic broadening agents showed that two distinct protein domains were spin-labeled, and spectral characteristics demonstrated that surface groups were considerably more mobile than buried groups. Paramagnetic broadening of the 2.0 TA-BR spectra by $Fe(CN)_6^{-3}$ selectively broadened the more mobile spectral characteristics. Since we found that $Fe(CN)_6^{-3}$ acted as a spin-exchange agent in the stearic acid model system, we conclude that these mobile groups reside at the surfaces of the purple membrane. The presence of the large immobilized component in 2.0 TA-BR (60% of the total spin) that remained in the presence of high $Fe(CN)_6^{-3}$ concentrations is strong evidence for the existence of buried label residues. These residues must reside in a protein domain, presumably hydrophobic, which is inaccessible to $Fe(CN)_6^{-3}$. Denaturation of TA-BR caused increased spin mobility and increased accessibility to charged quenching agents, consistent with the transfer of previously buried immobilized spin

residues to the aqueous environment.

$Ni^{+2}$ also caused paramagnetic broadening of the mobile spectral components. A smaller, more strongly immobilized signal relative to $Fe(CN)_6^{-3}$ remained at high concentrations. This may be due to the weak $Ni^{+2}$ dipolar interactions that extended at least to the level of the 5NS nitroxide. In addition, the different concentration dependent effects of $Cu^{+2}$, $Ni^{+2}$ and $Fe(CN)_6^{-3}$ can be ascribed in part to the negative surface potential of purple membrane sheets, which was previously determined to be almost -60 mV (Carmeli et al., 1980). As predicted by the Gouy-Chapman Theory (Barber, 1980), we found that high salt concentrations increased line broadening by $Fe(CN)_6^{-3}$ due to increased concentrations of these ions at the membrane surfaces.

The conclusion that both surface and buried groups are labeled, is supported by double-modification data. Blocking of surface groups with the permanently charged nucleophile, AES, showed that only immobilized spectral features could be observed upon subsequently spin-labeling the pre-treated BR. Comparison of the central line height reduction due to $Cu^{+2}$ interaction with the 5NS, 10NS, 16NS and AES/TA-BR shows that 16NS and AES/TA-BR are affected similarly and hence that the spin-labeled carboxyl group is deeply buried within the protein. Thus, to a first approximation, we would estimate the minimum distance of the buried carboxyl group(s) from the membrane surface to be 16.6 Å.

There are several possible sources of error in estimating accurately the effective intramembrane position of the buried carboxyl group(s). The first is that the presence of the nitroxide moiety may induce a local disordering effect on the acyl chain. Hence, in the distance calculation for 16NS, the use of 21° for the acyl chain segment from

carbons 1-5 and of 31° for the segment from carbons 5-10 probably over-estimates the tilt of those segments of the chain. This implies that the distance calculated for the position of the 16NS nitroxide group relative to the membrane surface should be considered to be a minimum value. A second possible error source is uncertainty about the surface structure of bacteriorhodopsin since this will determine the closest approach of quenching agents to the spin label. However, recent information from Zaccai and Gilmore (1979) about the hydration areas of purple membranes suggests that the protein surfaces are coplanar with the lipid headgroups to within about 1.5 Å. A third potential source of error is preferential association of copper ions with lipids rather than bacteriorhodopsin. This possibility is deemed to be an unimportant because the quenching behavior of the buried carboxyl group was essentially the same at concentrations of copper between 10 mM and 100 mM. A fourth potential source of error is possible heterogeneity in labeling, both with respect to the number of carboxyls modified and their distribution within a given protein molecule. Labeled sites at different distances from the membrane surfaces would be differentially broadened by $Cu^{+2}$ interactions. Greater $Cu^{+2}$-quenching of groups closer to the surface would bias the calculated distance of the more deeply buried groups such that their actual distance would be further from the surface than that which we calculated assuming a homogeneous population. In view of these considerations, we suggest that the 16.6 Å estimate for the minimum depth of the labeled carboxyl group(s) is conservative and includes reasonable allowances for errors.

b. **Mobility of the carboxyl-terminal tail**

Conversion of a weakly immobilized spectral component to a free component as a result of trypsin treatment, indicates that the C-terminal tail in the native BR structure is immobilized to some extent. This is supported by fluorescence depolarization data from a dansyl labeled carboxyl on the tail (Renthal et al., 1982). Since the carboxyl-terminal tail has not yet been resolved in electron density maps (Wallace and Henderson, 1982), the position it may occupy on the cytoplasmic face of the protein and the nature of its interaction with the membrane is open to speculation. The immobilization seen with spin-labeling may be due to ion-pairing between the carboxyls on the tail and some of the positively charged groups of the 5 lysines or 4 arginines thought to be present on the cytoplasmic surface. The structure and function of the C-terminal tail in BR remains unknown, although it may play a role in the proton pumping mechanism. Decreased $H^+$ release stoichiometries in purple membrane sheets after proteolysis of the tail have been reported, although its absence has no effect on photocycling activity (Govindjee et al., 1980, 1982).

c. **Identification of buried carboxyl residues in bacteriorhodopsin**

One of the more important implications of this study concerns the placement of buried charges in models of BR structure. To date, BR models place some aspartic and glutamic carboxyl residues within the hydrophobic membrane phase, although the majority of such residues have been placed at the cytoplasmic and extracellular surfaces (Agard and Stroud, 1982; Engelman et al., 1980, 1982; Huang et al., 1982). The requirement that buried charges form ion-pairs has been used as an

important criterion in selecting among possible models meeting other criteria (Engelman et al., 1980), but this was not directly shown. The ESR data suggest locations for the buried spin residue(s) that are consistent with three recent models of bacteriorhodopsin structure, each of which postulates 5 or 6 buried carboxyl groups with only a few residues located 16 Å or more from the membrane surface. We have determined the depths of the residue positions in the models based on a membrane thickness of 45 Å (Agard and Stroud, 1982). Agard and Stroud place Glu-9, Asp-85, Asp-96, Asp-115, Glu-166 and Asp-212 below the membrane surfaces, but only Asp-85, Asp-115 and Asp-212 are buried deeper than about 16 Å. Engelman et al. (1982) combined evidence from free-energy calculations for the insertion of bacteriorhodopsin into a lipid bilayer and chemical modification studies to derive a model which places five carboxyls: Asp-85, Asp-96, Asp-115, Glu-204 and Asp-212, in the hydrophobic membrane domain. Of these, only Asp-212 and Asp-115 are clearly buried deeper than 16 Å, while Asp-85 lies on the borderline. Huang et al. (1982) have arranged the polypeptide chain based on the cross-linking data of a photoaffinity derivative of retinal and a recent proposal of Steitz et al. (1982). The revised model includes the 5 buried residues of Engelman et al. (1982) plus one additional residue, Glu-9. The deepest buried residue in this model is Asp-212, while Asp-85 and Asp-115 are located about 15 Å from the surface. All three models assign residues Asp-85, Asp-115 and Asp-212 as the most deeply buried carboxyl residues ($d \geq 15$ Å). We consider these three residues as the most likely sites of labeling. Thus, our data are consistent with current models of bacteriorhodopsin structure.

IX.  GENERAL DISCUSSION

## Carboxyl Residues Essential for Photocycling Activity

The molecular mechanism of proton translocation by BR is intimately related to its photocycling function.  Photocycling activity of carboxyl modified BR demonstrated that carboxyl residues are essential for this function.  From an operational viewpoint, essential groups are those whose modification brings about loss of the photocycling activity due to a specific change in the group's chemical character.

The results indicate that modified carboxyl residues on the membrane surface (in which the retinal-protein chromophore is not substantially perturbed) are not essential for photocycle activity.  Of 19 carboxyl groups in the protein, 12 can form carboxyamidyl products of different ionic character with minimal effects on photocycle kinetics.  Although some modified samples had strongly inhibited kinetics, the $M_{412}$ yield indicated that all samples retained photocycling activity.  In addition, the pathway of the photocycle remained unchanged in all samples.

Conditions favoring modification of buried groups, however, resulted in loss of the retinal-protein chromophore and consequently, loss of photocycling activity.  This suggests that critical carboxyl groups essential for photocycling function may be located in the immediate chromophore vicinity in a hydrophobic environment.  This suggestion will only be valid if possible conformational changes in the modified protein can be ruled out.

## Carboxyl Residues From Ion-Pairs with Positively Charged Groups

The formation of ion-pairs between oppositely charged amino acids in the membrane environment of BR has been proposed (Engelman et al., 1980). It has been used as a distinguishing feature in the selection of models meeting other general criteria. Chemical modification using carboxyl activating reagents resulted in a single zero-length intramolecular cross-link between a carboxyl and lysine residue. A carboxyl-lysine pair must therefore be in close proximity in the native membrane, and are probably interacting ionically. This appears to be the best evidence to support the existence of an ion-pair in BR structure. The data indicate that this ion-pair may reside in the membrane. In the photocycle, the presence of the cross-linked residues inhibited the decay kinetics of the $M_{412}$ intermediate. This suggests that a conformational change in BR associated with $M_{412}$ decay affects the distance between the interacting carboxyl-lysine residues. The cross-link acts to constrain the normal protein movement occurring during the reprotonation phase of the photocycle.

The role of a carboxyl-lysine ion-pair in the photocycle mechanism may be analogous to the function of such ion-pairs in the cooperative allosteric interactions of hemoglobin (Perutz, 1970). BR may use such ion-pairs to store energy in the protein after the light-absorption event. A consequence of retinal isomerization would be to remove the positively charged Schiff base from a negatively charged carboxylate group. Alternatively, such a charge separation leading to a significant increase in free energy could occur in any buried ion-pair. Although the dielectric constant is not known, separating charges such as a carboxyl-lysine ion-pair, by a few angstroms can easily lead to

free-energy changes equal to or greater than 20 kcal/mole (Honig et al., 1979).

## Carboxyl Residues Involved in Protein-Chromophore Interactions

Several models of retinal-protein interactions for BR have postulated the placement of negatively charged residues in the chromophore environment. This study has identified a carboxyl group modified with a pH-sensitive reporter group that interacts with the retinal-protein chromophore. The nitrotyrosine methyl ester chromophore was used to monitor microenvironment of the protein near the retinal binding site. The results show that the chromophoric reporter group-retinal interactions occur in a hydrophobic membrane domain in the native state.

The exact mechanism of the NTME-retinal interaction cannot be ascertained at this point. The loss of NTME-retinal interactions subsequent to a configurational change argues for an electrostatic mechanism dependent on a particular geometry of the interacting groups. It makes a coupling mechanism such as Förster energy-transfer, which occurs over a wide range of distances (albeit with different efficiency), a much less likely explanation. These results provide additional evidence for the hypothesis (Honig et al., 1979) that electrostatic interactions between the retinal chromophore and charged groups on BR are responsible for regulation of the absorption maxima.

## The Topography and Mobility of Carboxyl Residues

This study has also explored the local topography and mobility of distinct protein domains in the vicinity of carboxyl residues. Chemical modification methods were employed to selectively spin-label carboxyl groups in BR. A combination of biochemical and biophysical procedures

definitively showed that at least 2 distinct classes of carboxyl groups exist in BR: (1) a strongly immobilized, buried membrane group(s) and (2) a weakly immobilized, surface set that includes carboxyls on the C-terminal tail. In addition, this study provided evidence for one of the distinguishing features of current models of BR structure; the placement of the charged residues of aspartic and/or glutamic acid in hydrophobic, buried membrane domains.

## Carboxyl Residues Involved in Proton Translocation Activity

A surprising finding of this investigation was that all carboxyl modified samples in which the retinal-protein chromophore was substantially unaltered retained proton pumping capabilities. However, under no conditions were all carboxyl residues modified, and thus their potential function as ion-translocating groups cannot be excluded. The difficulty in resolving this problem lies in obtaining conditions that yield extensive modification (particularly of buried residues) while retaining native protein and chromophore structure. Conditions that modify 3-4 buried groups also bleach the chromophore, and thus the proton translocation activity cannot be determined.

One current model for proton conduction in BR is based upon the concept of long-lived chains of hydrogen bonds between hydrogen bonding side groups in the protein (Nagle and Morowitz, 1981). This assumption appears favorable for BR because: (1) structural work has shown that the purple membrane is extremely ordered and rigid and (2) neutron diffraction data has determined that BR does not contain a bulk aqueous channel (Zaccai and Gilmore, 1979). This study further supports such an idea since strongly immobilized carboxyl group side chains could act as stable contributors to chains of hydrogen bonds. A combination of
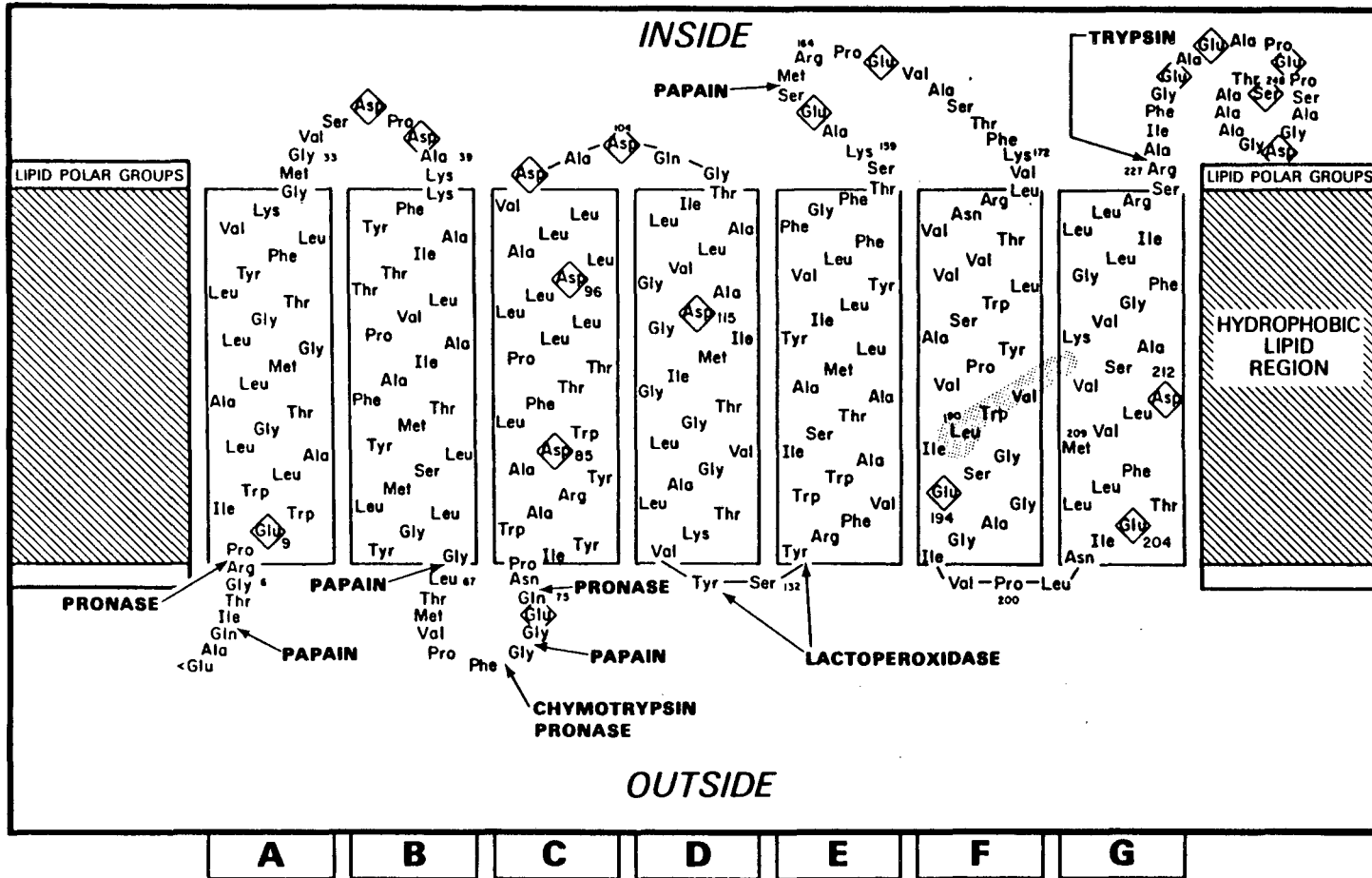
pK changes and/or configurational changes in retinal, or conformational changes in the protein, act as a gate or switch for proton conduction. Evidence for the participation of tyrosine in deprotonation and reprotonation reactions associated with the $M_{412}$ intermediate is the strongest (see background section). However, it is likely that other amino acid residues with lower pK values, such as carboxyl groups, could participate as members of the proposed proton wire. A group must act as the acceptor for the tyrosine proton since it does not appear immediately in solution. Calculations indicate that the pK of the groups that release the proton to the aqueous phase cannot exceed ≃6 (Kalisky et al., 1981). This data taken in conjunction with the Fourier transform and kinetic infrared spectroscopy data suggest that carboxyl residues may indeed act as proton translocating groups in the mechanism of the light-driven proton pump.

A Model of BR Structure

The data obtained in this study is consistent with several current models of BR structure (Agard and Stroud, 1982; Engelman et al., 1982; Huang et al., 1982). One representative model which incorporates all of the available data in the literature will be presented here and the results of this study will be related to the model.

A current model of the secondary structure of BR (Fig. 35) serves to illustrate the probable locations of the nineteen carboxyl groups of BR (Huang et al., 1982). The model is based on a combination of numerous lines of evidence that include: (1) x-ray diffraction and electron diffraction data which limit the length of the α-helical rods to about 45 Å, (2) circular dichroism measurements that indicate a 70-80% helix content, (3) proteolytic cleavage points, (4) chemical

Figure 35.    Model of the Secondary Structure of Bacteriorhodopsin

(Huang et al., 1982).  The nineteen carboxyl groups of

BR are identified by the boxed residues.  A possible

orientation of retinal is designated by the stippled

area originating from Lysine-216.  The α-helical protein

regions in hydrophobic protein domains are indicated as

they relate to the lipid bilayer structure and are denoted

by the rectangular areas.  Sites of proteolytic enzyme

cleavage of the polypeptide are indicated with arrows.

INSIDE

OUTSIDE

| A | B | C | D | E | F | G |

LIPID POLAR GROUPS

LIPID POLAR GROUPS

HYDROPHOBIC LIPID REGION

PRONASE

PAPAIN

PAPAIN

PRONASE

PAPAIN

CHYMOTRYPSIN PRONASE

LACTOPEROXIDASE

PAPAIN

TRYPSIN

PAPAIN

modification studies, (5) energy calculations for insertion of the polypeptide into the membrane, and (6) photoaffinity cross-linking studies with a retinal derivative. The surface groups in this model are located on the loops that are outside the hydrophobic lipid region. A number of these groups can be definitively placed on the surfaces since they reside on polypeptide loops or the C-terminal tail which are accessible to proteolytic enzymes. In this model, 12 of the 19 carboxyl groups (boxed residues) are defined as surface groups. There is a marked assymetric distribution of carboxyl groups between the two membrane surfaces since 11 of the 12 surface groups reside on the inside or cytoplasmic membrane surface. The C-terminal tail accounts for 5 of the 11 groups, and represents a region of high negative charge density on the inside surface. In the hydrophobic membrane domain, the remaining seven buried carboxyl residues are widely dispersed. Several of these groups appear in close proximity to the retinal moiety.

This study showed that a mild chemical modifiation procedure using a water-soluble carbodiimide and nucleophile resulted in the amide coupling of 12 residues. Previous carboxyl group modification studies of water-soluble globular enzymes and these identical modification reagents showed a strong correlation between crystallographic findings that placed carboxyls on the surface of the enzyme and modifiable groups. It is thus reasonable to assume that the 12 groups modified in BR by this procedure are on the surface, and that the remaining 7 are buried in a hydrophobic environment. Thus, the distribution of carboxyl groups determined by chemical modification is in strong agreement with that proposed in the model. In general, the surface groups have the following properties: (1) they do not interact with the retinal

chromophore, since the visible absorption and CD spectra of such samples
are unaltered, (2) they are not critical for photocycling activity of
BR, (3) they are not required for proton pumping functions, and (4) they
possess relatively high mobility as revealed by ESR spectra of spin-
labeled residues. However, recent reports by Govindjee et al. (1980)
suggest the C-terminal tail may influence the stoichiometry of the
proton pumping process. The proton pumping stoichiometry of carboxyl-
modified BR has not been determined and may be altered. Thus, the
surface carboxyl groups do not appear to be essential residues important
in the structure and function of BR.

In marked contrast, the seven buried carboxyl groups residing in
hydrophobic membrane domains (Fig. 35) appear particularly important to
both the structure and function of BR. The structural involvement of a
carboxyl residue in the photocycle was determined in this study.
Formation of a carboxyl-lysine zero-length intramolecular cross-link in
a relatively hydrophobic domain strongly limits the involvement of
possible groups. Buried groups that could form ion-pairs and bridge
different α-helical rods are Lysine-129 and either Glu-9 or Glu-204.

The presence of a hydrophobic carboxyl residue in close proximity
( ≃ 10 Å) to the retinal chromophore was determined. This group may
be capable of modulating BR absorption properties and influences photo-
cycling activity. Several buried groups in the model are sufficiently
close that one or more could function to modulate BR spectral properties
and activity through electrostatic interactions. The modified carboxyl
group in the chromophore environment is most likely to be Glu-194
(helix F), although Glu-204 (helix G) and Glu-9 (helix A) are also
candidates for the modified site.

A tentative role for a different set of buried carboxyl residues in the photocycle and proton translocation processes can be suggested from this study. Spin-label data shows that extensive modification of buried residues results in loss of the retinal-protein chromophore, and hence, loss of activity. These essential buried groups are likely located near the BR chromophore, but are distinct from the carboxyl labeled with the pH-sensitive reporter group. Essential buried groups in the hydrophobic membrane domain may be one of six residues: Asp-9, Asp-95, Asp-96, Asp-115, Glu-204 and Asp-212.

One of the more important implications of this study concerns the placement of buried carboxyl groups in models of BR structure. The ESR data definitively shows for the first time that at least one group is buried deeper than 16 Å. These observations confirm predictions that such groups reside within hydrophobic membrane environments. The most deeply buried carboxyl residues, Asp-85, Asp-115 and Asp-212, are considered the most likely sites of labeling (d $\geq$ 15 Å).

In summary, chemical modification and spin-label studies have identified several distinct functional roles for the buried carboxyl residues of BR in the mechanism of the light-driven proton pump. In addition, these studies obtained structural information which supports current models of BR protein structure in the purple membrane. The essential nature of carboxyl residues in the activity of membrane proton pumps has been recently demonstrated for the ATPase/synthase of chloroplasts, mitochondria and bacteria, cytochrome oxidase, and the plasma membrane ATPases of eukaryotic cells such as Neurospora. Hence, this study demonstrating essential carboxyl groups in BR appears

consistent with the idea that carboxyl residues in hydrophobic environments may be a general feature required for activity of membrane proton pumps.

## X. SUMMARY AND CONCLUSIONS

1. Chemical modification of carboxyl residues in BR located on or near the purple membrane surface does not affect the retinal-protein chromophore. When such residues are modified, the photocycle kinetics are minimally inhibited, indicating that surface groups are not essential for photocycle activity. However, modification of buried groups resulted in changes or loss of the retinal-protein chromophore and photocycling activity.

This indicates that carboxyl groups essential for photocycling function are located in a hydrophobic environment near the chromophore. This finding is of interest since carboxyl residues in hydrophobic domains are required for activity in many other membrane proton pump proteins.

2. Chemical modification of carboxyl groups in the absence of exogenous added nucleophiles resulted in strong inhibition of photocycle kinetics and the formation of a single zero-length intramolecular cross-link between a carboxyl and lysine residue. A carboxyl-lysine pair must, therefore, be in close proximity in the native membrane and interact ionically. Since the cross-link acts to constrain protein conformational changes, this finding provides additional evidence that conformational changes of BR are essential for the reprotonation phase of the photocycle and proton pumping activity.

3. A carboxyl residue involved in retinal-protein interactions was identified using a pH-sensitive reporter group, nitrotyrosine methyl ester. After modification, spectral and ionization properties indicated that the group resides in a hydrophobic environment and chromophore interactions depend upon a particular protein configuration. This

provides evidence for the hypothesis that electrostatic interactions between retinal and specific carboxyl groups modulate BR absorption properties.

4. The topography and mobility of carboxyl residues in the purple membrane was characterized using spin-labeled BR. Paramagnetic broadening agents showed that two distinct classes of carboxyl groups exist: (1) a strongly immobilized, buried membrane group and (2) a weakly immobilized set on the membrane surface that includes the C-terminal tail. These observations support current models of BR structure that place carboxyl residues deep within the purple membrane. Since removal of the C-terminal tail has been reported to affect proton pumping stoichiometry, the finding that the tail is moderately immobilized may be of significance in the proton translocation.

## X.  APPENDIX I

### Electron Spin Resonance Line Shape in a System of Two Interacting Spins

Leigh (1970) developed a theory to explain experimental observations that the ESR signal of a free radical covalently bound to a protein molecule was _not_ appreciably broadened by the binding of a paramagnetic ion in the same molecule. The theory describes the rigid-lattice line shape of an electron spin resonance signal which is influenced by dipolar coupling to a second spin. The theoretical curves generated by the theory compare extremely well with experimental results for a nitroxide radial interacting with a paramagnetic ion. The results of the theory allow the calculation of the distance between the two interacting spins using the experimentally measured value of the decrease in intensity of the spin signal.

The observed line width of the ESR signal will be given by:

$$\delta H = C (1 - 3 \cos^2 \theta_r')^2 + \delta H_o \qquad (1)$$

and

$$C = \frac{g \beta \mu^2 T_{1k}}{\hbar r^6} \qquad (2)$$

where $\delta H_o$ is the natural line width in the absence of the metal ion, $\theta_r'$ is the angle between the radial vector of magnitude r and the applied field, and C is the strength of the dipolar interaction. The value of C is in turn primarily dependent on $\mu$, the magnetic moment, $T_{1k}$ is the metal spin-lattice relaxation time, and $r^6$ is the sixth power of the distance between the interacting spins.

Computer-generated lineshapes taken from Leigh's paper are shown in figure 36. The main qualitative conclusion is that the ESR spectra

do not appear to change very much in shape but <u>appear</u> to lose intensity. This is due to the fact that Eq. 2 is sensitive to orientation changes. For a certain fraction of orientations where "r" with respect to $H_O$ is close to the magic angle of 54.7°, the dipolar interaction is near zero and the free radical spectrum is unaltered. Away from the magic angle, the dipolar broadening smears spectral intensity into a broad continuum with very small first derivative intensity.

As the spin-lattice relaxation time gets shorter and shorter, the dipolar interactions become increasingly well averaged, $\delta H \to \delta H_O$ in Eq. 2. Thus, relatively slowly relaxing metal ions such as $Cu^{+2}$, $Gd^{+3}$, and $Mn^{+2}$ are particularly effective dipolar broadening agents.

Hyde and Rao (1978) extended this type of calculation in order to consider a situation in which a number of metal ions could interact with each free radical. The occupation of potential metal-ion binding sites was allowed to vary over the full range of statistical probabilities. A large number of domains were considered in order to represent every combination of metal-ion occupations. The main conclusion of the analysis is that in a system of paramagnetic metal ions added to spin labels in which a wide range of radial distances is possible between the interacting spins, the observed magnetic interactions will be primarily determined by the distance of closest approach. The precise geometry is of little significance since the sixth power of the radius dominates the calculation.

Figure 36.  Computer nitroxide ESR spectral line-shape for an
immobilized spin interacting with a paramagnetic
metal ion of fixed geometry.  Figure taken from Leigh
(1970).

# LINE SHAPE OF TWO INTERACTING SPINS

## [after Leigh, J.S. (1970) J. Chem. Phys. 52, 2608-2612.]
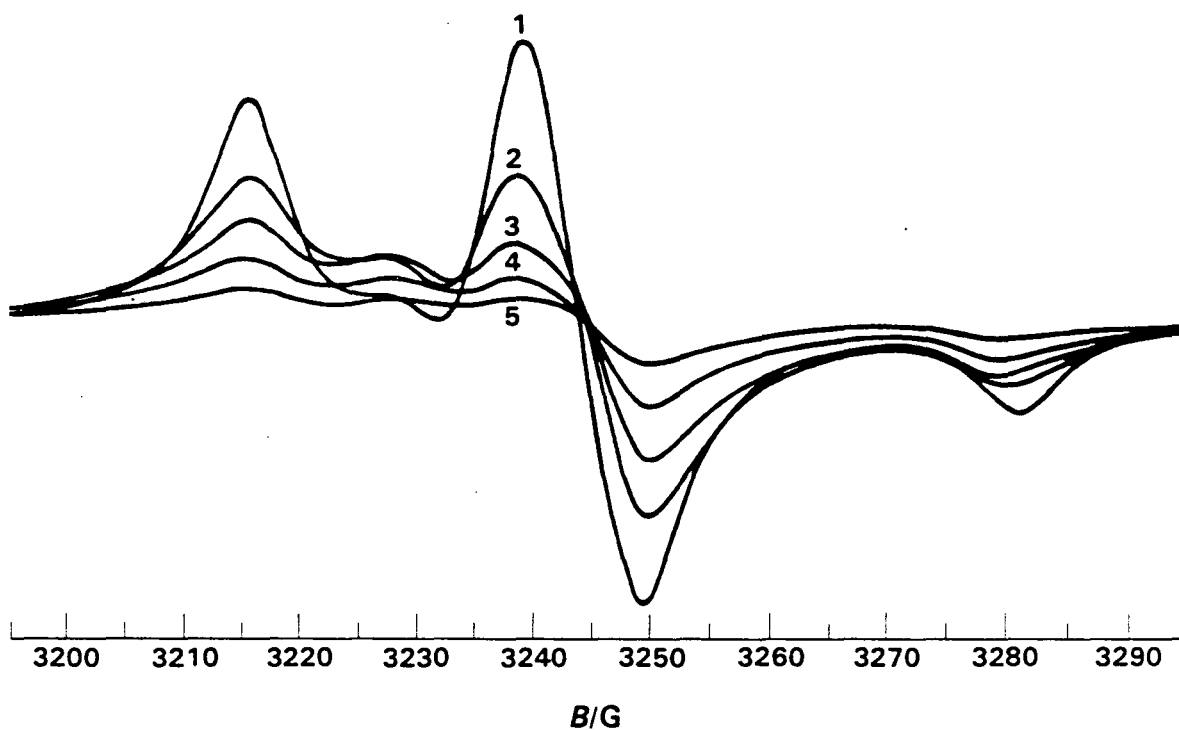


Computed nitroxide ESR spectra for an immobilized spin interacting with a paramagnetic metal ion of fixed geometry. The dipolar interaction results in an apparent loss of intensity without change in lineshape.

## XI. REFERENCES

Agard, D.A. and Stroud, R.M. (1982) Biophys. J. 37, 589-602.

Balogh-Nair, V., Carriker, B., Honig, B., Kamat, V., Motto, M.,
Nakanishi, K., Sen, R., Sheves, M., Tanis, M. and Tsujimoto, K.
(1981) Photochem. Photobiol. 33, 483-488.

Barber, J. (1980) Biochim. Biophys. Acta 594, 253-308.

Basch, J.J. and Timasheff, S.N. (1967) Arch. Biochem. Biophys.
118, 37-47.

Bayley, H., Huang, K.-S., Radhakrishnan, R., Ross, A.H., Takagaki, Y.
and Khorana, H.G. (1981) Proc. Natl. Acad. Sci. USA 78, 2225-
2229.

Becher, B.M. and Cassim, J.Y. (1975) Prep. Biochem. 5, 161-178.

Becher, B.M. and Ebrey, T.G. (1977) Biophys. J. 17, 185-191.

Belleau, B. and Malek, G. (1968) J. Am. Chem. Soc. 90, 1651-1652.

Blatz, P.E., Mohler, J.H., and Navangul, H.V. (1972) Biochemistry
11, 848-855.

Blaurock, A.E. (1975) J. Mol. Biol. 93, 139-158.

Blaurock, A. and Stoeckenius, W. (1971) Nature New Biol. 233, 152-155.

Bogomolni, R., Hwang, S.-B., Tseng, Y.-W., King, G.I. and Stoeckenius, W.
(1977) Biophys. J. 17, 98a.

Bogomolni, R., Stubbs, L. and Lanyi, J.K. (1978) Biochemistry 17,
1037-1041.

Bohlen, P., Stein, S., Dairman, W. and Udenfriend, S. (1973) Arch.
Biochem. Biophys. 155, 213-220.

Bridgen, J. and Walker, I.D. (1976) Biochemistry 15, 792-796.

Burley, R.W., Seidel, J.C. and Gergely, J. (1972) Arch. Biochem. Biophys.
150, 792-796.

Burr, M. and Koshland, D.E. (1964) Proc. Natl. Acad. Sci. USA 52, 1017–1021.

Callendar, R. and Honig, B. (1977) Ann. Rev. Biophys. Bioenerg. 6, 33–55.

Carmeli, C., Quintanilha, A.T., and Packer, L. (1980) Proc. Natl. Acad. Sci., USA 77, 4707–4711.

Carraway, K.L. and Koshland, D.E. (1968) Biochim. Biophys. Acta 160, 272–274.

Carraway, K.L. and Koshland, D.E. (1972) in Methods in Enzymology (Hirs, C.H.W. and Timasheff, S.N., eds.) Academic Press, New York. Vol. 25, pp. 616–623.

Champeil, P., Rigaud, J.-L. and Gary-Bobo, C.M. (1980) Proc. Natl. Acad. Sci. U.S.A. 77, 2405–2409.

Cherry, R.J., Muller, V., Henderson, R. and Heyn, M.P. (1978) J. Mol. Biol. 121, 283–298.

Chignell, C.F. and Chignell, D.A. (1975) Biochem. Biophys. Res. Commun. 62, 136–143.

Cohen, L.A. and Jones, W.M. (1963) J. Am. Chem. Soc. 85, 3397–3402.

Cornell, C.N. and Kaplan, L.J. (1978) Biochemistry 17, 1750–1754.

Dencher, N. and Heyn, M. (1979) FEBS Lett. 108, 307–310.

Edgarton, M.E., Moore, T.A. & Greenwood, C. (1978) FEBS Lett. 95, 35–39.

Engelman, D.M., Henderson, R., McLachlan, A.D. and Wallace, B.A. (1980) Proc. Natl. Acad. Sci. USA 77, 2023–2027.

Engelman, D.M., Goldman, A. and Steitz, T.A. (1982) in Methods in Enzymology, (Packer, L., ed.) Academic Press, New York. Vol. 88, pp. 81–88.

Eyl, A. and Inagami, T. (1971) J. Biol. Chem. 246, 738-746.

Fairbanks, G., Steck, T.L. and Wallach, D.F.H. (1971) Biochemistry 10, 2606-2617.

Fischer, U. and Oesterhelt, D. (1979) Biophys. J. 28, 211-230.

Frankel, R.D. and Forsyth, J.M. (1982) in Methods in Enzymology (Packer, L., ed.) Academic Press, New York. Vol. 88, pp. 272-281.

Fukumoto, J., Hopewell, W., Karvaly, B. and El-Sayed, M. (1981) Proc. Natl. Acad. Sci. USA 78, 252-255.

Gerber, G.E., Gray, C.P., Wildenauer, D. and Khorana, H.G. (1977) Proc. Natl. Acad. Sci. USA 74, 5426-5430.

Glazer, A.N., Delange, R.J. and Sigman, D.S. (1976) in Chemical Modification of Proteins: Selected methods and analytical procedures. North-Holland Pub. Co., Amsterdam.

Godin, D.V. and Schrier, S.L. (1970) Biochemistry 9, 4068-4077.

Govindjee, R., Ebrey, T.G. and Crofts, A.R. (1980) Biophys. J. 30, 231-242.

Govindjee, R., Ohno, K. and Ebrey, T.G. (1982) Biophys. J. 38, 85-87.

Hartmann, R. and Oesterhelt, D. (1977) Eur. J. Biochem. 77, 325-335.

Hayward, S.B., Grano, D.A., Glaeser, R.M. and Fisher, K.A. (1978) Proc. Natl. Acad. Sci. USA 75, 4320-4324.

Hayward, S.B. and Stroud, R.M. (1981) J. Mol. Biol. 151, 491-517.

Henderson, R. (1975) J. Mol. Biol. 93, 123-138.

Henderson, R. and Unwin, P.N.T. (1975) Nature 257, 28-32.

Herz, J.M. and Packer, L. (1981) FEBS Lett. 131, 158-164.

Herz, J.M., Mehlhorn, R. and Packer, L. (1983) J. Biol. Chem., in press.

Hess, B. and Kushmitz, D. (1979) FEBS Lett. 100, 334-340.

Hoare, D.G. and Koshland, D.E. (1967) J. Biol. Chem. 242, 2447-2453.

Honig, B., Dinur, V., Nakanishi, K., Balogh-Nair, V., Gawinowicz, M.A., Arnaboldi, M. and Motto, M.G. (1979a)  J. Am. Chem. Soc. 101, 7084-7086.

Honig, B., Ebrey, T., Callender, R.H., Dinur, V. and Ottolenghi, M. (1979b)  Proc. Natl. Acad. Sci. USA 76, 2503-2507.

Honig, B. and Hubbell, W. (1983)  Biophys. J. 41, 203a.

Huang, K.S., Bayley, H. and Khorana, H.G. (1980)  Proc. Natl. Acad. Sci., USA 77, 323-327.

Huang, K.S., Bayley, H., Liao, M.J., London, E., and Khorana, H.G. (1981)  J. Biol. Chem. 256, 3802-3809.

Huang, K.-S., Radhakrishnan, R., Bayley, H. and Khorana, H.G. (1983) J. Biol. Chem., in press.

Hyde, J.S. and Rao, K.V.S. (1978)  J. Magn. Reson. 29, 509-516.

Hyde, J.S. and Sarna, T. (1978) J. Chem. Phys. 68, 4439-4446.

Hyde, J.S., Swartz, H.M. and Antholine, W.E. (1979) in Spin Labeling Two (Berliner, L.J., ed.) Academic Press, New York.  pp. 71-113.

Kalisky, O., Feitelson, J. and Ottolenghi, M. (1981)  Biochemistry 20, 205-209.

Kalisky, O., Ottolenghi, M., Honig, B. and Korenstein, R. (1981) Biochemistry 20, 649-655.

Kates, M., Kushwaha, S.C. and Sprott, G.D. (1982)  in Methods in Enzymology (Packer, L., ed.) Academic Press, New York.  Vol. 88, pp. 98-111.

Katre, N.V., Wolber, P.K., Stoeckenius, W. and Stroud, R.M. (1981) Proc. Natl. Acad. Sci. USA, 78, 4068-4072.

Keefer, L.M. and Bradshaw R.A. (1977)  Fed. Proc. 36, 1799-1804.

Keith, A.D., Snipes, W., Mehlhorn, R.J., and Gunter, T. (1977) Biophys. J. 19, 205-218.

Khorana, H.G., Gerber, G.F., Herlihy, W., Gray, C.P., Anderegg, R.J., Nihei, K. and Biemann, K. (1979) Proc. Natl. Acad. Sci. USA 76, 5046-5050.

King, G.I., Stoeckenius, W., Crespi, H.L. and Schoenborn, B.P. (1979) J. Mol. Biol. 130, 395-404.

Klein, G., Satre, M., Dianoux, A.C. and Vignais, P.V. (1980) Biochemistry 19, 2919-2925.

Kokesh, F.C. and Westheimer, F.H. (1971) J. Am. Chem. Soc. 93, 7270-7274.

Konishi, T. and Packer, L. (1976) Biochem. Biophys. Res. Commun. 72, 1473-1441.

Konishi, T. and Packer, L. (1977) FEBS Lett. 79, 369-373.

Konishi, T., Tristram, S. and Packer, L. (1979) Photochem. Photobiol. 29, 353-358.

Kushawa, S.C., Kramer, J.K.G., Gates. M. (1975) Biochim. Biophys. Acta 398, 303-314.

Kushner, D.J. (1964) J. Bacteriol. 5, 1147-1156.

Kushwaha, S.C., Kates, M. and Martin, W.G. (1975) Can. J. Biochem. 53, 284-292.

Laemmli, V.K. (1970) Nature 227, 680-685.

Lanyi, J. (1978) Microbiological Reviews 42, 682-706.

Lanyi, J.K. and MacDonald, R.E. (1979) in Methods in Enzymology (Packer, L. and Fleischer, S., eds.) Academic Press, New York. Vol. 56, pp. 398-407.

Leigh, J.S. (1970) J. Chem. Phys. 52, 2608-2612.

Lemke, H.D. and Oesterhelt, D. (1981)   Eur. J. Biochem. 115, 595-604.

Lewis, A., Marcus, M.A., Ehrenberg, B. and Crespi, H. (1978)   Proc. Natl. Acad. Sci. USA 75, 4642-4646.

Lewis, A., Spoonhower, J., Bogomolni, R.A., Lozier, R.H. and Stoeckenius, W. (1974)   Proc. Natl. Acad. Sci. USA 71, 4462-4466.

Likhtenshtein, G.I. (1976)   Spin Labeling Methods in Molecular Biology, J. Wiley and Sons, New York.

Lin, T.-S. and Koshland, D.E. (1969)   J. Biol. Chem. 244, 505-508.

Long, M.M., Urry, D.W. and Stoeckenius, W. (1977)   Biochem. Biophys. Res. Commun. 75, 725-731.

Lowry, O., Rosebrough, N., Farr, L. and Randall, R. (1951)   J. Biol. Chem. 193 365-474.

Lozier, R.H., Bogomolni, R.A. and Stoeckenius, W. (1975)   Biophys. J. 15, 955-962.

Lozier, R., Niederberger, W., Bogomolni, R., Hwang, S.-B. and Stoeckenius, W. (1976)   Biochim. Biophys. Acta 440, 545-556.

Malan, P.G. and H. Edelhoch (1970)   Biochemistry 9, 3205-3214.

Matsuno-Yagi, A. and Mukohata, Y. (1980).   Arch. Biochem. Biophys. 199, 297-303.

Means, G.E. and Feeney, R.E. (1971)   Chemical Modifcation of Proteins, Holden-Day, Inc., San Francisco.

Mehlhorn, R.J. and Keith, A. (1972) in Membrane Molecular Biology (Fox, C.F. and Keith, A., eds.) Sinauer Associates, Stamford, Conn. pp. 192-227.

Michel, H. and Oesterhelt, D. (1976)   FEBS Lett. 65, 175-178.

Michel, H. and Oesterhelt, D. (1980)   Biochemistry 19, 4615-4619.

Moore, T.A., Edgarton, M.E., Parr, G., Greenwood, C. and Perham, R.N. (1978) Biochem. J. 171, 469-476.

Morrisett and Broomfield, J. (1971) J. Am. Chem. Soc. 93, 7297.

Morrisett, J.D. (1976) in Spin Labeling (Berliner, L.J., ed.) Academic Press, New York. pp. 273-338.

Mowery, P.C., Lozier, R.H., Chae, Q., Tseng. Y.W., Taylor, M. and Stoeckenius, W. (1979) Biochemistry 18, 4100-4107.

Muccio, D.D. and Cassim, J.Y. (1979) J. Mol. Biol. 135, 595-609.

Mukohata, Y., Sugiyama, Y. Kaji, Y., Usukura, J. and Yamada, E. (1981) Photochem. Photobiol. 33, 593-600.

Myers, B. and Glazer, A.N. (1971) J. Biol. Chem. 246, 412-419.

Nagle, J.F. and Morowitz, H.J. (1981) J. Chem. Phys. 74, 1367-1372.

Oesterhelt, D. and Hess, B. (1973) Eur. J. Biochem. 37, 316-326.

Oesterhelt, D. and Stoeckenius, W. (1971) Nature New Biol. 233, 149-152.

Oesterhelt, D. and Stoeckenius, W. (1973) Proc. Natl. Acad. Sci. USA 70, 2853-2857.

Ovchinnikov, Y.A., Abdulaev, N.G., Feigina, M., Kiselev, A.V. & Lobanov, N.A. (1977) FEBS Lett. 84, 1-4.

Ovchinnikov, Y., Abdulaev, N., Feigina, M., Kiselev, A. and Lobanov, N.A. (1979) FEBS Lett. 100, 219-224.

Packer, L., Tristram, S., Herz, J.M., Russell, C. and Borders, C.L. (1979) FEBS Lett. 108, 243-248.

Packer, L., Quintanilha, A., Carmeli, C., Sullivan, P.D., Scherrer, P., Tristram, S., Herz, J., Pfeifhofer, A. and Mehlhorn, R.J. (1981) Photochem. Photobiol. 33, 579-585.

Parsegian, A. (1969) Nature 221, 844-846.

Perutz, M.F. (1970) Nature 228, 726-739.

Pettei, M., Yudd, A., Nakanishi, K., Henselman, R. and Stoeckenius, W. (1977) Biochemistry 16, 1955-1959.

Pougeois, R., Satre, M. and Vignais, P. (1978) Biochemistry 17, 3018-3022.

Quintanilha, A.T. and Mehlhorn, R.J. (1978) FEBS Lett. 91, 104-108.

Racker, E. (1973) Biochem. Biophys. Res. Commun. 55, 224-230.

Racker, E. and Stoeckenius, W. (1974) J. Biol. Chem. 249, 662-663.

Renthal, R. (1981) J. Biol. Chem. 256, 11471-11476.

Renthal, R., Harris, G.J. and Parrish, R. (1979) Biochim. Biophys. Acta 547, 259-269.

Renthal, R., Dawson, N. and Horowitz, P. (1982) Biophys. J. 37, 227a.

Rothschild, K.J., Zagaeski, M. and Cantore, W.A. (1981) Biochem. Biophys. Res. Commun. 103, 483-489.

Salikhov, K.M., Doctorov, A.B. and Molin, Yu.N. (1971) J. Magn. Reson. 5, 189-205.

Satre, M., Lunardi, J., Pougeois, R. and Vignai, P.V. (1979) Biochemistry 18, 3134-3140.

Scherrer, P., Packer, L. and Seltzer, S. (1981) Arch. Biochem. Biophys. 212, 589-601.

Schreckenback, T., Walckhoff, B. and Oesterhelt, D. (1978) Biochemistry 17, 5353-5358.

Schreckenback, T., Walckhoff, B. and Oesterhelt, D. (1977) Eur. J. Biochem. 76, 499-511.

Sheehan, J.C., Cruickshank, P.A. and Boshart, G.L. (1961) J. Org. Chem. 26, 2525-2528.

Sherman, W.V., Korenstein, R. and Caplan, S.R. (1976) Biochim. Biophys. Acta 439, 454-458.

Sherman, W.V., Eicke, R.R., Stafford, S.R. and Wasacz, F.M. (1979) Photochem. Photobiol. 30, 727-729.

Sheves, M., Nakanishi, K. and Honig, B. (1979) J. Am. Chem. Soc. 101, 7086-7088.

Shichi, H. and Rafferty, C.N. (1980) Photochem. Photobiol. 31, 631-639.

Siebert, F., Mäntele, W. and Kreutz, W. (1982) FEBS Lett. 141, 82-87.

Spackman, D.H., Stein, W.H. and Moore, S. (1958) Anal. Chem. 30, 1190-1206.

Stamatoff, J., Lozier, R.H. and Gruner, S. (1982) in Methods in Enzymology (Packer, L., ed.) Academic Press, New York. Vol. 88, pp. 282-286.

Stoeckenius, W., Lozier, R. and Bogomolni, R.A. (1979) Biochim. Biophys. Acta 505, 215-278.

Sullivan, P.D., Quintanilha, A.T., Tristram, S. and Packer, L. (1980) FEBS Lett. 117, 359-362.

Swanson, M.S., Quintanilha, A.T. and Thomas, D.D. (1980) J. Biol. Chem. 255, 7494-7502.

Tanford, C. (1962) Adv. Protein Chem. 17, 70-165.

Taylor, J.S., Leigh, J.S. and Cohn, M. (1969) Proc. Natl. Acad. Sci. U.S.A. 64, 219-226.

Terner, J., Hsieh, C.L., Burns, A.R. and El-Sayed, M.A. (1979) Biochemistry 18, 3629-3634.

Tsuji, K. and Rosenheck, K. (1979) FEBS Lett. 98, 368-372.

Walker, J.E., Carne, A.F. and Schmitt, H.W. (1979) Nature 278, 653-654.

Wagner, S., Keith, A., and Snipes, W. (1980) Biochim. Biophys. Acta 600, 367-375.

Wallace, B.A. and Henderson, R. (1982) Biophys. J. 39, 233-239.

Warshel, A. (1978)  Proc. Natl. Acad. Sci. USA 75, 2558-2562.

Zaccai, G. and Gilmore, D. (1979)  J. Mol. Biol. 132, 181-191.